PRELIMINARY GEOLOGIC AND HYDROLOGIC STUDIES OF SITES HU1A AND HU1B IN HUDSPETH COUNTY, TEXAS

by

C. W. Kreitler, J. A. Raney, W. F. Mullican III,
E. W. Collins, and R. Nativ

Bureau of Economic Geology
W. L. Fisher, Director
The University of Texas at Austin
Austin, Texas 78713

Final report prepared for the
Low-Level Radioactive Waste Disposal Authority
under contract no. IAC(86-87)-1061

November 1986

CONTENTS

FIGURES

Appendix Figures

Tables

Plate (in pocket)

EXECUTIVE SUMMARY

The Bureau of Economic Geology, The University of Texas at Austin, conducted preliminary investigations of the geology and hydrology of northern Hudspeth County for the Texas Low-level Radioactive Waste Disposal Authority. The Authority had previously identified two sites, HU1A and HU1B, as possible sites for an above-ground disposal facility for low-level radioactive wastes.

Regional and site-specific investigations were conducted to characterize the geology and hydrology of HU1A and HU1B. The two sites are underlain by different bedrock lithologies covered by alluvium, which necessitated drilling for site-specific investigations. Because of the lack of exposed bedrock, studies of the regional geologic setting were used to infer the probable nature of the bedrock geologic environment at each site. Hydrologic studies were predominantly regional because of the limited data available at either site and the availability of water-level data and water samples from previously drilled wells in the region.

The host rocks at HU1A and HU1B are Precambrian rhyolite porphyry and Cretaceous limestone interbedded with some silty and muddy interbeds, respectively. The rhyolite porphyry is very fractured; the fractures strike in many directions and dip from vertical to horizontal. Most fractures contain no mineral fillings, indicating that they are not sealed. Cretaceous limestone at HU1B is not as fractured as the rhyolite porphyry at HU1A. There is evidence of carbonate dissolution and formation of some solution permeability.

The Babb flexure is north of both sites; however, fractures that are evident away from the inferred margins of the flexure may be related to flexure deformation. The flexure may be the Permian or post-Permian expression of a major pre-Permian strike-slip fault (Hodges, 1975). It is unknown if Cretaceous rocks have been warped by recurrent movement along the structure.

Regional ground-water flow is from southwest to northeast. The ground-water divide is not located along the Babb flexure but is close to the southern edge of the Diablo Plateau, an escarpment that overlooks the Rio Grande basin. Two aquifers are present, a shallow aquifer in the southwestern area with depths to water generally less than 200 ft (61 m) and a deeper aquifer through most of the region with depths to water of as much as 700 ft (213 m).

Recharge occurs over the entire study area and is not restricted to the updip part of the potentiometric surface in the areas of higher elevation. Tritium occurs in nearly all wells regardless of their location on the regional water table. Most recharge probably occurs during flooding of the arroyos that traverse the plateau. Recharge along fractures permits recently recharged water to move rapidly through a thick unsaturated section. Three separate fracture sets were identified during a pumping test. Because of the fracture control on ground-water flow, flow velocities cannot be estimated but are expected to be high. Discharge is either by evaporation on the salt flats or through pumping wells.

The shallower aquifer may or may not be present at either site, though it is not used in the vicinity of either site. Depth to ground water in the deeper aquifer beneath the sites is probably greater than 600 ft (183 m). Fractures in bedrock beneath the arroyos are probably important pathways for recharge in the vicinities of the sites.

Flooding down Antelope Draw, which bounds site HU1A, may be very intense for short durations, and consideration should be given to any siting with respect to this potential flooding.

Additional work on flooding potential, recharge potential, and aquifer hydraulic characteristics is recommended.

INTRODUCTION

In June 1986 the Bureau of Economic Geology (BEG) was asked by the Texas Low-level Radioactive Waste Disposal Authority to conduct a preliminary study of the geology and hydrology of two sites being considered for construction of a low-level radioactive waste repository. Both sites are located in northern Hudspeth County, Texas.

The rocks below potential sites are Precambrian rhyolite porphyry and Cretaceous limestone interbedded with some sandstone and mudstone. The geologic investigations provide data for evaluation of the general geologic framework of the proposed sites and provide site-specific data for evaluation of the physical and structural character of the rock units.

The hydrologic investigations address the following questions:

(1) Are there any regional aquifers below these sites? Aquifers are defined as water-bearing formations capable of producing water from a well.

(2) What is the thickness of the unsaturated zone (the depth to the uppermost regional ground-water table) at each site? What is the permeability of the unsaturated zone? Are there fracture zones in the unsaturated zone in which water and solute migration could be rapid?

(3) What are the flow directions of ground water in the aquifers?

(4) What is the residence time of water in the regional aquifers?

(5) What are the methods and rates of recharge to these aquifers? How much of the recharge comes from direct precipitation and surface flooding? How much recharge water could percolate through the layers being considered as host rocks for the repository?

(6) Where are the discharge points (natural and wells) of these aquifers, and what is their distance from the site?

Hydrogeologic study of both the unsaturated and saturated zones at each site was conducted to provide an initial assessment of these questions.

C. W. Kreitler and J. A. Raney are co-principal investigators for the hydrologic and geologic studies. W. F. Mullican III investigated the hydrology of the sites and supervised the drilling program. E. W. Collins studied the geology of the area. R. Nativ assisted with chemical and isotopic analysis and interpretation of the pumping test. We are appreciative of the cooperation of the local landowners during our investigations.

SITE INVESTIGATIONS

Location

The Texas Low-level Radioactive Waste Disposal Authority selected two sites (HU1A and HU1B) within an area in Hudspeth County, Texas, for consideration as the location of a low-level radioactive waste repository. The sites are on land owned and administered by The University of Texas System and are located approximately 15 mi (24 km) west of the Salt Basin in the vicinity of the Pump Station Hills on University Block K, sections 5, 6, 7, and 8, and University Block N, sections 16, 17, 31, 32, and 33, respectively (fig. 1). HU1A and HU1B are in the Hueco Station and Scratch Ranch 7.5-minute quadrangles, respectively. Site HU1A is 2 mi (3 km) south of the intersection of U.S. Highway 62-180 and Ranch-to-Market Road 1111. Site HU1B is about 1.5 mi (2.4 km) south of Scratch Ranch. Precambrian rhyolite porphyry bedrock is partly covered by alluvium at HU1A, whereas at HU1B alluvium covers Cretaceous limestone interbedded with some sandstone and mudstone. Both sites can be accessed from Ranch-to-Market Road 1111.

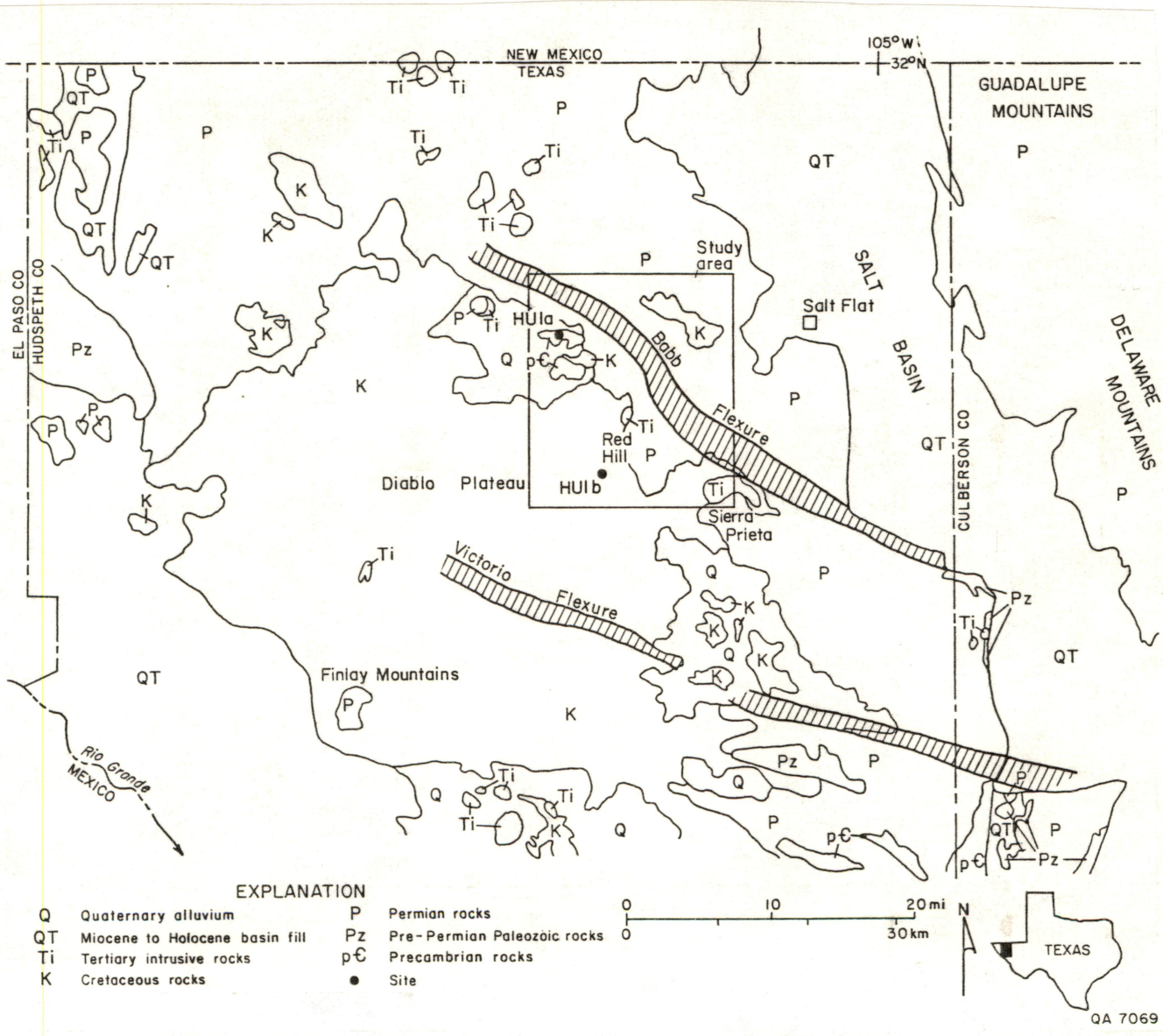

Figure 1. Location and regional setting of Pump Station Hills study area, Hudspeth County, Texas. Geology from Henry and Price (1985).

Methods

Aerial photographs at a scale of 1:12,000 (1 inch = 1,000 ft, 1 cm = 120 m) were acquired for a large area in the vicinity of the sites. The interpretations of the aerial photographs were compared with published maps. Field studies refined interpretations made from aerial photographs, and fracture data were collected.

Water-level data for the regional aquifers near the proposed sites were collected from several sources and are presented in appendix 1. Thirty static water-level values were obtained either by direct measurement using an electric water probe and steel tape, or from information provided by the well owner (fig. 2). Data for the Dell City and Salt Basin areas were taken from Texas Natural Resources Information System (TNRIS) computerized data base and from Nielson and Sharp (1985) and Boyd and Kreitler (in press). Information on the Fort Hancock area, southwest of the study sites, had previously been collected by BEG personnel (Kreitler and others, 1986).

No data were available on porosities, hydraulic conductivities, or transmissivities of the unsaturated or saturated zones at the sites.

Drilling Program

The drilling program for sites HU1A and HU1B was designed to provide data on the subsurface stratigraphy and rock characteristics at the sites and to drill boreholes for hydrologic testing.

Byrl Binkley, drilling contractor, drilled four test holes to complete the drilling objectives. At each site a 150 ft (45.7 m) deep stratigraphic test hole was drilled (HU1A-BEG#1 and HU1B-BEG#1), and continuous core from top of bedrock to total depth was recovered to characterize the nature of the subsurface bedrock. The

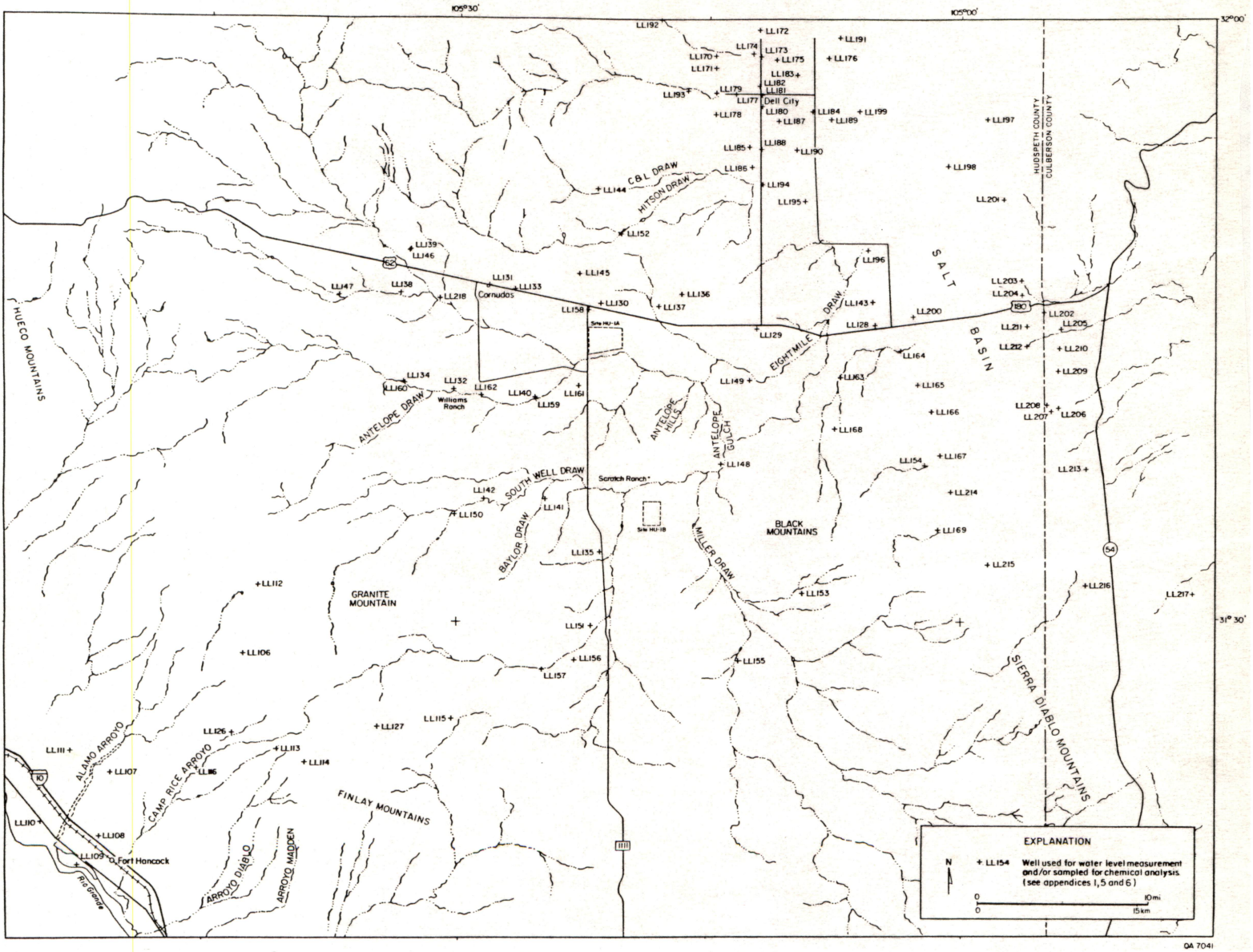

Figure 2. Surface drainage and location of wells within the study area. Thirty water level measurements were taken, as were 30 ground-water samples that were analyzed for general chemistry, $\delta^{18}O$, δD, tritium, $\delta^{34}S$, $\delta^{13}C$, and ^{14}C. Water level data and chemical analyses of ground-water in the Del City area taken from Texas Natural Resources Information System (TNRIS), Nielson and Sharp (1985), and Boyd and Kreitler (in press).

top of unweathered bedrock was determined at each site, and 15 ft (4.5 m) west of each stratigraphic test hole, a permeability test hole was cored (HU1A-BEG#2 and HU1B-BEG#2) to the top of unweathered bedrock. Casing was run to bottom and cemented to surface in each permeability test hole, and an additional 30 ft (9.1 m) was cored below casing. Constant head permeability tests were conducted for the intervals below casing to determine the hydraulic conductivity of the unweathered section of the unsaturated zone (appendix 2).

The permeability test holes were drilled with fresh water circulated only once instead of using a gel-based mud system. This procedure was used to reduce potential contamination by mud-cake buildup on the walls of the borehole. The nature of the rhyolite and dense limestone prevented use of air for circulation as tremendous heat buildup occurred on the coring bit while drilling with compressed air. It was determined that drilling with compressed air was not feasible, and the system was converted to fresh water.

Previous drilling of the shallow subsurface (Dames and Moore, 1985) at both sites documented variability in thickness of bedrock cover and depths of weathered bedrock. Permeability tests on such heterogeneous units may be of only local significance and not applicable to the site as a whole. Unweathered rhyolite penetrated at HU1A, however, may be very homogeneous (assuming uniform fracture distribution), and permeability tests on this interval could be applicable to a larger area. The heterogeneity of alluvial cover and weathered bedrock strata at HU1B also indicates that permeability tests on these units are of only local significance.

Two permeability tests were performed during this study in the unsaturated zone. At HU1A the tested interval is the upper 30 ft (9 m) of unweathered rhyolite, and at HU1B the tested interval is the upper 30 ft (9 m) of unweathered Cretaceous Campagrande limestone. A pumping test in the saturated zone of the

regional aquifer (assumed to be in Permian Victorio Peak - Bone Spring strata) was conducted. Data from the permeability tests and pumping test are presented in appendices 2 and 3, respectively.

Geologic and hydrologic data were obtained from eight water wells drilled and operated by the El Paso Natural Gas Company (EPNG) for their now-abandoned Pump Station #2 (appendix 4). Pump Station #2 is located 7.5 mi (12.2 km) west-southwest of site HU1A.

Chemical and Isotopic Analysis

Chemical analyses of ground water from wells in the Dell City area and in the Salt Basin were obtained from Texas Water Commission files. Data for wells near sites HU1A and HU1B were unavailable, but 30 active water wells within the study region were sampled. All samples were analyzed for general chemistry, $\delta^{18}O$, δD, tritium, $\delta^{34}S$, $\delta^{13}C$, and ^{14}C. Chemical analyses were performed by Mineral Studies Laboratory (BEG); ^{14}C analyses, by Radioisotopes Laboratory, Balcones Research Center (UT-Austin); other isotopic analyses ($\delta^{18}O$, δD, tritium, $\delta^{34}S$, and $\delta^{13}C$), by Environmental Isotope Laboratory, University of Waterloo, Ontario, Canada. Replicate analyses were performed on 26 isotope samples (8.6% of total) by Environmental Isotope Laboratory. Methods and applications of isotopic data ($\delta^{18}O$, δD, $\delta^{34}S$, $\delta^{13}C$, tritium, ^{14}C) are discussed in Kreitler and others (1986; appendix 3). Water temperatures were measured at the sampling sites. All chemical and isotopic data collected during this study are reported in appendix 5. Additional data used in this report from Kreitler and others (1986) and Texas Water Development Board (1985) are in appendix 6.

REGIONAL SETTING AND SEISMICITY

The study area lies within the Diablo Plateau region, Hudspeth County, Trans-Pecos Texas, at the eastern part of the Basin and Range structural province (fig. 1). This province consists of topographically high ranges separated by major normal faults from adjacent topographically low basins. Structural development of the province began about 24 million years ago (ma) during east-northeast-oriented extension. Faulting and associated relative subsidence of the basins began at that time and continue to the present. The basins were progressively filled by detritus eroded from the adjacent ranges. The study area lies about 15 mi (24 km) west of the Salt Basin, a large Basin and Range graben at the eastern edge of Hudspeth County.

No detailed studies of seismicity are available for Hudspeth County. Information on possible seismic activity in these areas is based on a consideration of the tectonic setting of Trans-Pecos Texas, including the presence of Quaternary fault scarps, and on recent seismicity in adjacent areas and in the Basin and Range structural province. Quaternary fault scarps occur throughout much of Trans-Pecos Texas and are abundant in the Salt Basin (Muehlberger and others, 1978; Henry and Price, 1985). Quaternary scarps have not been found within the study area, although some parallel the eastern part of the Babb flexure in the Salt Basin (Goetz, 1977). The west-northwest-trending Babb flexure extends from the Salt Basin across the study area (fig. 1).

Recent compilations of regional seismicity data include (1) the entire Basin and Range province (Askew and Algermissen, 1983), (2) southeastern New Mexico (Sanford and Toppozada, 1974), and (3) southern Culberson County and adjacent areas (Dumas, 1980). Askew and Algermissen (1983) show six epicenters in the Trans-Pecos region between 1803 and 1977, two with Richter magnitudes (surface

waves) of 5 and 6. Both of these latter earthquakes occurred near Valentine, Texas; one, the 1931 Valentine earthquake, had a modified Mercalli intensity of VIII and was the strongest reported earthquake in Texas. The 1955 earthquake near Valentine had a modified Mercalli intensity of IV (Reagor and others, 1982). Dumas (1980) detected about 300 earthquakes, all with magnitudes less than 3.7, between 1976 and 1980 near the site of the Valentine earthquake. Dumas (1980) also identified a seismically active area along the eastern margin of the Salt Basin near abundant Quaternary fault scarps. However, this area could not be located precisely because it was outside the seismic network. Sanford and Toppozada (1974) listed 11 felt earthquakes prior to 1961 and 6 instrumentally detected quakes between 1961 and 1972 in southeastern New Mexico and West Texas. Askew and Algermissen (1983) identified a swarm of earthquakes, all having Richter magnitudes of less than 4, centered near Juarez, Chihuahua, Mexico, about 45 mi (70 km) west of Hudspeth County.

Geology

The sites lie on the Diablo Plateau, west of the Salt Basin. Rocks in the area range in age from Precambrian to Recent (fig. 1 and plate). Strata most important to this investigation are Precambrian rhyolite porphyry at site HU1A and Cretaceous limestone interbedded with sandstone and mudstone at site HU1B.

Precambrian rhyolite porphyry crops out in the northwestern part of the study area in low rounded hills (plate). The petrology and age of the rhyolite porphyry were discussed by King and Flawn (1953), Stead and Waldschmidt (1953), Flawn (1956), Masson (1956), and Wasserburg and others (1962). The dark red rhyolite porphyry has pink feldspar and clear glassy quartz phenocrysts that range in size

from 0.1 to 0.4 inches (0.2 to 1.0 cm). Chlorite is a common alteration product. It is unknown if the rhyolite is intrusive or extrusive. Masson (1956) suggested that a complex of both extrusive and intrusive Precambrian rocks is present. The general age determined by strontium isotopic analysis is 1,060 mya, whereas the age determined by the lead-uranium method on zircon is 1,150 to 1,200 mya (Wasserburg and others, 1962). Lithologic descriptions of core from HU1A are in appendix 7. Core and good exposures in an abandoned quarry indicate that fractures are locally abundant. The fractures are discussed in the structure section of this report.

Permian strata that crop out in the study area include the Victorio Peak limestone and undivided Leonardian rocks (plate). These thin- to thick-bedded fossiliferous limestones and dolomites have interbeds of sandstone and siltstone (King, 1965). The Permian Cutoff shale also crops out in the eastern part of the study area, and the Hueco limestone is present on the south side of Sierra Prieta in the southeastern part of the area.

Cretaceous strata include the Campagrande Formation, Cox sandstone, and Finlay Formation (plate). Washita Group marl and fossiliferous shale also crop out at Sierra Prieta. The Campagrande Formation in the study area consists of thin-bedded, nodular, partly conglomeratic limestone with marl and clay interbeds (Barnes, 1983). It is commonly mottled yellow and red. The Cox conformably overlies the Campagrande Formation and consists of siltstone, sandstone, shale, and fossiliferous limestone (Barnes, 1983). Throughout most of the study area the Campagrande and Cox are poorly exposed and are undivided (plate). Test holes at site HU1B penetrate both Cox and Campagrande strata. Core descriptions are in appendix 7. Overlying the Cox are thick- to thin-bedded fossiliferous limestone interbedded with marl, shale, and sandstone of the Finlay Formation (Albritton and Smith, 1965; Barnes, 1983).

Two Tertiary intrusive bodies are present in the study area. The Red Hills (Antelope Hills) intrusion lies in the central part of the area and is about 6 mi (10 km) southeast of HU1A and 4 mi (6 km) north of HU1B (plate). The quartz trachyte intrusion is locally discordant but generally resembles a sill (Sullins, 1971). The intrusion has a Rb-Sr age of 28.2 $\pm$ 3.2 mya (Haley, 1971). The Sierra Prieta syenite intrusion (Black Mountains) lies 6 mi (10 km) east of HU1B. Hodges (1975) described Sierra Prieta as a "trap door" intrusion overlain by Permian strata and floored by Cretaceous rocks. Emplacement of the syenite intrusion was 35.0 $\pm$ 2.0 mya (Hodges, 1975).

Quaternary alluvial deposits cover much of the bedrock in the area. The alluvium consists of silt and sand with some pebbles and cobbles derived from local bedrock. Caliche layers up to 3 ft (1 m) thick occur near the surface.

Structure

Babb Flexure

The Babb flexure is a west-northwest-trending monocline with downward displacement of strata on the north side of the flexure (King, 1949, 1965). It can be traced about 40 mi (65 km) northwestward from the Salt Basin across the study area and is approximately 1 to 2 mi (1.5 to 3 km) wide (fig. 1 and plate). Permian rocks exposed on the flexure usually dip 10° to 15° north. The Victorio Peak Formation is displaced about 1,000 ft (305 m), and the Cutoff shale occurs only on the north side of the flexure (east of the study area). An angular unconformity exists between Permian and Cretaceous strata. Cretaceous rocks are not well enough exposed to determine if they have been warped by recurrent movement along the structure. Hodges (1975) mentioned that the flexure may be the Permian or post-Permian expression of a major pre-Permian strike-slip fault. Basement relief across the flexure could be greater than 4,500 ft (1,370 m) based on

the difference in elevation between exposed Precambrian rhyolite porphyry and the Jones No. 1 Mowry test hole, located 12 mi (19 km) northeastward, that bottomed in Ordovician strata at 500 ft (150 m) below sea level. The great amount of basement relief across the flexure indicates that the basement may be faulted.

Faults, Folds, and Joints

Faults present in outcrop are associated with the two Tertiary intrusions and do not extend far from the extrusive bodies. An east-west-trending anticline occurs west of Sierra Prieta. The anticline could have been caused by an unexposed intrusion that warped the overlying strata during emplacement. The buried intrusion may be related to the nearby Sierra Prieta intrusion.

Minor faults, flexures, and zones of closely spaced joints are mapped in well-exposed Permian strata in the northeastern part of the study area (plate). Displacement across the minor normal faults and flexures is commonly a few feet. Joint spacing in the fractured zones is as great as 10 joints per 3 ft (1 m) for limestone beds 1.5 ft (0.5 m) thick. Most of the fractured zones are about 6 ft (2 m) wide. These minor structures are probably related to the regional deformation along the Babb flexure but occur in strata well beyond the margins of the regional flexure.

Joints and minor normal faults also occur in the Precambrian rhyolite porphyry. Joint spacing of nearly vertical joints locally approaches 6 joints per 3 ft (1 m). Many of the joints extend vertically throughout the 15 to 20 ft (6 m) height of available exposures. Subhorizontal joints with dips of less than 30° also are abundant. Iron staining is a common feature on the joint surfaces, indicating that the joints have acted as ground-water conduits. Limonite and hematite stains also

occur on fracture surfaces in core, and some fractures are filled with dolomite and/or calcite (appendix 7). Fifty percent of the rhyolite porphyry core from site HU1A is fractured (appendix 7). Fractures in the core have dips ranging from horizontal to vertical, similar to fractures observed in outcrop.

Nearly vertical joints in the Precambrian rhyolite porphyry have multiple strike orientations (station 2 on the plate, and fig. 1). Three minor normal faults present in the rhyolite strike west-northwestward, similar to the regional trend of the Babb flexure. Permian and Cretaceous strata usually have two major joint sets that vary in strike regionally across the area (plate). Across most of the study area, nearly vertical joints strike northwest at 300° to 340° and northeast at 050° to 070° (stations 2, 3, 4, and 5, plate). North of Sierra Prieta, joints striking 010° to 030° are also common (station 6, plate). West of Sierra Prieta, joints strike north-northwest at 330° to 000° and east-west at 250° to 290° (stations 7 and 8, plate). The east-west trend parallels the anticline axis and faults at Sierra Prieta. Joints at site HU1B may strike in the same direction as joints in bedrock at stations 7 and 8 (plate). Core from test holes at HU1B was not as fractured as core from HU1A.

HYDROLOGIC SETTING

Surface Flow

HU1A

All surface streams in this region are ephemeral and, except for small local depressions, discharge east of the sites into the Salt Basin (fig. 2). Antelope Draw, one of the larger ephemeral streams in the area, is located 1.5 mi (2.4 km) south of

HU1A. Dames and Moore (1985) report that this draw drains more than 650 mi^2 of the Diablo Plateau west of the site. Final discharge of Antelope Draw is into Eight Mile Draw, which discharges into the Salt Basin approximately 18 mi (28.9 km) east.

During field activities for this study, several thunderstorms occurred. Flooding of Ranch-to-Market Road 1111 created a body of water 2 ft (0.6 m) deep and as much 200 to 300 ft (60 to 91 m) across (fig. 3). Duration of the flooding was very brief, and the road became passable almost as soon as rainfall terminated.

A smaller unnamed draw in the northern part of this site drains a very small area and is not considered as potentially hazardous as the larger draws. The National Flood Insurance Rate Map (FIRM) for HU1A (Community-panel number 480361 0400 B) (fig. 4) classifies both Antelope Draw and this smaller unnamed draw as Zone A, defined as areas of 100-year flood; base flood elevations and flood hazard factors were not determined. The site itself is classified as Zone C, defined as areas of minimal flooding.

HU1B

The northern and western portions of HU1B are within the mapped floodplain of Antelope Gulch, a large ephemeral draw that discharges into Antelope Draw several miles to the north (FIRM, Community-panel number 480361 0550 B) (fig. 5). This draw is also classified as Zone A, and the remaining area is mapped as Zone C (U.S. Department of Housing and Urban Development, 1985).

Methodologies utilized by the National Flood Insurance Program (NFIP) to classify potential areas of flooding may be divided into three basic types: (1) existing sources, such as the U.S. Army Corps of Engineers; (2) USGS flood-prone area quadrangles; and (3) normal depth equations actually calculated for

Figure 3. Photograph of flooding at Antelope Draw where it crosses Ranch-to-Market Road 1111. The flood created a body of water 2 ft (0.6 m) deep and as much 200 to 300 ft (60 to 91 m) across. Duration of flooding was very brief, and the highway became passable almost as soon as rainfall terminated.

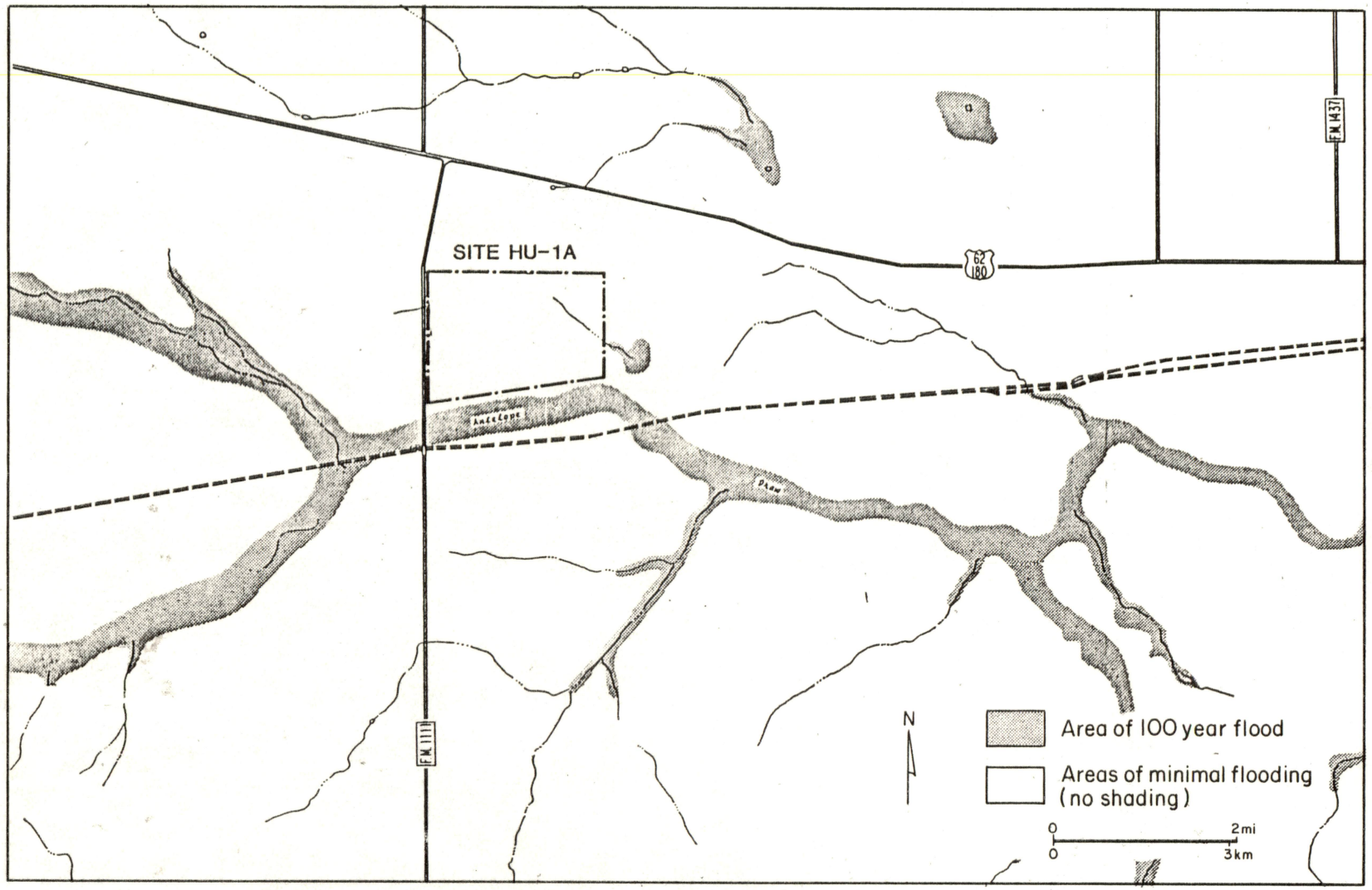

Figure 4. Flood Insurance Rate Map (FIRM) for area around site HU1A (Community-panel number 480361 0400 B). Both Antelope Draw and a smaller unnamed draw are enclosed as Zone A, defined as an area of 100-year flood. Base flood elevations and flood hazard factors were not determined. The site itself is classified as Zone C, defined as area of minimal flooding (U.S. Department of Housing and Urban Development, 1985).

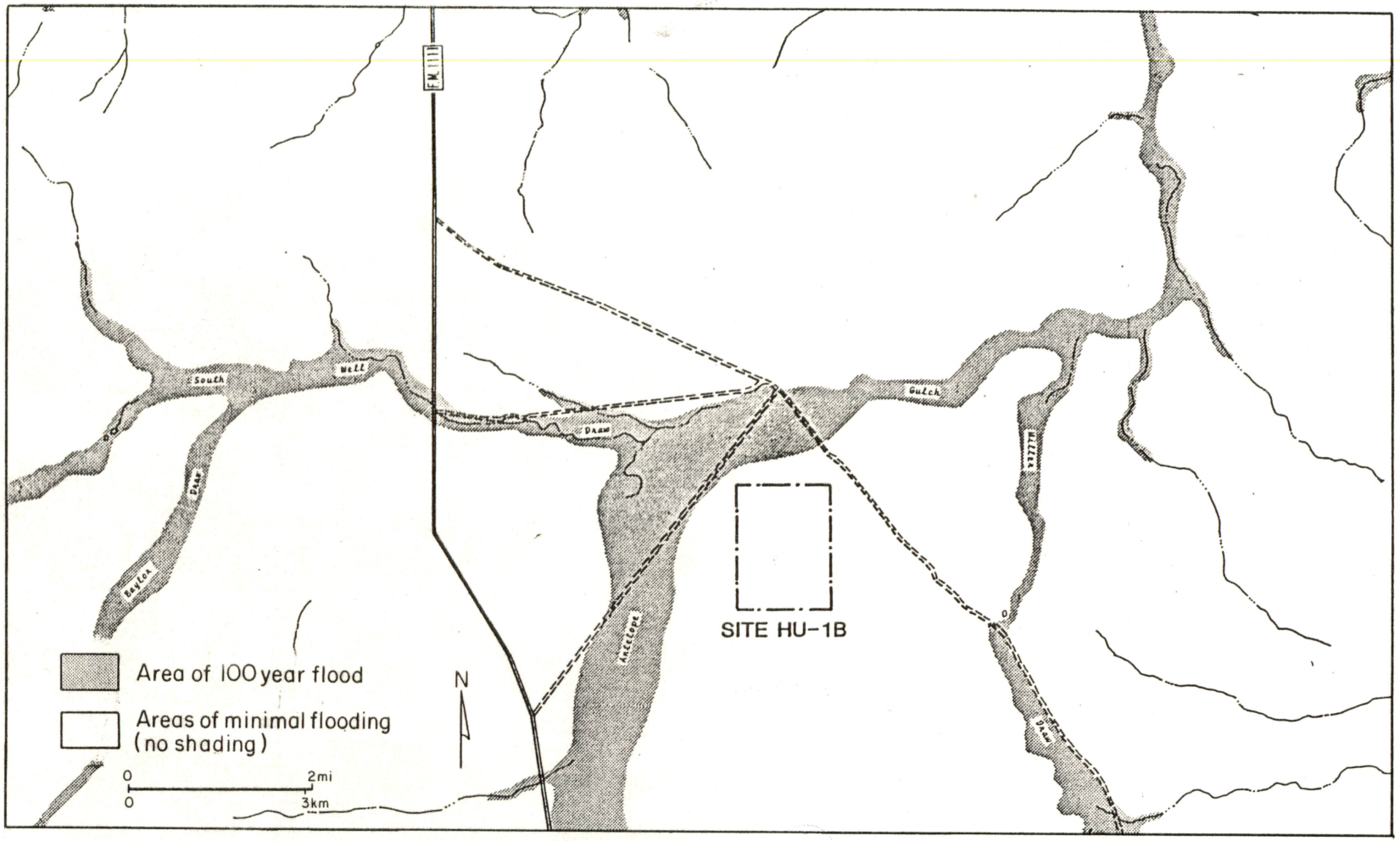

Figure 5. Flood Insurance Rate Map (FIRM) for area around site HU1B. The northern and western portions of HU1B are within the mapped floodplain of Antelope Gulch, a large ephemeral draw that discharges into Antelope Draw several miles to the north (FIRM, Community-panel number 480361 0550 B). This draw is also classified as Zone A, defined as area of 100-year flood. The remaining area is mapped as Zone C, defined as area of minimal flooding (FIRM, 1985).

specific areas. A formal request has been made to the Risk Studies Division to determine the methods used to map sites HU1A and HU1B. Additional study is needed to determine the different approaches used by the Risk Studies Division, to evaluate the extent of flooding from the heavy rains of this past summer (1986) and to discover whether flooded areas are consistent with those areas mapped by the NFIP.

Unsaturated Zone

The thickness of the unsaturated zone in the study area ranges from 3 ft (0.9 m) in the salt flats to 709 ft (216 m) in LL132 (fig. 6). The unsaturated zone is made up of Cenozoic alluvium and colluvium, Cretaceous sandstones and limestones, Paleozoic carbonates and clastics, and Precambrian rhyolites.

Vertical permeabilities of cores through the alluvial cover at HU1A range from 2×10^{-4} to 2×10^{-5} cm/sec (Dames and Moore, 1985). In situ horizontal permeability measurements from the upper 30 ft (9.1 m) of unweathered bedrock (Precambrian rhyolite) indicate a hydraulic conductivity value of 2.59×10^{-5} cm/sec (8.19 m/yr) (appendix 2). This value falls within the range of fractured igneous and metamorphic rocks as reported by Freeze and Cherry (1979, their table 2.2).

Vertical permeabilities of cores through the alluvial cover at HU1B range from 7×10^{-4} to 4×10^{-6} cm/sec (Dames and Moore, 1985). In situ horizontal permeability measurements taken on the upper 30 ft (9.1 m) of Cretaceous Cox sandstone and Cretaceous Campagrande limestone below the alluvium indicate a hydraulic conductivity of 1.226×10^{-4} cm/sec (38.6 m/yr). This value is within the range of limestones, dolomites, and sandstones (Freeze and Cherry, 1979).

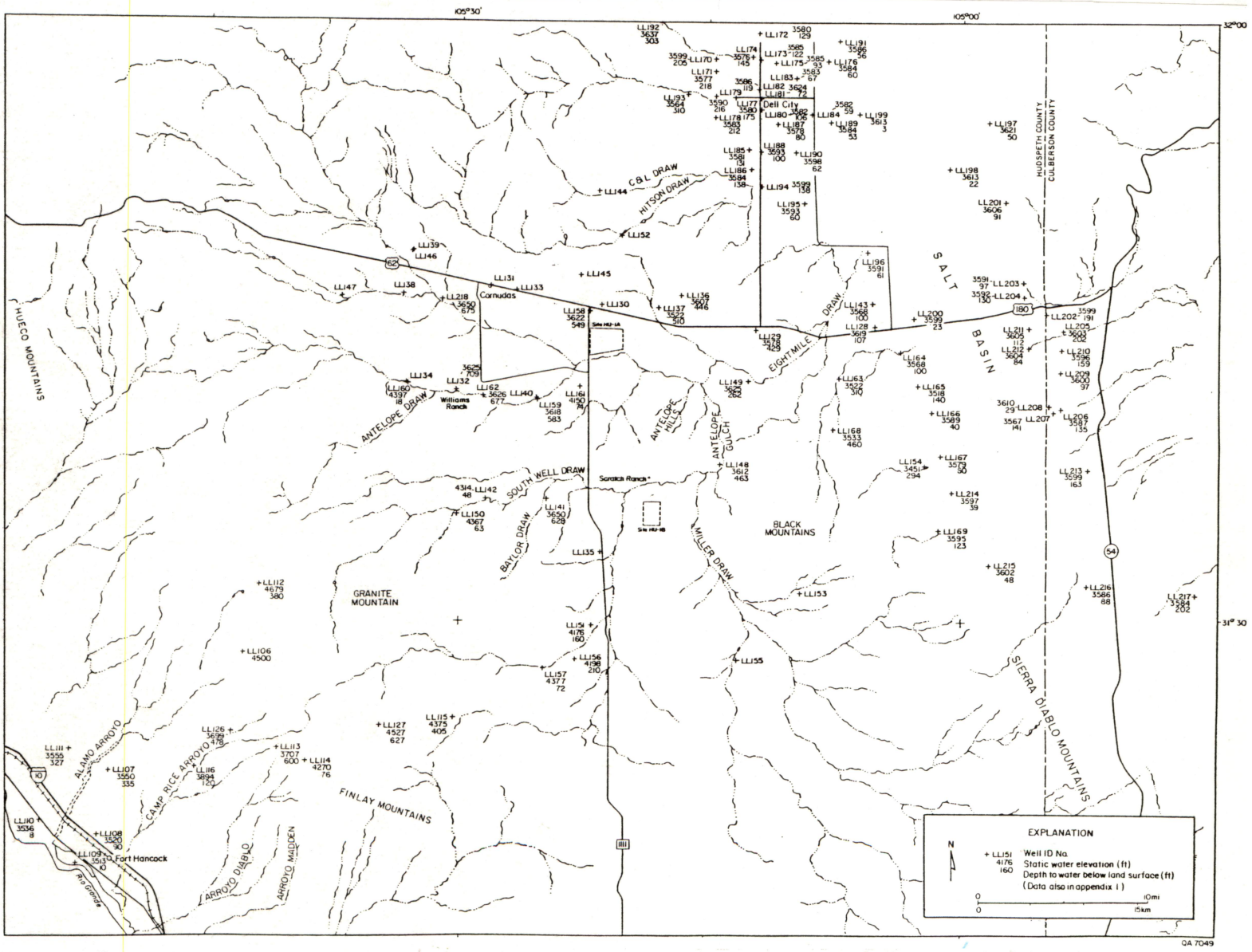

Figure 6. Map showing potentiometric surface elevations in the study area. Land surface elevation changes from 3,450 ft (1,050 m) at the salt flats and Dell City area to greater than 4,500 ft (1,370 m) in higher regions in the west, but the elevation of the water table in Aquifer A rises only 200 ft (61 m) (from 3,445 ft to 3,650 ft, or 1,050 to 1,113 m) across the same region, resulting in increasing depth to water at higher elevation. Thickness of the unsaturated zone in the study area ranges from 3 ft (0.9 m) in the salt flats to 702 ft (214 m) in well LL132 in the west.

Natural fracturing occurs in cored bedrock at both sites and in an abandoned quarry southeast of the test holes at HU1A. Natural fractures are more abundant in the rhyolite. Most of the fractures in the rhyolite are still open with only thin layers of limonite and hematite lining the fractures and providing no appreciable restriction to ground-water flow. Fractures in the limestones of HU1B, however, are partially to totally occluded by brown calcite and dolomite cements. The degree of restriction to ground-water flow that results from these cements is unknown. At least two examples of fracture enlargement by solutioning were recorded from the limestone core. In addition to fracture solutioning, partially occluded biomolds, initially a result of solutioning, were also observed. The apparent increase in fracturing from HU1B to HU1A may be a result of closer proximity to the Babb flexure. Higher permeabilities at HU1B, however, could result from more efficient connection of fracture systems due to the effects of solutioning. Permeability tests on the unsaturated zone at HU1A (appendix 2) also confirmed the presence of fracture systems in the subsurface rhyolite.

Saturated Zone

The primary aquifer, Aquifer A, (see potentiometric surface section for a detailed discussion) in the study area is part of a regional aquifer that extends across much of the Diablo Plateau. Previous studies of the Dell City area have reported that locally the water-bearing formation is the Bone Spring limestone of the Leonard series of Permian age (Scalapino, 1950; Peckham, 1963; Young, 1976; Gates and others, 1980). In the nearby Guadalupe Mountains, the Bone Spring limestone attains a thickness of several thousand feet (King, 1948). In the Dell City area, the Victorio Peak member of the Bone Spring limestone crops out, and locally the

aquifer is referred to as the Victorio Peak - Bone Spring aquifer. Peckham (1963) reports that the Bone Spring limestone is a black, cherty, dense, fine-textured, thin-bedded limestone at least 500 ft (152 m) thick, and the Victorio Peak limestone is a thick-bedded succession of gray limestone with a total thickness of about 800 ft (243 m). Lithologic control for this aquifer outside the Dell City area is extremely limited. Two driller's logs were obtained from El Paso Natural Gas Company records (appendix 4) for water wells drilled at Pump Station #2. These logs record lithologies that could reasonably be correlated with Permian strata of the area.

The shallow aquifer, Aquifer B (fig. 7), is a local aquifer located in the southwestern portion of the study area. Although no previous studies report aquifer host rock, stratigraphic thicknesses, coring at HU1B, and discussions with local well drillers make possible some inferences. Aquifer B is probably a Cretaceous limestone aquifer with permeabilities controlled by the presence of fracturing and solutioning. Cretaceous rocks in the area are typically reported to have minimum thicknesses of 200 ft (61 m) and because all but one of the wells producing from Aquifer B are shallower than 200 ft (61 m), a Cretaceous host rock seems reasonable.

Water-bearing Characteristics

The occurrence and quantity of ground water both in the Dell City area and throughout this regional aquifer appear to be controlled by fractures. Subsurface joints and fractures, caused by structural movement along the Babb and Victorio flexures (fig. 1), have contributed to both porosity and permeability development of the aquifer.

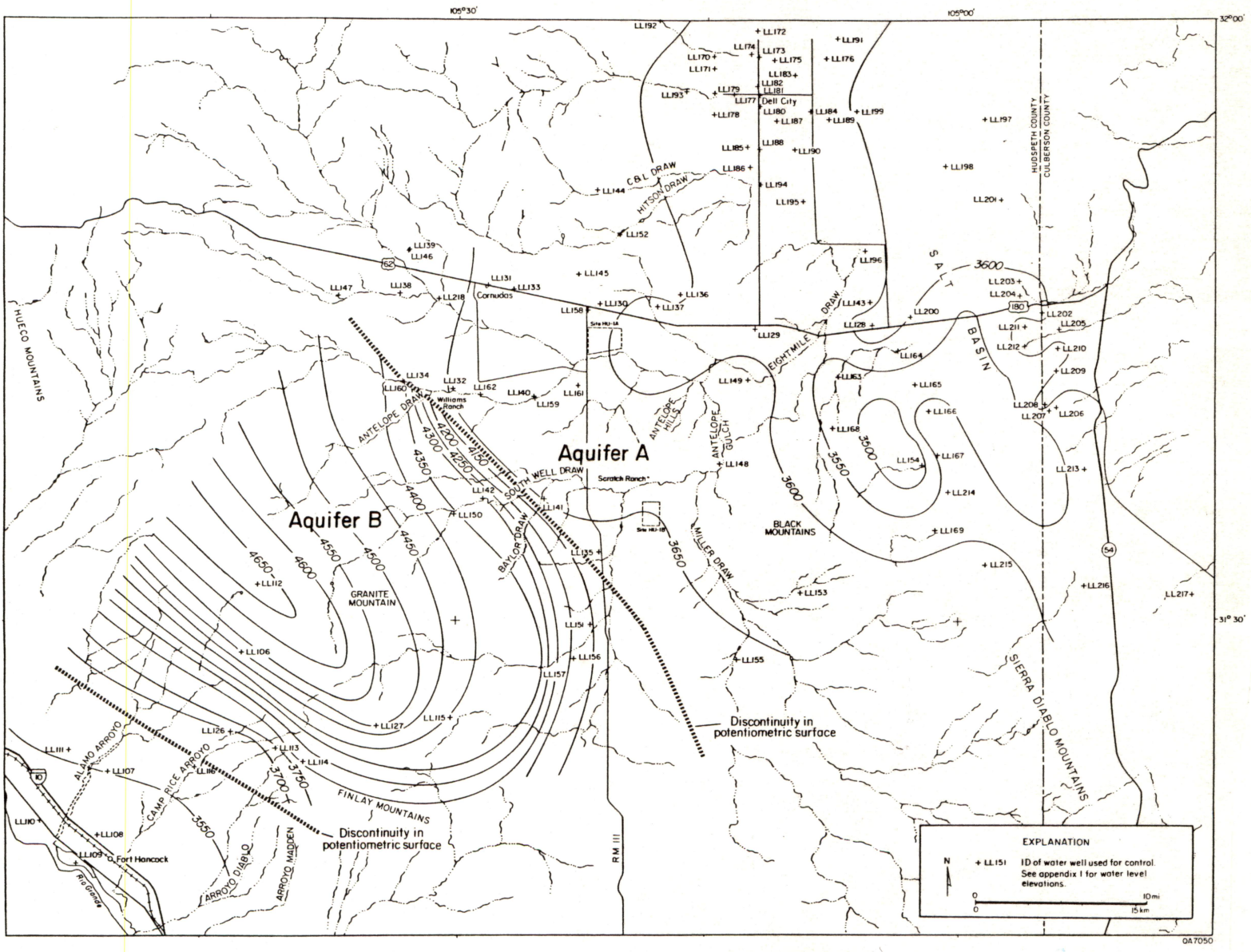

Figure 7. Potentiometric surface map, Aquifers A and B. Ground-water flows predominantly to the northeast. A ground-water divide is located north of the Diablo Plateau scarp. The abrupt change of the potentiometric surface together with the difference in gradients and depth to water suggests the presence of two separate aquifers: The primary deep aquifer, Aquifer A, and a shallower aquifer, Aquifer B.

Fractures in the carbonate rock may be enhanced by solution from the flow of fresh ground water through initial primary and secondary porosity. The presence of recent sinkholes 12 ft (3.6 m) deep and 12 ft (3.6 m) in diameter (Young, 1976) is evidence of active solution in the Dell City area. Well drillers in the area also report the regular occurrence of lost circulation zones indicative of large openings or caverns (Scalapino, 1950). Although the extent of fractures has not been clearly defined, inferences may be drawn from the low hydraulic gradients recorded for Aquifer A and from field observations.

A pump test was conducted on the Williams' Ranch using one producing well (LL162) and two observation wells (LL219 and LL220). Data collected from this test are included in appendix 3. Values of transmissivity calculated by the methods of Walton, Jacob, and Theis for both semiconfined leaky aquifer and confined nonleaky aquifer conditions range from 64 gpd/ft to 252 gpd/ft. The mean transmissivity calculated from all methods utilized during interpretation is 129 gpd/ft (17 ft^2/d or 6 m^2/d). At present, this is the only known pumping test for the study region outside of the Dell City area. In the Dell City area specific capacity data range from 5 to 64 gpm/ft (93 to 1,141 m^2/d) of drawdown (Peckham, 1963).

Potentiometric Surface

The potentiometric surface (fig. 7) on the Diablo Plateau shows that regional ground water flows predominantly to the northeast. A ground-water divide is located just to the north of the Diablo Plateau scarp. No divide is evident in the region of the Babb flexure. Recharge from either site HU1A or HU1B would flow in the general direction of the Dell City irrigation region and toward the salt flats.

Two separate aquifers may exist. Aquifer A is located in the northeast section of the study area and includes the Dell City irrigation and salt flat areas (fig. 7). Elevations of the water table range from 3,445 ft (1,050 m) in the Dell City and salt flat regions in LL154 to 3,650 ft (1,112 m) for wells LL141 and LL218. Depth to water varies from 3 ft (1 m) on the salt flats to more than 700 ft (213 m) in areas of higher land elevations (fig. 6). Land surface elevation changes from ≃ 3,450 ft (1,051 m) at the salt flats to more than 4,500 ft (1,372 m) in higher regions of the Diablo Plateau, but the elevation of the water table only rises 200 ft (61 m) across the same region. This explains why the depth to water increases significantly at higher elevations. The maximum hydraulic gradient measured between LL218 and LL154 is 6.9 ft/mi (1.3 m/km). A more typical gradient for the area, however, is 2.5 ft to 5 ft/mi (0.5 to 0.9 m/km) as measured between several wells.

Southwest of Aquifer A is a local aquifer (referred to as Aquifer B) with water-table elevations that are significantly higher than in Aquifer A (fig. 7). Aquifer B is bounded on the southwest by the escarpment of the Diablo Plateau. Water elevations for this area range from 4,397 ft (1,340 m) in LL160 to 4,176 ft (1,272 m) in LL151. The depth to ground water at Aquifer B is significantly less than that observed at Aquifer A; depth of water ranges from 18 to 210 ft (5 to 64 m), and the water depth for most wells is less than 100 ft (30 m). Ground water flows predominantly to the northeast. Limited flow is southwestward toward the Rio Grande valley. The hydraulic gradients measured for Aquifer B are higher than those of the regional Aquifer A, values being as high as 90 ft/mi (17 m/km) between wells LL156 and LL157.

The two different potentiometric surfaces in Aquifer A and Aquifer B suggest two permeable zones beneath the Diablo Plateau. Aquifer B represents a perched

aquifer; Aquifer A is predicted to lie beneath Aquifer B in the southwestern part of the study area. In the north-northeastern part of the study area there are three examples of Aquifer B overlying Aquifer A: (1) The water elevation of well LL161, a geothermal test well drilled on the flanks of one of Pump Station Hills, is 4,150 ft (1,265 m), which is similar to water-table elevation of the shallow aquifer. This well was not used in potentiometric mapping of Aquifer A because of its apparently anomalous nature. (2) Wells LL160 and LL134 are located 100 ft (30 m) apart from each other on the Williams' Ranch at Hobo Tank, west of HU1A, and have significantly different water levels. LL160, a shallow windmill located in the bottom of an arroyo, has a depth to water of 18 ft (5.4 m), whereas the water depth in LL134, a deep pumpjack in the same area, was greater than 750 ft (229 m) (as reported by the owner). (3) The driller's logs for the abandoned El Paso Natural Gas Company Pump Station #2 well, which was used as an observation well for the pumping test (appendix 3), indicate that three water-bearing zones were encountered during drilling. During this study, water was always observed on the electric-line probe at depths of less than 200 ft (60.9 m), although static water level was recorded at 673 ft (205.1 m). In addition, water could be heard cascading down the borehole. (There was no casing below 100 ft (30.5 m) depth.)

The difference in water levels, the difference in gradients, and the abrupt change in water levels that exist between the deep water table (Aquifer A) and the shallow water table (Aquifer B) found in the southwestern part of the study area suggest a change in hydrologic properties between the two regions. Aquifer A may be more fractured because of its location over or proximate to the Babb flexure. Fractures would permit greater leakage through possible aquitards between Aquifer A and Aquifer B and drain any ground water in overlying permeable zones. Greater fracture permeability would also permit a lower hydraulic gradient for Aquifer A than

for Aquifer B. The Jacob plot for the aquifer test of Aquifer A at the Williams' Ranch shows a segmented drawdown curve with time, which indicates drawdown in a fractured medium (appendix 3). In this plot the first straight-line segment (a) represents drawdown in the fracture(s) penetrated by the well. These fractures have a transmissivity of 111 gpd/ft (1.38 m^2/d). A barrier was hit at 40 minutes. The cone of depression hit another set of fractures at $\simeq$ 80 minutes. Transmissivity measured at the second set of fractures is 84 gpd/ft (1.05 m^2/d); a higher transmissivity (158.6 gpd/ft; 1.97 m^2/d) representing a third set was intersected at 900 minutes. The different transmissivities measured with increased time do not represent transmissivity values specific to each fracture set but do represent the cumulative value for the area affected by the cone of depression. The increased transmissivity evident at the end of the test may only indicate that more fractures are being intersected by the cone of depression, not that the fractures are more permeable. There was no drawdown in either of the observation wells, further indicating fracture control of ground-water flow and distribution. The abrupt change in water-table elevations between Aquifer A and Aquifer B may be due to a structural feature that functions as a hydrologic barrier between the two regions.

Recharge

Recharge for the general study area is by infiltration of stream runoff and recirculation of irrigation water (primarily in the Dell City area). Flash flooding in arroyos probably is the major source of recharge. Most shallow wells that catch this recharge in Aquifer B are located in arroyos. Peckham (1963) reported recharge occurring to the west in the Dell City, Texas area, and to the north in New Mexico.

Principal recharge has been attributed to the Sacramento River drainage basin (Young, 1976). The unsaturated section in the Dell City area consists of 5 to 150 ft (1.5 to 45 m) of alluvial cover. Peckham (1963) and Young (1976) also noted that, to a lesser extent, recharge may occur by precipitation on the land surface, but apparently most of this precipitation evaporates (Boyd and Kreitler, in press). Recharge through the alluvium in the interarroyo areas is expected to be minor. Vegetation changes observed during field work may also influence or indicate active surface recharge. Preliminary studies dealing with climate and vegetation are presented in appendix 8.

Discharge

The potentiometric map of Aquifer A (fig. 7) indicates that ground water flows toward the salt flats. Peckham (1963) and Young (1976) also reported that ground-water flow is in the direction of the salt flats. Discharge occurs naturally by evaporation in geographically extensive areas where depths to water may be as shallow as 3 ft (0.9 m) in the salt flats. Boyd and Kreitler (in press) and Chapman (1984) consider the salt flats to be the major discharge zone for the area. The potentiometric map of the study region confirms this hypothesis.

Water levels measured in 1961 had dropped an average of 18.5 ft (5.6 m) since irrigation became prominent in the area around 1948. This decline of the potentiometric surface in the Dell City area has caused the wells in the Dell City area to be discharge points for the northern part of Aquifer A. It is uncertain whether flow from site HU1A would be toward Dell City. Flow from HU1B is expected to ultimately discharge at the salt flats. Young (1976) reports that water levels in this area have declined an average of 1.5 to 1.7 ft (0.45 to 0.51 m) per

year from 1948 to 1968. During the same period of record, water salinity at Dell City tripled because of return flow from irrigation that leached salts from the soil. Production yields from these wells range from 160 to 2,240 gpm (875 to 12,250 m^3/d) (Peckham, 1963). In 1960, about 200 wells pumped 100,000 acre-ft (123×10^6 m^3) of water from the aquifer.

Discharge of this system has also occurred through naturally flowing springs. Crow Springs, located east-northeast of Dell City, was an important water oasis until the 1950's when an irrigation well was drilled adjacent to the spring. Flow of the spring terminated overnight (Brune, 1981). Other springs in the area that dried up due to pumpage are Washburn and Persimmon Springs north of Cornudas, Cove Spring on the south side of the Paint Waterhole Mountains, Shot Springs in the Antelope or Red Hills, Sulphur Springs on the east side of salt flat, Cottonwood Springs southeast of salt flat, and Aparejo or Harness Springs on the south side of Black Mountain (Brune, 1981).

No exterior drainage from Aquifer A was recorded during this study. Nielson and Sharp (1985) offer the possibility, however, that intrabasinal flow to the east may occur in the southern portion of the Salt Basin.

Ground-water Geochemistry

Chemical and isotopic analyses of ground-water samples from Hudspeth County collected during this study are presented in appendix 5. Additional chemical and isotopic analyses used during the evaluation of the southern site in Hudspeth County (Kreitler and others, 1986) and chemical analyses from the Texas Water Development Board (1985) are presented in appendix 6.

Ground water in the study area is fresh to brackish; total dissolved solids (TDS) range from 715 to 3,803 mg/L. Generally, there is no consistent pattern in TDS distribution (fig. 8); however, occurrence of relatively fresh water is restricted to Aquifer B and its vicinity, where elevation of the water table is higher and the unsaturated section is thinner (figs. 6 through 8). Elevated values of TDS are a result of increasing concentrations of Na and SO_4 and, to a lesser extent, increasing concentrations of Ca and Cl (figs. 8 and 9).

Water facies vary from mainly Ca-Na-HCO_3 and Na-SO_4 types in the west (Aquifers A and B) to Na-SO_4, Ca-SO_4, and Na-Cl facies in the east (Aquifer A) (figs. 10 through 12). The shift in facies may be the result of the changing lithology from Cretaceous limestone interbedded with marl and clay to Permian limestone that may include Ca, SO_4, and Cl-rich evaporites. Typically, high sulfate waters change chemically from Ca-SO_4 waters to Na-SO_4 waters as they flow because of cation exchange of Na for Ca. Waters in the study area, however, appear to change in the opposite direction, from Na to Ca facies, as they flow toward the salt flats, and this direction for chemical change is considered anomalous.

Aquifer B typically contains higher NO_3 concentrations (three wells had NO_3 concentrations of 100 mg/L or greater) than Aquifer A (fig. 13). The shallower depth to ground water permits more rapid recharge. The source of the nitrate may be anthropogenic (stock water tanks, barnyards, corrals, septic tanks). High nitrate in wells typically relates to an animal waste or cultivation source. All high-NO_3 wells in Aquifer B were proximal to contaminant sources, and fracture permeability would facilitate rapid recharge of animal wastes. Some of the wells with high NO_3, however, contain no tritium, which suggests that animal waste is not the source. At present the source of nitrates in these wells cannot be determined. High nitrates

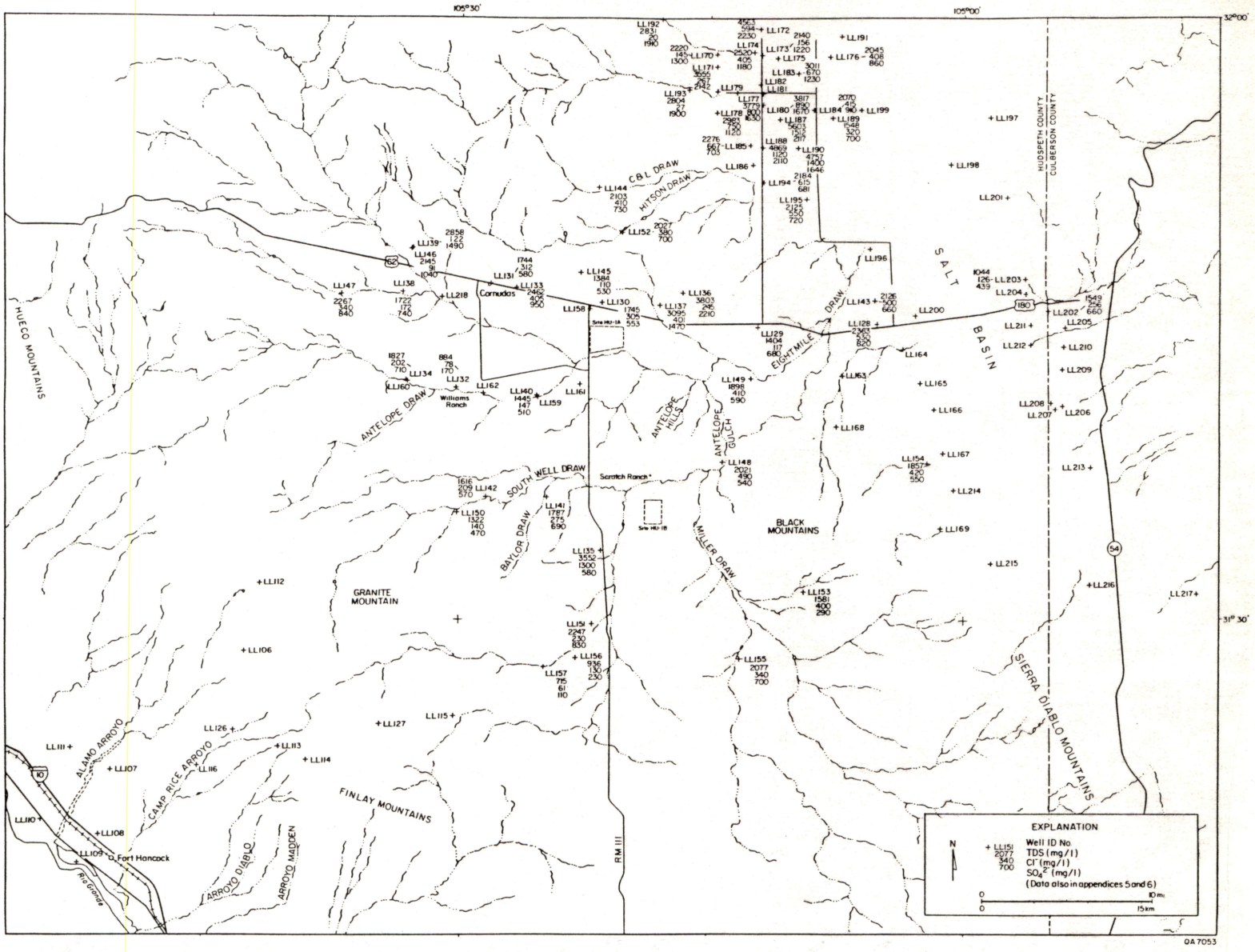

Figure 8. Map of TDS, Cl, and SO_4 (mg/L) distribution. Ground water in the study area is fresh to brackish, TDS ranging from 715 to 3,803 mg/L. Generally, there is no consistent pattern in TDS distribution; however, occurrence of relatively fresh water is restricted to Aquifer B and its vicinity. Elevated values of TDS are a result of increasing Na and SO_4 concentrations and, to a lesser extent, increasing concentrations of Ca and Cl.

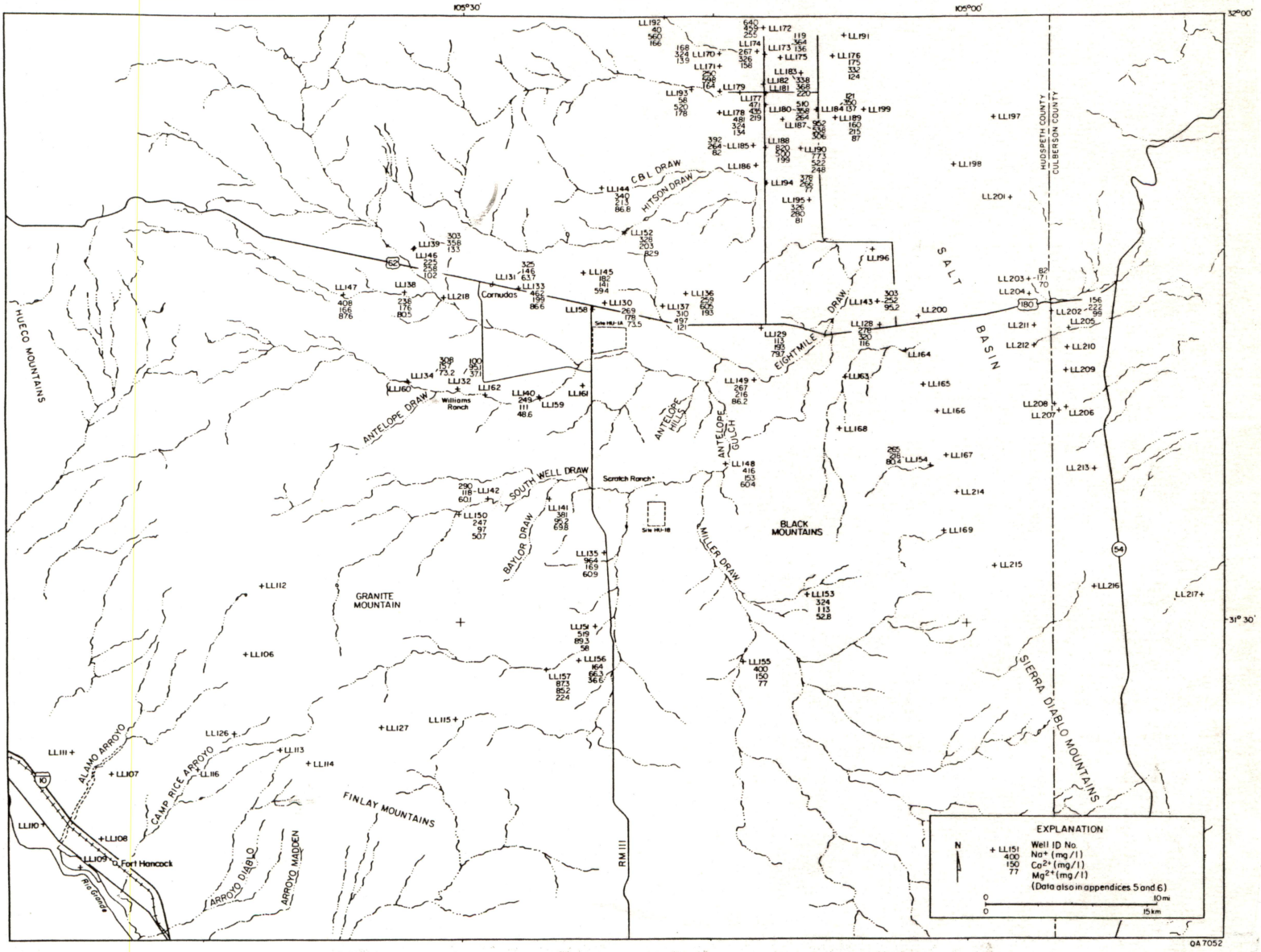

Figure 9. Map of Na, Ca, and Mg (mg/L) distribution.

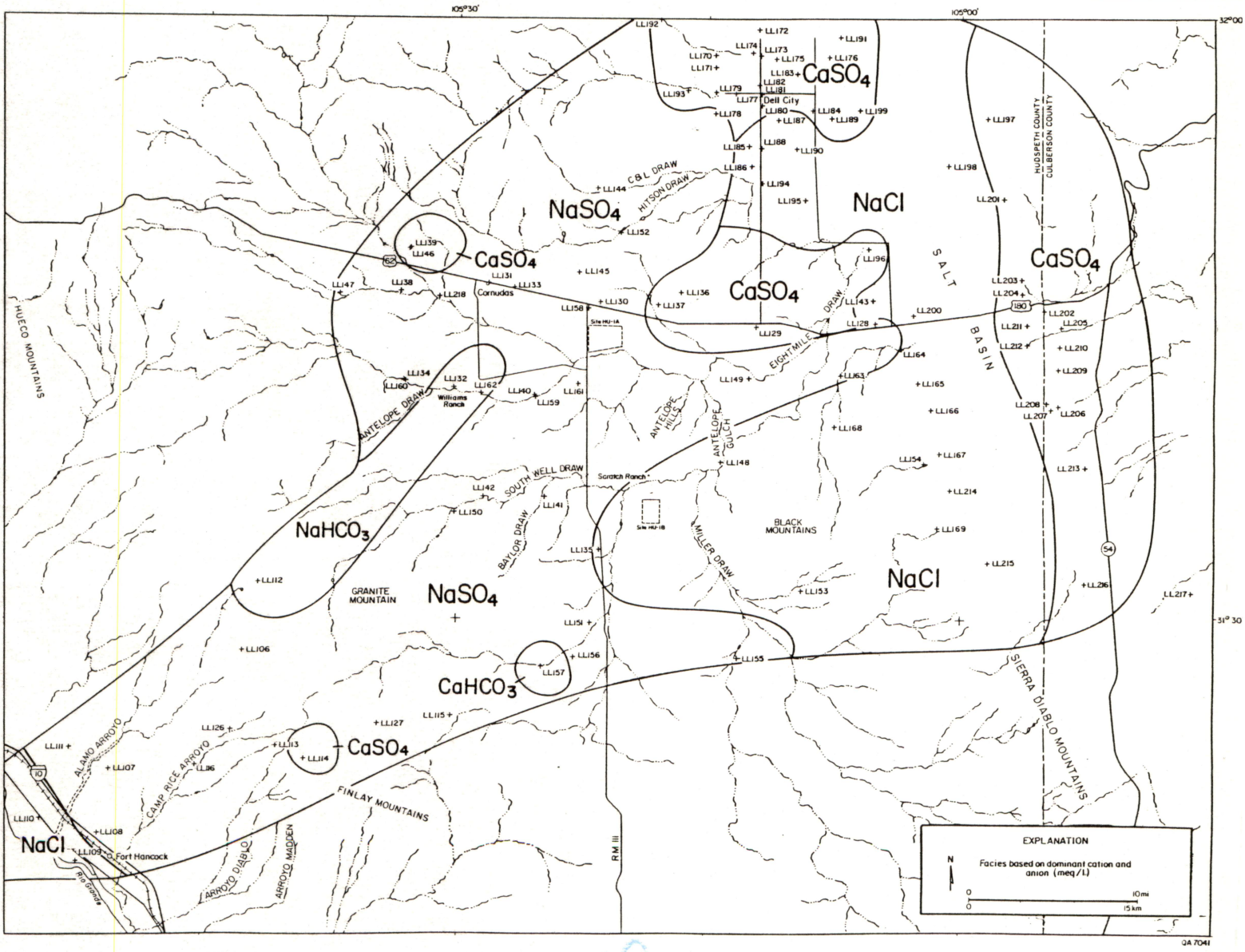

Figure 10. Chemical facies map, Aquifers A and B. Water chemical facies vary from mainly Ca-Na-HCO_3 and Na-SO_4 in the southwest (Aquifers A and B) to Na-SO_4, Ca-SO_4, and Na-Cl facies in the northeast. This shift in facies may be the result of the changing lithology from Cretaceous limestone interbedded with marl and clay to Permian limestone that may include Ca, SO_4, and Cl-rich evaporites.

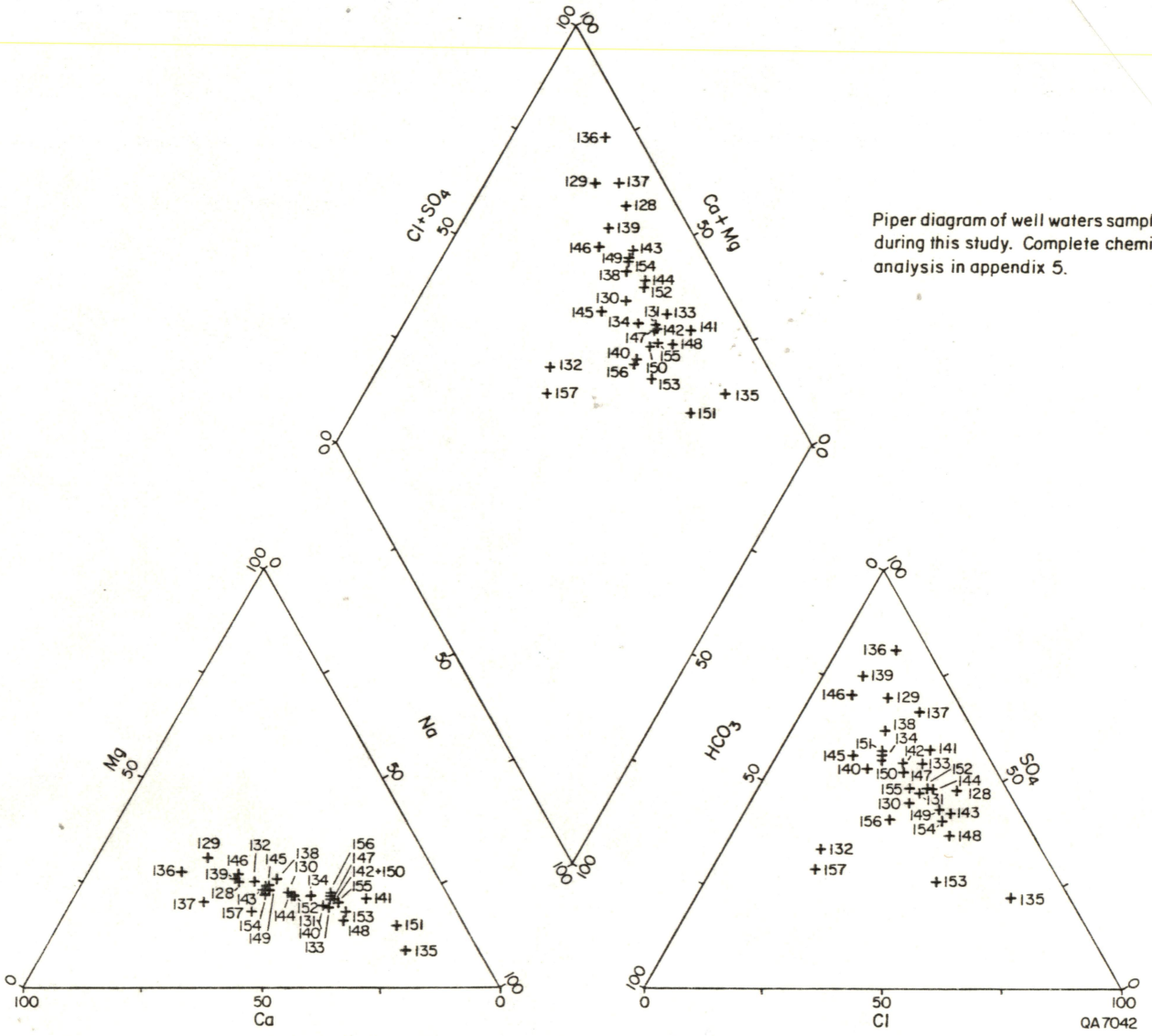

Piper diagram of well waters sampled during this study. Complete chemical analysis in appendix 5.

Figure 11. Piper diagram, Aquifers A and B.

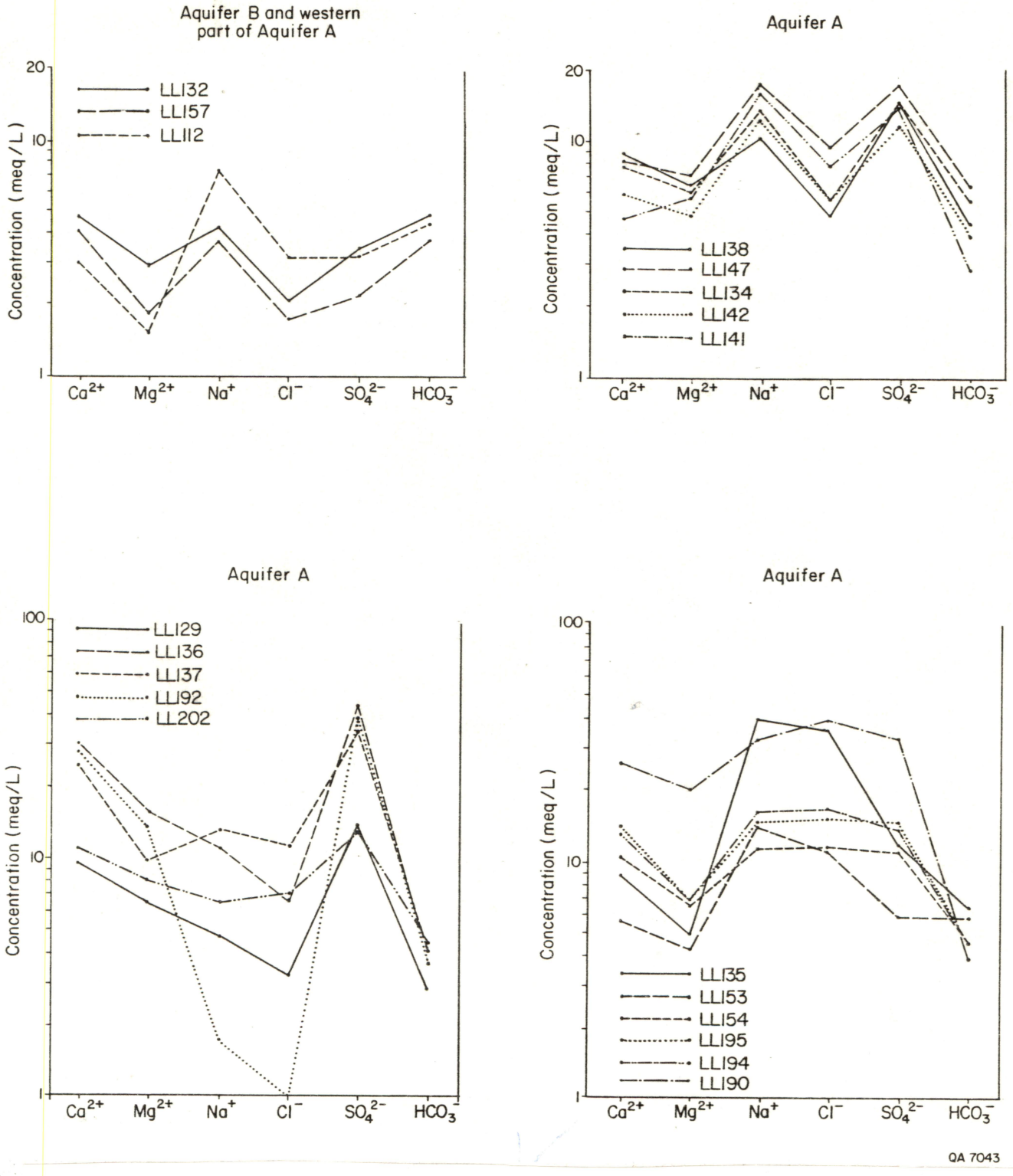

Figure 12. Salinity diagrams, Aquifers A and B, at different regions within the study area.

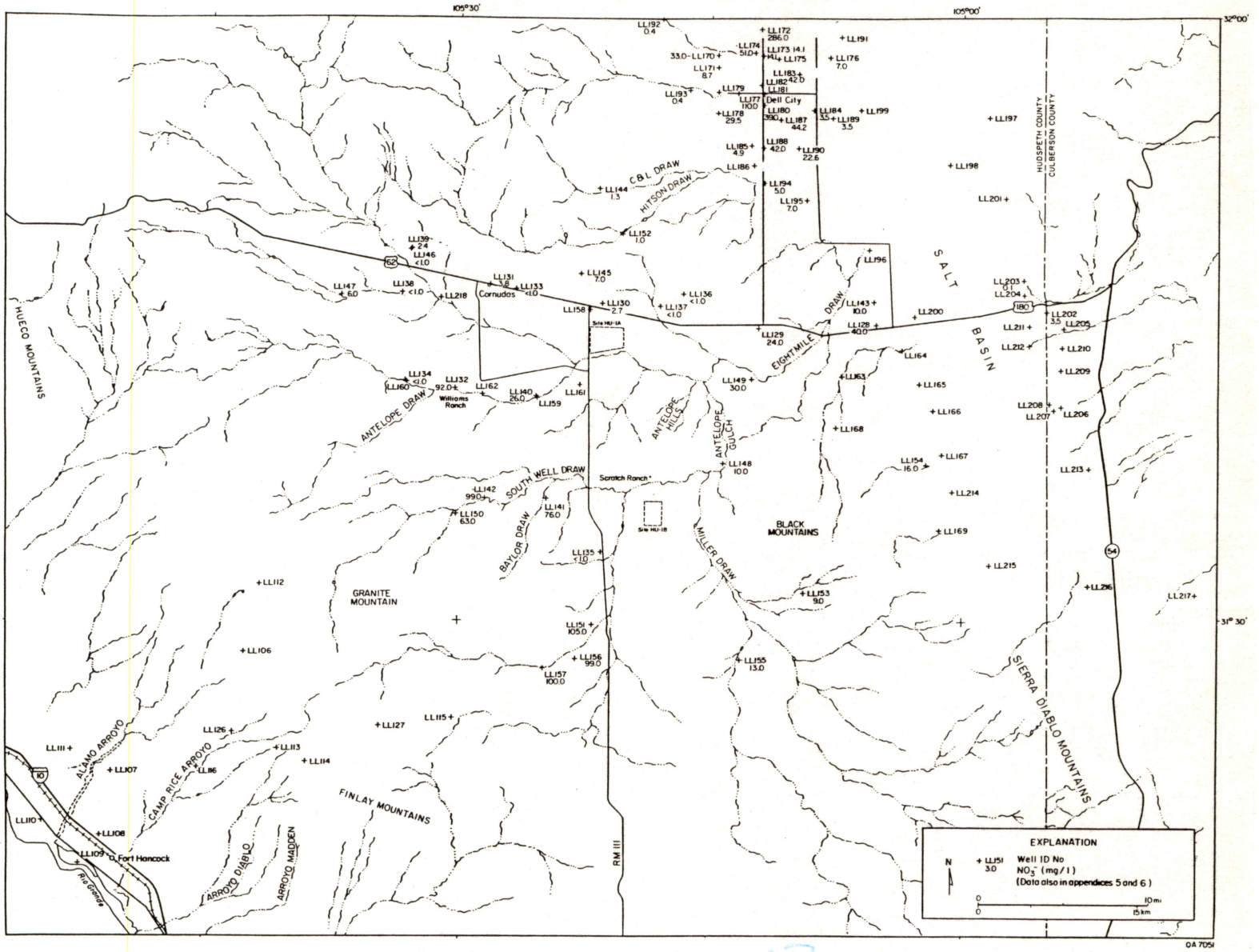

Figure 13. Map of NO_3 distribution. Higher NO_3 concentrations (mg/L) exist in Aquifer B than in Aquifer A. Shallower depth to ground water in Aquifer B permits more rapid recharge. The source of nitrates may be anthropogenic, and contaminant can rapidly reach water table through fracture permeability. Some of the wells with high NO_3, however, contain no tritium, suggesting other sources of NO_3.

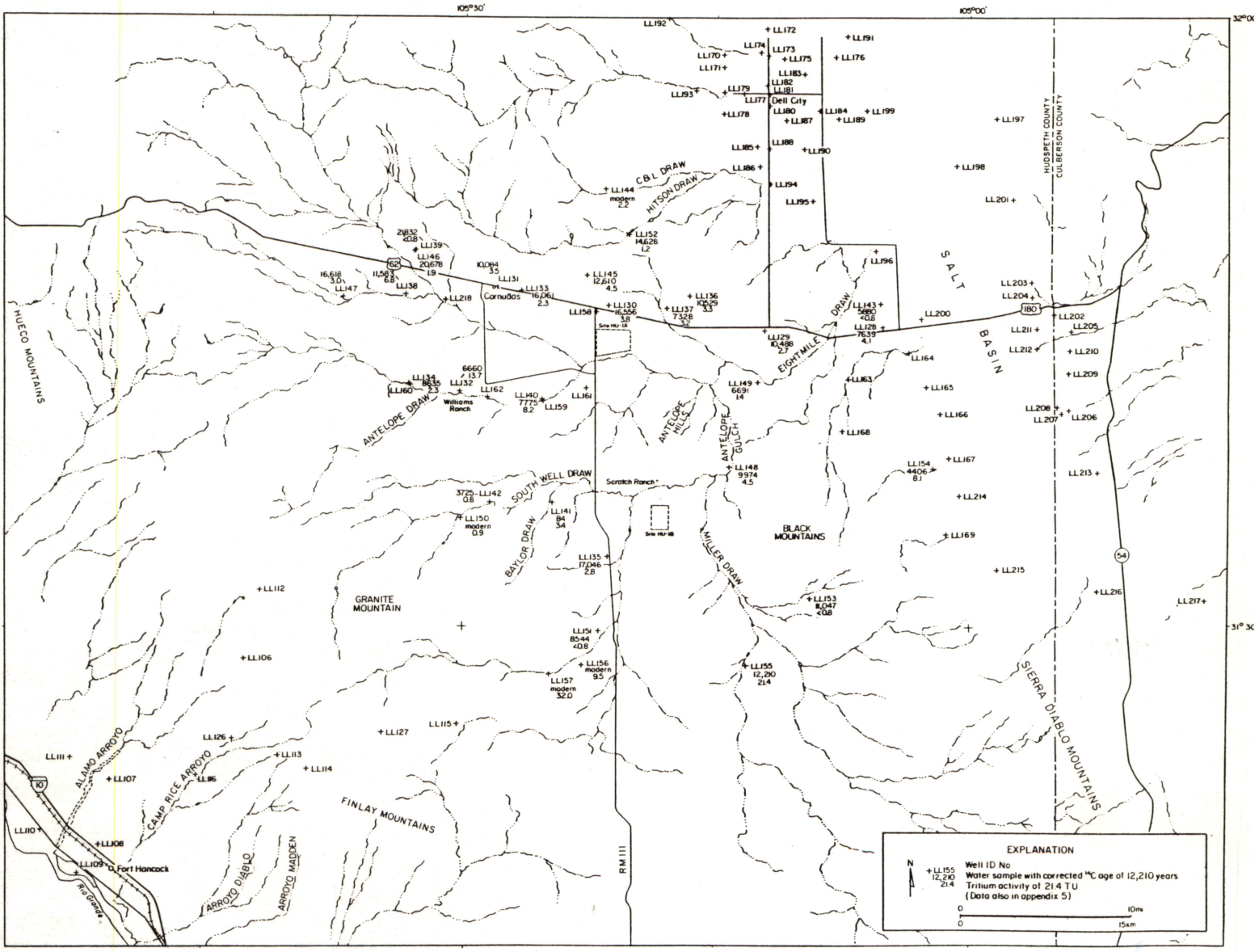

Figure 14. Map of ^{14}C and tritium distribution. Tritium activity data range from 0 to 32 TU and, except for four ground-water samples, all samples had varying amounts of tritium, indicating active recharge into both Aquifer A and Aquifer B. Ground-water ages determined by ^{14}C ranged from recently recharged modern water to 22,831-yr-old water. Presence of tritium in water with old ^{14}C corrected age may indicate mixing of very young water with older waters, or it may indicate that the calculated ^{14}C ages are erroneous. Tritium and ^{14}C activities vary significantly within short distances and do not show a clear distribution pattern, suggesting the importance of fracture flow.

have been observed in other arid regions where they could not be related to anthropogenic sources.

Tritium activity data ranged from 0 to 32 TU and, except for four ground-water samples, all samples had varying amounts of tritium, indicating active recharge into both Aquifer A and Aquifer B (fig. 14). Ground-water ages determined by ^{14}C ranged from recently recharged modern water to 22,831-yr-old water (fig. 14). Tritium and ^{14}C activities vary significantly within short distances and do not show a clear distribution pattern. However, the youngest ^{14}C values and highest tritium values occur in the southwestern part of the study area in Aquifers A and B. The oldest water (> 20,000 yr old) can be found in the northern area of Aquifer A (fig. 14). The variable distribution of tritium (and variable chemical composition) across the study area strongly suggests the importance of fracture flow. The presence of tritium in ground water throughout the entire region and even where the water table is greater than 700 ft (213 m) below land surface indicates that rapid recharge occurs along fractures in all regions of the study area and is not restricted to Aquifer B or to hydrologically updip areas in Aquifer A.

The ^{14}C ages are considered rough approximations. The presence of tritium in the waters indicates recharge that occurred post-1950. Some waters with high tritium concentrations have a low percent modern carbon (PMC) and old corrected ages (e.g., LL155). This disparate situation may indicate mixing of very young waters with older waters or it may indicate that the calculated ^{14}C ages are erroneous. The $\delta^{13}C$ values of the bicarbonate are in a range of -10 to -3°/oo, heavier than those observed in most aquifers and significantly heavier than those of recently recharged ground waters. This suggests complex chemical reactions controlling the carbonate geochemistry and possibly altering the PMC values and the $\delta^{13}C$ values, both of which are necessary for calculating ^{14}C age.

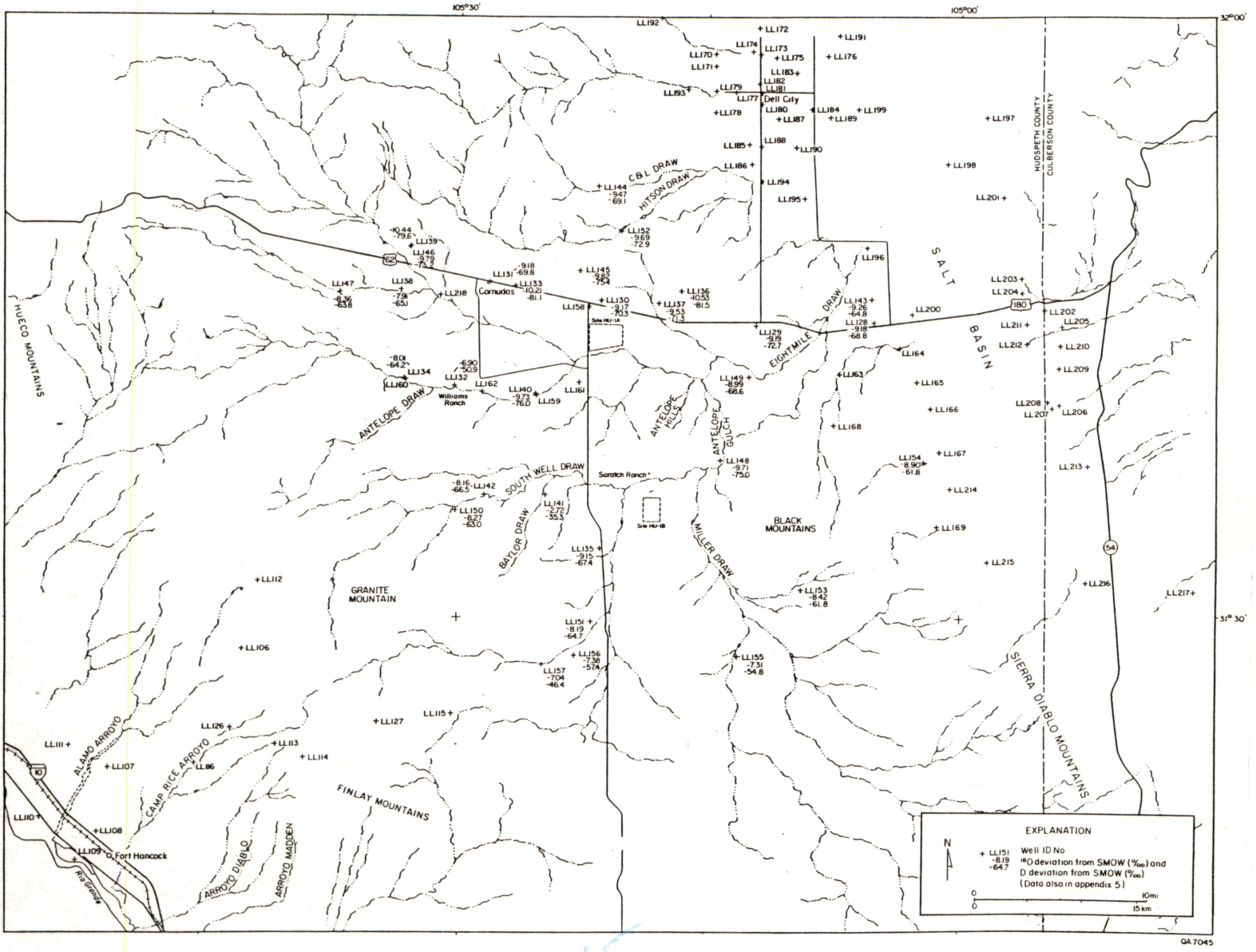

Figure 15. Map of $\delta^{18}O$ and δD distribution. Ground-water samples vary in $\delta^{18}O$ values from -6.90 to -10.53 °/oo, and δD values vary from -46.4 to -81.5 °/oo (with the exception of well LL141). Enriched values, which resemble current annual mean rainfall values in Midland, are encountered at the west and southwest parts of the study area (in both Aquifer A and Aquifer B), where ground-water salinities are relatively low tritium activities are high and the age of the water is young. The most depleted values of δ^{18} and δD occur in the north, where water has the oldest ^{14}C dates and lacks tritium.

Ground-water samples vary in $\delta^{18}O$ values from -6.90 to -10.53°/oo, and δD values vary from -46.4 to 81.5°/oo (with the exception of one sample [LL141] which had relatively enriched values of -2.72 and 35.3°/oo, respectively) (fig. 15). Heavier values (-6.90 to -8.27°/oo for $\delta^{18}O$, and -46.4 to -64.2°/oo for δD) are encountered at the western and southwestern parts of Aquifers A and B, where ground-water salinities are relatively low (fig. 8), and the age of water (determined by ^{14}C and tritium) is young (fig. 14). Annual weighted means of $\delta^{18}O$ and δD in rainfall sampled in Midland are -6.9 and -45°/oo, respectively (Nativ and Riggio, in preparation), similar to the values encountered in ground water in these parts of the study area. Based on these observations, it is suggested that the ground water of these areas represents the recharge end-member of the hydrologic system.

The most depleted values of $\delta^{18}O$ and δD occur in the northern part of Aquifer A where water has the oldest ^{14}C dates and lacks tritium (fig. 14). Similarly depleted values of $\delta^{18}O$ and δD were observed in Gunsight well (LL115) during the previous study at the southern Hudspeth County site (Kreitler and others, 1986). Depleted values of stable isotopes in ground water can result from several mechanisms (Dansgaard, 1964). Cool, humid climatic conditions during recharge or an elevated recharge source are the more probable mechanisms relevant to this area. Occurrence of these exceptionally depleted values can be explained either by a cooler or more humid climate that may have prevailed in the area 20,000 years ago, when the water recharged the aquifer (based on the ^{14}C age of these ground-water samples), or by an elevated source of recharge to this area, other than the Diablo Plateau.

In the study area $\delta^{18}O$ and δD values of ground water generally plot parallel to and below the meteoric water line (Craig, 1961) (fig. 16). Ground-water samples collected from the southern Hudspeth County and Culberson County sites (Kreitler

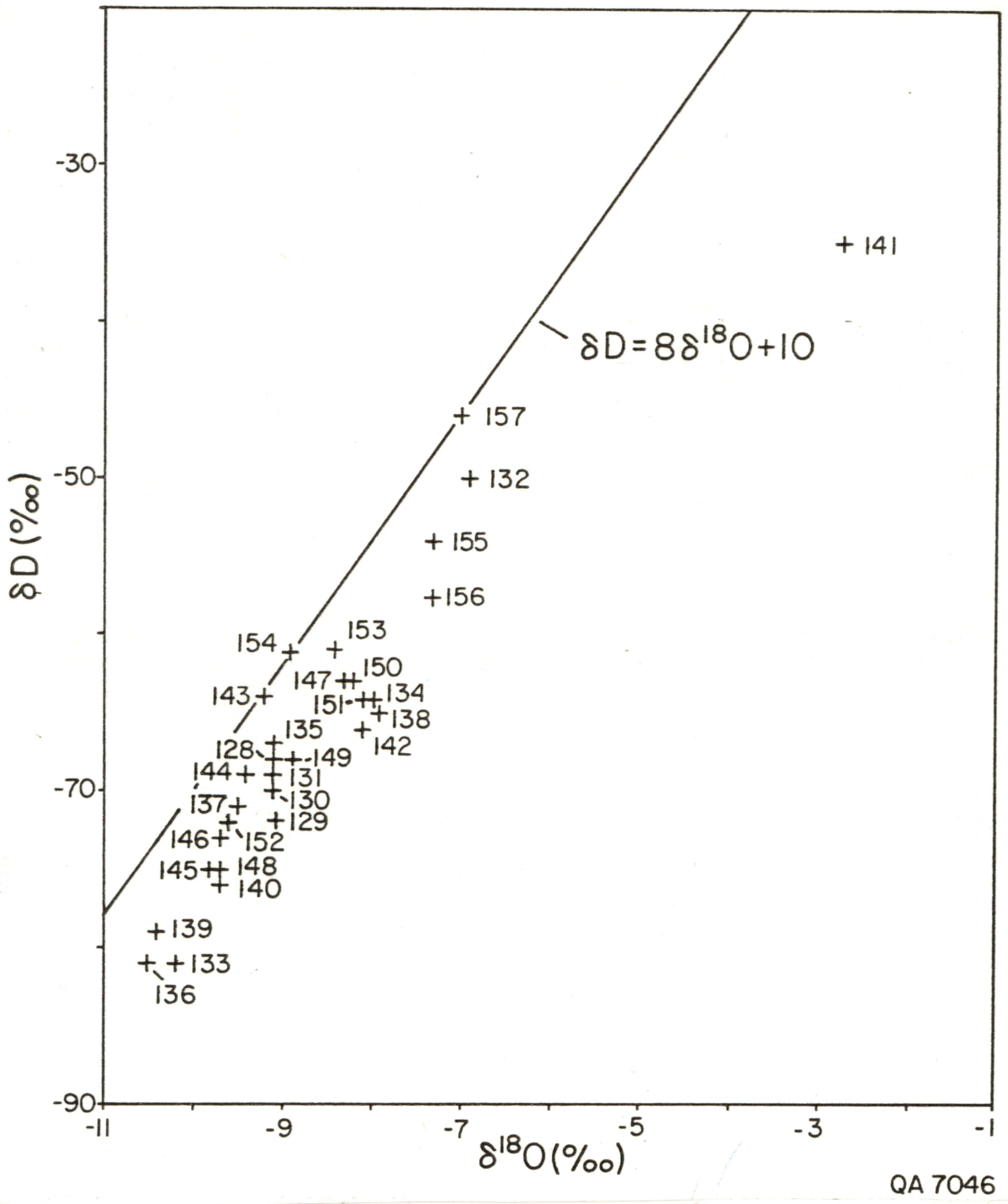

Figure 16. Plot of $\delta^{18}O$ versus δD. Values of $\delta^{18}O$ and δD in ground-water in the study area generally plot parallel to and below the meteoric water line (Craig, 1961), similar to ground-water in the southern Hudspeth County and Culberson County sites (Kreitler and others, 1986). These data may reflect a local version of the meteoric water line, high temperatures and evaporation rates prevailing in the study area.

and others, 1986, their figs. 21 and 36) had similar plots. These data may reflect a local version of the meteoric line. Stable isotope data on ground water from Roswell basin, eastern New Mexico (Hoy and Gross, 1982), indicate a shift of the local line to fit the line equation $\delta D = 7.27\delta^{18}O + 5.36$, rather than Craig's equation (1961) $\delta D = 8\delta^{18}O + 10$. Hoy and Gross (1982) related this shift to the higher temperatures and increased evaporation rates that prevail in eastern New Mexico. However, isotope data from the Ogallala, Dockum, and Cretaceous aquifers of the Texas Panhandle (Nativ and Smith, 1985), where climatic conditions are similar, plot along the meteoric line, rather than below it.

Values of $\delta^{34}S$ range from -1.24 to +16.11°/oo, (fig. 17); two-thirds of the samples have values above +6°/oo. Heavier values (9.28 to 16.11°/oo) were encountered in the north and northeast of Aquifer A toward the discharge zone (fig. 7) and suggest that the dissolved SO_4 in ground water in this area is from dissolution of anhydrite in the host rock. These $\delta^{34}S$ values of dissolved sulfate are typical of Permian sulfate minerals (10 to 15°/oo) (Hoefs, 1973; Claypool and others, 1980). The $\delta^{34}S$ of the ground water SO_4 from Block 46 and S-15 (Culberson County) occupies a narrow range of +9 to +11°/oo and indicates simple Permian evaporite dissolution. In other parts of the study area, values are less enriched, possibly because of shorter reaction time with the host rock, or in the case of Aquifer B because of different $\delta^{34}S$ values of sulfate minerals in the Cretaceous host rock or a mixing of sulfates from Cretaceous and Permian rocks. The most depleted $\delta^{34}S$ values are found in the northern part of Aquifer A, where ground water has other unique features regarding ^{14}C, tritium, $\delta^{18}O$, and δD values.

Values of $\delta^{13}C$ range from -10.35 to -3.64°/oo (fig. 17). These values are heavier than those encountered in the southern Hudspeth County site (Kreitler and others, 1986). Most marine carbonate rocks have $\delta^{13}C = 0$°/oo, whereas common

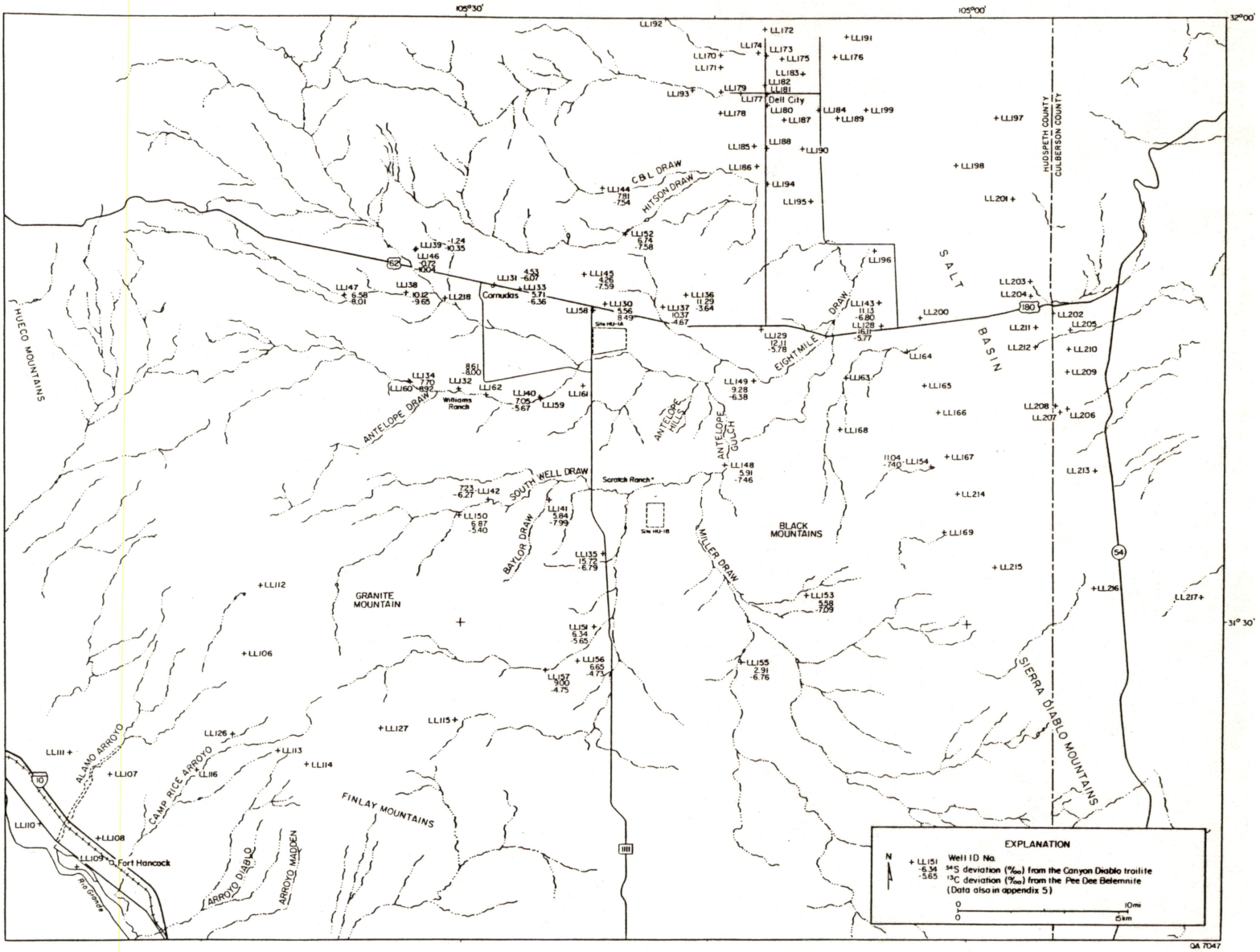

Figure 17. Map of $\delta^{34}S$ and $\delta^{13}C$ distribution. Values of $\delta^{34}S$ range from -1.24 to $+16.11^{o}$/oo; two-thirds of the samples have values above $+6^{o}$/oo. Values of $\delta^{13}C$ range from -10.35 to -3.64^{o}/oo and are heavier than those in the southern Hudspeth County site (Kreitler and others, 1986). Old ground water in the north has the most depleted $\delta^{13}C$ values, whereas young water in the south and southwest has enriched values.

values for organic material and CO_2 in soil are -25 to -20°/oo. The concentration of $\delta^{13}C$ in ground water is determined by the input with recharge water and by reaction with the rock. However, the assumption that the enriched values found in ground water in the study area can be related to longer interaction time with the host rocks is not supported by the distribution of $\delta^{13}C$ values. Old ground water in the northern part of Aquifer A has the most depleted $\delta^{13}C$ values, whereas young water with elevated tritium values in Aquifer B has enriched values. Therefore, a different mechanism controls the range and distribution of $\delta^{13}C$ in this area.

CONCLUSIONS

The host rocks at HU1A and HU1B are Precambrian rhyolite porphyry and Cretaceous limestone interbedded with some silty and muddy interbeds, respectively. The rhyolite porphyry is fractured. The fractures strike in many directions, dip from vertical to horizontal, and have limonite and hematite stains on the fracture surfaces. Most fractures contain no mineral fillings, indicating that they are not sealed. Cretaceous limestone at HU1B is not as fractured as the rhyolite porphyry at HU1A.

The Babb flexure is north of both sites; however, fractures away from the inferred margins of this regional structure may be related to deformation of the flexure. The flexure may be the Permian or post-Permian expression of a major pre-Permian strike-slip fault (Hodges, 1975). It is unknown if Cretaceous rocks have been warped by recurrent movement along the structure.

Flooding down Antelope Draw at HU1A may be very intense for short durations and should be considered during site selection.

Regional ground-water flow is from southwest to northeast. The ground-water divide is located close to the Diablo Plateau, the escarpment that defines the northern edge of the Rio Grande basin, not along the Babb flexure. In the study area, two aquifers are present, a shallow aquifer in the southwestern area with depths to water generally less than 200 ft (60 m) and a deeper aquifer through most of the region, with depths to water up to 700 ft (213 m).

Recharge occurs over the entire study area and is not restricted to the updip part of the potentiometric surface in the areas of higher elevation. Tritium is found in nearly all wells regardless of their location on the regional water table, indicating rapid recharge throughout the area. Most recharge probably occurs during flooding of the arroyos that drain the plateau. Minimal recharge is expected through the interarroyo areas. Fractures are probably important pathways for recharge. Recharge along fractures is the best mechanism to move recent recharge water rapidly through a thick unsaturated section.

Ground-water flow appears to be fracture controlled. Three separate fracture sets were identified during a pumping test. Because of the fracture control on ground-water flow, flow velocities cannot be estimated but are expected to be high. The pumping test measured low transmissivities (64 to 252 gpd/ft); these numbers should, however, be used with caution because the calculations are based on assumptions of porous media flow and not fracture flow and represent only one pumping test. The fractures may cause a very anisotropic system, and flow may not be directly down the potentiometric gradient. Discharge is either by evaporation on the salt flats or through pumping wells.

Total dissolved solids content ranges from 715 to 3,803 mg/L. The dominant water types are Na-SO_4 and $CaSO_4$. Many of the waters have high NO_3

concentrations, which suggests recent recharge and possible contamination by animal wastes. The chemical composition of the waters appears to be randomly distributed; there is no coherent chemical evolution of the water as it flows down the potentiometric gradient. This may be due to control of flow by fracture pathways and by local recharge across the entire Diablo Plateau.

The shallower aquifer may or may not be present at either site, although it is not used in the immediate vicinity of either site. Depth to ground water in the deeper aquifer beneath the sites is probably greater than 600 ft (180 m). Fractures are probably important pathways for recharge over the entire study area.

RECOMMENDATIONS FOR FUTURE STUDIES

Additional studies need to be conducted to accurately characterize the hydrology and geology of sites HU1A and HU1B. These studies concern surface runoff, permeability distribution, and recharge through interarroyo areas.

1. Heavy rains fell during the summer of 1986, which caused flooding of the arroyos and salt flat area. The extent of flooding within arroyos in the sites needs to be investigated by looking for flood sediment distribution to determine whether the sites were flooded or not, and to determine whether flooded areas conform to those mapped on the Flood Insurance Rate maps (figs. 4 and 5).

2. Recharge to Aquifer A is suspected to be occurring through the arroyos and not through the alluvium in the interarroyo areas. Recharge studies at a site need to be conducted to ensure that the interarroyo areas are not active recharge sites. A recommended approach at this reconnaissance level is to measure chloride distribution in the soil profile (0 to 50 ft) at selected locations at site HU1B. High chloride in the shallow soils indicates that evapotranspiration is preventing recharge.

The lack of high chloride concentrations in the shallow soils suggests active recharge. This technique was used at the Fort Hancock area to determine where recharge was occurring at that site.

3. Additional pumping tests are needed to better determine the transmissivity distribution and type of permeability of Aquifer A. This information would help determine whether these Permian formations represent an aquifer or not and to better define rates and directions of ground-water flow. The aquifer test at the Williams' Ranch indicated low transmissivities and fracture permeability, suggesting small volumes of ground water but possible high ground-water flow rates. Additional aquifer tests in the study area are needed to develop a larger data base. These additional tests could be conducted in producing water wells in the region.

ACKNOWLEDGMENTS

We would like to thank Skeet and Jay Williams of the Williams Ranch for their hospitality, time, information, and use of their water wells during this study. Kenneth Moore and Syd Sullenger of the University Lands Office were a great help in water well location and plant identification. Richard Bowen of El Paso Natural Gas Company provided assistance in locating water well records for Pump Station No. 2. All the ranchers in the study area of Hudspeth County were true "West Texans," as shown through their daily assistance and cooperation. We owe special thanks to George and Ethyl Temple of Salt Flat, Texas, for their always open door after a hot day in the field. Thanks are also given to Alan Dutton of the Bureau of Economic Geology for his technical assistance and supervision during pumping test operations.

Arten Avakian and Gay Nell Gutierrez of the Bureau of Economic Geology helped with data processing, mapping, sample processing, and drafting. Word processing was by Virginia C. Zeikus, Dorothy C. Johnson, and Rosanne M. Wilson under the supervision of Lucille C. Harrell. Figures were drafted by Don W. Thompson, Nan Minchow-Newman, T. B. Samsel III, and Annie Kubert-Kearns under the supervision of Richard L. Dillon. The report was edited by Amanda R. Masterson. Funding for this study was provided by the Texas Low-level Radioactive Waste Disposal Authority under contract no. IAC(86-87)-1061.

REFERENCES

Albritton, C. C., Jr., and Smith, J. F., 1965, Geology of the Sierra Blanca area, Hudspeth County, Texas: U. S. Geological Survey Professional Paper 479, 131 p.

Askew, B., and Algermissen, S. T., 1983, An earthquake catalog for the Basin and Range province, 1803-1977: U.S. Geological Survey Open-File Report 83-86, 21 p.

Barnes, V. E., project director, 1983, Van Horn - El Paso Sheet: The University of Texas at Austin, Bureau of Economic Geology Geologic Atlas of Texas, scale 1:250,000.

Bebout, D. G., and Loucks, R. G., 1984, Handbook for logging carbonate rocks: The University of Texas at Austin, Bureau of Economic Geology Handbook 5, 43 p.

Boersma, L., 1965, Field measurement of hydraulic conductivity above water table, in Black, L., A., ed., Methods of soil analysis: American Society of Agronomy, p. 222-234.

Boyd, F. M., and Kreitler, C. W., in press, Hydrology of a gypsum playa, northern Salt Basin, Texas: The University of Texas at Austin, Bureau of Economic Geology Report of Investigations No. 160.

Brune, G., 1981, The springs of Texas: Fort Worth, Branch-Smith, 566 p.

Chapman, J. E. B., 1984, Hydrogeochemistry of the unsaturated zone of a salt flat in Hudspeth County, Texas: The University of Texas at Austin, Master's thesis, 132 p.

Claypool, G. E., Holser, W. T., Kaplan, I. R., Sakai, H., and Zak, I., 1980, The age curves of sulfur and oxygen isotopes in marine sulfate and their mutual interpretation: Chemical Geology, v. 28, p. 199-260.

Correll, D. S., and Johnston, M. C., 1970, Manual of vascular plants in Texas: Renner, Texas, Texas Research Foundation, 1881 p.

Craig, H., 1961, Isotopic variations in meteoric waters: Science, v. 133, p. 1702-1703.

Dames and Moore, 1985, Siting of a low-level radioactive waste disposal facility in Texas: evaluation of State-owned lands: v. 2, Attachment C.

Dansgaard, W., 1964, Stable isotopes in precipitation: Tellus, v. 16, p. 436-469.

Dougherty, J. P., 1975, Evaporation data in Texas: Texas Water Development Board Report 192, 237 p.

Dumas, D. B., 1980, Seismicity in the Basin and Range province of Texas and northeastern Chihuahua, Mexico, in Dickerson, P. W., Hoffer, J. M., and Callender, J. F., eds., Trans-Pecos region, southeastern New Mexico and West Texas: New Mexico Geological Society 31st Annual Field Conference Guidebook, p. 77-81.

Flawn, P. T., 1956, Basement rocks of Texas and southeast New Mexico: University of Texas, Austin, Bureau of Economic Geology Bulletin 5605, 261 p.

Freeze, R. A., and Cherry, J. A., 1979, Groundwater: Englewood Cliffs, New Jersey, Prentice-Hall, Inc., 604 p.

Gates, J. S., White, D. E., Stanley, W. D., and Ackermann, H. D., 1980, Availability of fresh and slightly saline ground waters in the basins of westernmost Texas: Texas Department of Water Resources Report 256, 108 p.

Goetz, L. K., 1977, Quaternary faulting in Salt Basin graben: The University of Texas at Austin, Master's thesis, 136 p.

Haley, J. F., 1971, Rb-Sr geochemistry of alkalic igneous intrusions, northern Trans-Pecos Texas: The University of Texas at Austin, Master's thesis, 62 p.

Henry, C. D., and Price, J. G., 1985, Summary of the tectonic development of Trans-Pecos Texas: The University of Texas at Austin, Bureau of Economic Geology Miscellaneous Map No. 36, 8 p.

Hodges, F. N., 1975, Petrology, chemistry and phase relations of the Sierra Prieta nepheline-analcime syenite intrusion, Diablo Plateau, Trans-Pecos Texas: The University of Texas at Austin, Ph.D. dissertation, 184 p.

Hoefs, J., 1973, Stable isotopes geochemistry: New York, Springer-Verlag, 112 p.

Hoy, R. N., and Gross, G. W., 1982, A baseline study of oxygen 18 and deuterium in the Roswell, New Mexico, groundwater basin: New Mexico Water Resources Research Institute, partial technical completion report for U.S. Department of the Interior, Office of Water Research and Technology, Project No. B-059-nmex.

King, P. B., 1948, Geology of the Southern Guadalupe Mountains, Texas: U.S. Geological Survey Professional Paper 215, 183 p.

_____ 1949, Regional geologic map of parts of Hudspeth and Culberson Counties, Texas: U.S. Geological Survey Oil and Gas Investigations Preliminary Map 90.

_____ 1965, Geology of the Sierra Diablo region, Texas: U.S. Geological Survey Professional Paper 480, 185 p.

King, P. B., and Flawn, P. T., 1953, Geology and mineral deposits of pre-Cambrian rocks of the Van Horn area, Texas: University of Texas, Austin, Bulletin 5301, 218 p.

Kreitler, C. W., Raney, J. A., Nativ, R., Collins, E. W., Mullican, W. F., III, Gustavson, T. C., and Henry, C. D., 1986, Final report for the Low-level Radioactive Waste Disposal Authority: preliminary geologic and hydrologic studies of selected areas in Culberson and Hudspeth Counties, Texas: The University of Texas at Austin, Bureau of Economic Geology, report prepared for the Texas Low-level Radioactive Waste Disposal Authority under interagency contract no. IAC(86-87)-0828, 184 p.

Kruseman, G. P., and De Ridder, N. A., 1976, Analysis and evaluation of pumping test data (3d ed.): Wageningen, The Netherlands, International Institute for Land Reclamation and Improvement, Bulletin 11, 200 p.

Larkin, T. J., and Bomar, G. W., 1983, Climatic atlas of Texas: Texas Department of Water Resources Publication LP-102, 151 p.

Masson, P. H., 1956, Age of igneous rocks at Pump Station Hills, Hudspeth County, Texas: American Association of Petroleum Geologists Bulletin, v. 40, no. 3, p. 501-518.

Muehlberger, W. R., Belcher, R. C., and Goetz, L. K., 1978, Quaternary faulting in Trans-Pecos Texas: Geology, v. 6, no. 6, p. 337-340.

National Weather Service, 1986a, Texas water oriented data bank-NWS maximum temperature for ID 00002012: 328 p.

_____ 1986b, Texas water oriented data bank-NWS minimum temperature for ID 00002012: 328 p.

_____ 1986c, Texas water oriented data bank-NWS precipitation for ID 00002012: 411 p.

Nativ, R., and Riggio, R., in preparation, Rain events in the Southern High Plains - their distribution and isotopic composition patterns.

Nativ, R., and Smith, D. A., 1985, Characterization study of the Ogallala aquifer, northwest Texas: The University of Texas at Austin, Bureau of Economic Geology, prepared for the U.S. Department of Energy, Office of Nuclear Waste Isolation under Contract No. DE-AC97-83WM46651, 103 p.

Nielson, P. D., and Sharp, J. M., Jr., 1985, Tectonic controls on the hydrogeology of the Salt Basin, Trans-Pecos Texas, in Structure and tectonics of Trans-Pecos Texas: West Texas Geological Society Guidebook, Publication 85-81, p. 231-234.

Orton, R. B., 1964, The climate of Texas and adjacent Gulf waters: Washington, D.C., U.S. Department of Commerce, Weather Bureau, 195 p.

Peckham, R. C., 1963, Summary of the ground-water aquifers in the Rio Grande Basin: Texas Water Commission, Circular No. 63-05, 16 p.

Reagor, B. G., Stover, C. W., and Algermissen, S. T., 1982, Seismicity map of the state of Texas: U.S. Geological Survey Miscellaneous Field Studies, map MF-1388.

Sanford, A. R., and Toppozada, T. R., 1974, Seismicity of proposed radioactive waste disposal site in southeastern New Mexico: New Mexico Bureau of Mines and Mineral Resources Circular 143, 15 p.

Scalapino, R. A., 1950, Development of ground water for irrigation in the Dell City area, Hudspeth County, Texas: Texas Board of Water Engineers, Bulletin 5004, 38 p.

Stead, F. L., and Waldschmidt, W. A., 1953, Regional significance of the Pump Station Hills, in Haigh, B. R., and others, Sierra Diablo, Guadalupe, and Hueco areas of Trans-Pecos Texas: West Texas Geological Society Guidebook, p. 70-85.

Sullins, C. J., 1971, Red Hills intrusion, northern Hudspeth County, Texas: The University of Texas at Austin, Master's thesis, 63 p.

Texas Water Development Board, 1985, Texas water oriented data bank-ground water quality system ID PD-115 for Hudspeth County, 24 p.

U.S. Department of Housing and Urban Development, Federal Insurance Administration, 1985, Flood hazard boundary maps, Hudspeth County, Texas: Community Panel Nos. 480361 0400 B and 480361 0550B.

Walton, W. C., 1970, Groundwater resource evaluation: New York, McGraw-Hill, 664 p.

Wasserburg, G. J., Wetherill, G. W., Silver, L. T., and Flawn, P. T., 1962, A study of the ages of the Precambrian of Texas: Journal of Geophysical Research, v. 67, no. 10, p. 4021-4047.

Young, P. W., 1976, Water resources survey of Hudspeth County: West Texas Council of Governments, 156 p.

Appendix 1. Records of wells and springs in Hudspeth County sites.
Depths are in feet.

BEG ID	Well name	TDWR ID	Coordinates		Ground-level elevation	Water-level depth	Water-level elevation	Total depth
LL106	Alamo Arroyo Spring				4,500		4,500	
LL107		48-42-1	31°22'12"	105°50'52"	3,855	335	3,550	450
LL108		48-42-404	31°18'56"	105°51'27"	3,610	90	3,520	267
LL109		48-41-618	31°17'31"	105°52'45"	3,523	10	3,513	305
LL110	Miller Feedlot	48-41-2	31°19'37"	105°54'55"	3,545	8	3,536	160
LL111		48-33-9	31°23'18"	105°53'18"	3,882	327	3,555	367
LL112	Head of Canyon Wm		31°31'42"	105°42'05"	5,059	380	4,679	720
LL113	Wilkey Well No. 1		31°23'23"	105°40'48"	4,307	600	3,707	730
LL114	Wilkey Well No. 2		31°22'48"	105°39'07"	4,346	76	4,270	200
LL115	Gunsight Well 2		31°25'03"	105°30'20"	4,780	405	4,375	480
LL116	Owen Well		31°22'31"	105°45'50"	4,014	120	3,894	300
LL126	Low Level Well		31°24'14"	105°43'32"	4,179	478	3,699	530
LL127	Gunsight Well 1		31°24'43"	105°34'45"	5,154	627	4,527	690
LL128	Temple Well	48-24-1	31°44'40"	105°05'25"	3,726	107	3,619	
LL129	Guillen E on Well	48-23-201	31°44'48"	105°12'06"	4,007	429	3,578	
LL130	Desert Inn Well	48-14-7	31°45'56"	105°21'22"	4,135			
LL131	Cornudas Cafe Well	48-13-7	31°46'45"	105°28'09"	4,304			
LL132	Williams Ranch House Well	48-20-6	31°41'31"	105°30'09"	4,334	709	3,625	
LL133	Puett Well	48-13-8	31°46'38"	105°26'53"	4,341			
LL134	Hobo Well-Deep	48-20-5	31°41'44"	105°33'07"	4,416			
LL135	Jardin Well	48-30-4	31°33'27"	105°21'25"	4,282			
LL136	Sparks Windmill	48-14-9	31°46'18"	105°16'45"	4,053	446	3,607	
LL137	Sparks House Pump Well	48-14-8	31°45'39"	105°18'04"	4,032	510	3,522	
LL138	Williams #4 Well	48-12-8	31°46'21"	105°33'09"	4,409			
LL139	Stewart #2 Well	48-12-5	31°48'30"	105°32'52"	4,447			
LL140	Adobe House Tank Well	48-21-5	31°41'10"	105°25'18"	4,200			
LL141	Bravo Well	48-29-3	31°36'14"	105°24'27"	4,278	628	3,650	
LL142	Three Sisters Well	48-29-1	31°36'10"	105°28'18"	4,362	48	4.314	
LL143	Sumrall Well	48-16-7	31°45'57"	105°05'20"	3,668	100	3,568	
LL144	Foster House Well	48-14-1	31°51'44"	105°21'44"	4,186			
LL145	Foster South Well	48-13-9	31°47'15"	105°22'47"	4,182			
LL146	Stewart #1 Well	48-12-5	31°48'29"	105°32'56"	4,445			
LL147	Beard #1 Well	48-12-7	31°46'07"	105°37'02"	4,523			
LL148	Red Well	48-23-7	31°37'47"	105°14'20"	4,075	463	3,612	
LL149	Sampson Well	48-23-1	31°42'04"	105°12'45"	3,886	262	3,625	
LL150	South Well	48-28-3	31°35'29"	105°30'08"	4,430	63	4,367	
LL151	Dyer #1 Ranch House	48-38-1	31°29'45"	105°21'59"	4,336	160	4,176	
LL152	Gibbs Well	48-14-4	31°49'17"	105°20'17"	4,081			
LL153	Dyer #2 Black Mountain South Well	48-31°9	31°31'20"	105°09'33"	4,509			
LL154	Flattop Well- Figure 2 Ranch	48-24-9	31°37'49"	105°02'10"	3,745	294	3,451	
LL155	Dyer #3 Well	48-39-1	31°28'16"	105°13'16"	4,368			
LL156	Baylor-New Well	48-37-3	31°28'05"	105°22'59"	4,408	210	4,198	
LL157	Baylor-Old Well	48-37-3	31°27'38"	105°24'51"	4,449	72	4,377	
LL158	Desert Inn Abnd. Well	48-14-7	31°45'38"	105°22'05"	4,170	549	3,622	

BEG ID	Well name	TDWR ID	Coordinates		Ground-level elevation	Water-level depth	Water-level elevation	Total depth
LL159	Abnd. Adobe House Tank	48-21-5	31°41'06"	105°25'15"	4,201	583	3,618	
LL160	Hobo Well-Shallow	48-20-5	31°41'48"	105°33'08"	4,415	18	4,397	
LL161	Geothermal Well (UTEP)	48-21-6	31°41'47"	105°22'40"	4,224	74	4,150	
LL162	Williams Pump Jack #1	48-21-4	31°41'18"	105°28'50"	4,303	677	3,626	
LL163	Cavender Well	48-24-4	31°42'15"	105°07'19"	3,832	310	3,522	
LL164	Graham Well	48-24-2	31°43'34"	105°03'40"	3,668	100	3,568	
LL165	Bill Crane Well	48-24-5	31°41'54"	105°02'38"	3,658	140	3,518	
LL166	Morrison Well	48-24-6	31°40'34"	105°01'48"	3,629	40	3,589	
LL167	Wesley West Well	48-24-9	31°38'20"	105°01'11"	3,659	80	3,579	
LL168	Black Mountain Well	48-23-9	31°39'39"	105°07'34"	3,993	460	3,533	
LL169	Babbs Well	48-32-6	31°34'38"	105°01'22"	3,718	123	3,595	
LL170		48-07-101	31°58'08"	105°14'39"	3,804	205	3,599	700
LL171		48-07-102	31°57'33"	105°14'40"	3,795	218	3,577	962
LL172		48-07-206	31°59'25"	105°12'02"	3,709	129	3,580	215
LL173		48-07-207	31°58'10"	105°12'01"	3,707	122	3,585	712
LL174		48-07-210	31°58'15"	105°12'27"	3,721	145	3,576	240
LL175		48-07-214	31°57'56"	105°10'57"	3,678	93	3,585	500
LL176		48-07-304	31°58'00"	105°07'55"	3,644	60	3,584	
LL177		48-07-405	31°56'17"	105°13'27"	3,755	175	3,580	230
LL178		48-07-414	31°55'13"	105°14'39"	3,795	212	3,583	680
LL179		48-07-418	31°56'17"	105°14'39"	3,805	216	3,590	886
LL180		48-07-501	31°55'37"	105°11'51"	3,688	106	3,582	
LL181		48-07-504	31°56'11"	105°12'00"	3,696	72	3,624	175
LL182		48-07-516	31°56'37"	105°12'02"	3,705	119	3,586	300
LL183		48-07-606	31°57'10"	105°09'51"	3,651	67	3,583	
LL184		48-07-607	31°55'23"	105°08'51"	3,641	59	3,582	
LL185		48-07-706	31°53'34"	105°12'38"	3,712	131	3,581	835
LL186		48-07-708	31°52'37"	105°12'32"	3,722	138	3,584	1,583
LL187		48-07-801	31°54'53"	105°10'56"	3,658	80	3,578	200
LL188		48-07-803	31°53'31"	105°12'00"	3,693	100	3,593	278
LL189		48-07-901	31°54'56"	105°07'49"	3,637	53	3,584	300
LL190		48-07-904	31°53'27"	105°09'51"	3,660	62	3,598	780
LL191		48-08-102	31°59'03"	105°07'17"	3,642	56	3,586	392
LL192		48-06-201	31°59'59"	105°17'54"	3,940	303	3,637	1,100
LL193		48-06-601	31°56'20"	105°16'15"	3,874	310	3,564	1,505
LL194		48-15-203	31°51'43"	105°11'55"	3,715	138	3,599	325
LL195		48-15-301	31°50'53"	105°09'19"	3,652	60	3,593	320
LL196		48-16-402	31°48'26"	105°05'31"	3,652	61	3,591	140
LL197	(Eclipse Well)	47-01-7	31°54'57"	104°58'24"	3,671	50	3,621	
LL198		48-08-9	31°52'37"	105°00'45"	3,635	22	3,613	
LL199		48-08-4	31°55'23"	105°06'05"	3,616	3	3,613	
LL200		48-16-8	31°45'11"	105°02'50"	3,622	23	3,599	
LL201		47-09-1	31°50'58"	104°57'21"	3,697	91	3,606	
LL202		47-09-803	31°45'19"	104°55'01"	3,790	191	3,599	
LL203		47-09-805	31°46'51"	104°56'17"	3,696	97	3,591	515
LL204		47-09-8	31°46'10"	104°56'16"	3,722	130	3,592	

Appendix 1 (cont.)

BEG ID	Well name	TDWR ID	Coordinates		Ground-level elevation	Water-level depth	Water-level elevation	Total depth
LL205	(Black John Well)	47-17-3A	31°44'27"	104°53'57"	3,805	202	3,603	
LL206		47-17-6A	31°40'51"	104°53'50"	3,722	135	3,587	
LL207		47-17-6B	31°40'39"	104°54'06"	3,708	141	3,567	
LL208		47-17-6C	31°40'51"	104°54'59"	3,639	29	3,610	
LL209	(Hardluck Well)	47-17-3B	31°42'20"	104°54'06"	3,697	97	3,600	
LL210		47-17-3C	31°43'31"	104°54'02"	3,755	159	3,596	
LL211		47-17-2A	31°44'33"	104°56'00"	3,717	112	3,605	
LL212		47-17-2B	31°43'38"	104°56'03"	3,688	84	3,604	
LL213		47-18-4A	31°37'37"	104°52'25"	3,762	163	3,599	
LL214		48-32-3	31°36'30"	105°00'39"	3,636	39	3,597	
LL215	(Curton Well?)	47-25-4	31°32'45"	104°58'24"	3,650	48	3,602	
LL216		47-26-7	31°31'44"	104°52'30"	3,674	88	3,586	
LL217		47-26-9	31°31'18"	104°46'02"	3,786	202	3,584	
LL218	Abandoned Well	48-12-9	31°46'13"	105°30'51"	4,325	675	3,650	

Appendix 2. Hydraulic conductivity measurements in unweathered bedrock of the unsaturated zone, Diablo Plateau.

The hydraulic conductivity of two intervals of unweathered bedrock was measured at sites HU1A and HU1B to characterize potential migration rates in the area. Procedure and interpretations follow those reported by Boersma (1965) and Freeze and Cherry (1979). The method used is referred to as the shallow well - pump-in method, the piezometric method, or the dry-auger-hole method. This method requires an uncontaminated borehole, drilled with either a hollow-stem auger or a rotary rig, and a drill bit utilizing compressed air to circulate cuttings to the surface. At site HU1A, the interval to be tested consisted of unweathered rhyolite porphyry. Attempts to core this section with air proved unsuccessful (because of tremendous heat buildup), and fresh water had to be used to circulate cuttings and cool the core bit. To a lesser extent, a similar situation existed at HU1B in Cretaceous Campagrande limestones and was also cored with fresh water. To reduce borehole contamination, the fresh water was circulated only once to keep the borehole flushed of cuttings.

Water was then supplied to the test interval and maintained at a constant level. The rate of water input was adjusted until a steady state was achieved. Hydraulic conductivity was then calculated using the following equation:

$$K = \frac{[\ln(h/r + \sqrt{(h/r)^2 - 1}) - 1]\, Q}{2\pi h^2}$$

where

K = hydraulic conductivity (cm/hr)

h = depth of water maintained as measured from the bottom of the hole

r = the radius of the test hole (cm)

Q = rate at which water flows into the test interval.

Tests performed during this study were conducted on two different units, unweathered rhyolite porphyry and unweathered limestone. In previous tests in the Fort Hancock area (Kreitler and others, 1986), uniform coarse sand was added to the test hole before adding water to stabilize the walls of the hole. This was not necessary for these tests, however, due to the competent nature of the intervals tested. Results of the two tests are presented in the following table.

Tested lithology (cm)	Depth of borehole (cm)	Length of the tested interval (cm)	Radius of the borehole	Final rate of flow into the borehole (cc/hr)	K (cm/hr)
Rhyolite	1,524	914	3.7846	240,000	.0935
Limestone	1,524	914	4.8133	1,182,000	.4415

Hydraulic conductivity of the rhyolite was calculated to be 26.8 ft/yr (8.19 m/yr) and that of the limestone was 126.6 ft/yr (38.6 m/yr).

Appendix 3. Pumping test data and interpretation.

In order to determine the hydraulic parameters of the regional aquifer, a pumping test was conducted in well LL162 at Williams Ranch, Hudspeth County (fig. 2). The well is located 6.7 mi (10.8 km) west-northwest of the intersection between Ranch-to-Market Roads 1111 and 2317 (fig. A3-1). This well was drilled by El Paso Natural Gas Company to serve as a water supply well for their pump station #2. It was drilled into probable Victorio Peak - Bone Spring limestones of Permian age to an original total depth of 1,214 ft (370 m). Wellbore diameter was 8 inches (20.3 cm). Static water level in this well was measured at 677 ft (206.3 m) below land surface, and the saturated thickness is approximately 400 ft (121.9 m). Two adjacent wells, LL219 and LL220, located 468 ft (142.6 m) north-northwest and 1,326 ft (404 m) northwest of LL162, respectively, served as observation wells for the test. Water levels in these wells were measured at 671.5 ft (204.6 m) and 682.5 ft (208.0 m), respectively, below land surface. A shallow aquifer (see hydrologic setting, this report) was found in observation well LL219 at a depth of about 200 ft (61 m) below land surface. Cascading ground water from this level to the bottom of the well was clearly audible in this borehole and was also observed on the electric line-probe from 200 ft (60.9 m) down to the producing aquifer.

The test started at 12:40 p.m. on September 26, 1986. Production rates were essentially constant throughout the drawdown phase at 9.7 to 10.1 gpm (table A3-1). During the pumping period, which lasted 32 hours and 50 minutes, the recorded water level dropped 60.5 ft (18.4 m) in the pumping well (fig. A3-2, table A3-1), but no drawdown was detected in the observation wells. When the pump was turned off at 9:31 p.m. on September 27, the recovery of water level was monitored for another 31 hours and 30 minutes, until 5:00 a.m., September 28. By

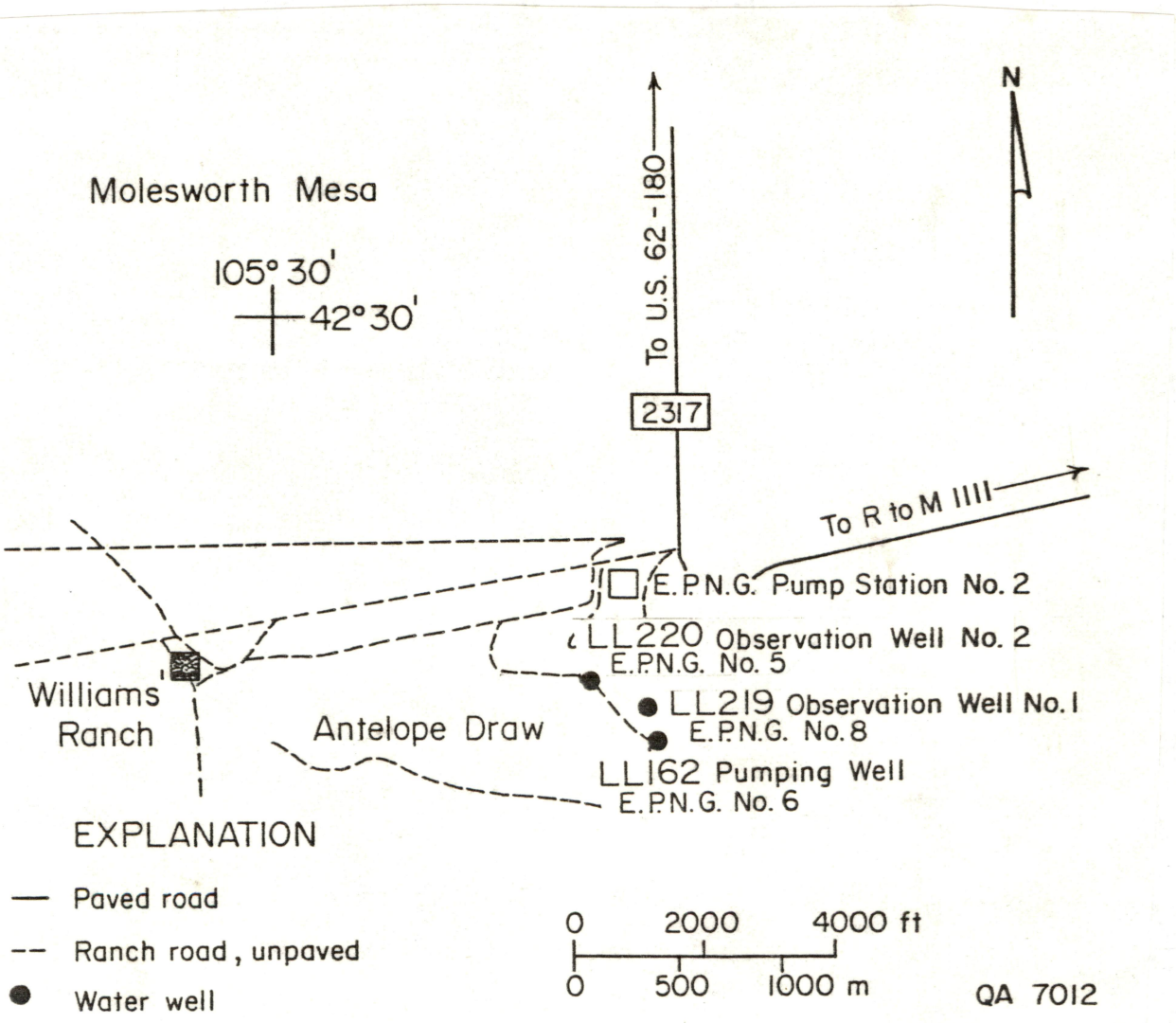

Figure A3-1. Location map for the pumping test site. Well LL162 was pumped while wells LL219 and LL220 served as observation wells.

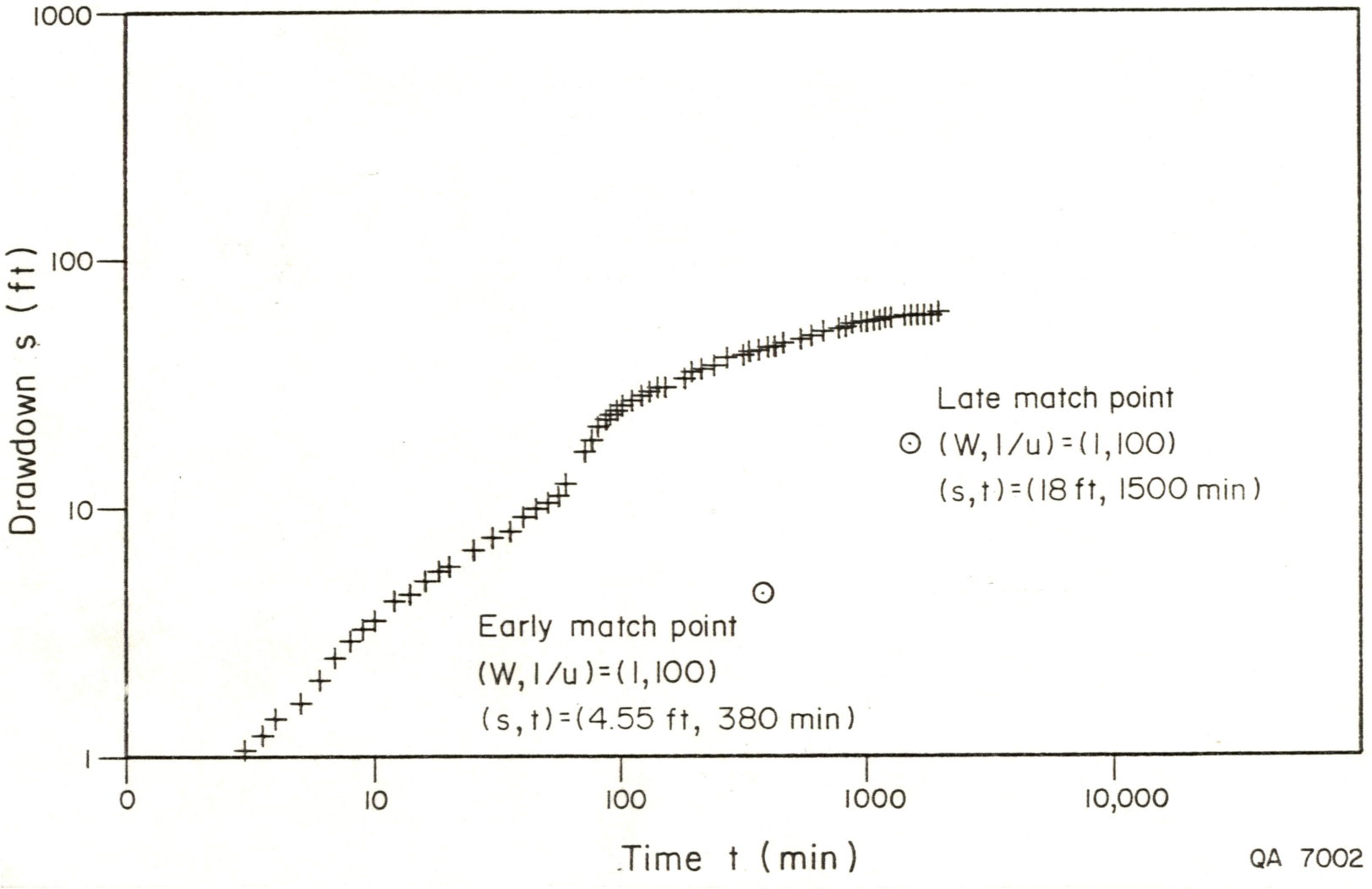

Figure A3-2. Time-drawdown curve that was matched to Walton type curves. Two distinct segments appear on the curve, suggesting (1) leakage from Aquifer B to Aquifer A after a short drawdown which was caused by early pumpage or (2) dewatering of additional fracture systems as the test proceeded.

Table A3-1. Drawdown data from pumping test on Williams' Ranch.

Time (hr)	Time from beginning of pumpage (min)	Depth to water level (ft)	Water level drawdown (ft)	Flow meter reading (gal)	Well Discharge (gpm)
12:40:00	0.0	680.00	0.00	3,353	0
12:40:30	0.5	680.00	0.00	-	-
12:41:00	1.0	680.27	0.27	3,361	8.0
12:41:30	1.5	680.625	0.625	3,365	8.0
12:42:00	2.0	680.792	0.792	3,371	12.0
12:42:30	2.5	680.917	0.917	3,378	14.0
12:43:00	3.0	681.083	1.083	-	-
	3.5	681.208	1.208	3,387	9.0
12:44:00	4.0	681.396	1.396	3,390.5	7.0
12:45:00	5.0	681.688	1.688	3,403	12.5
12:46:00	6.0	682.042	2.042	-	-
12:47:00	7.0	682.458	2.458	3,424	10.5
12:48:00	8.0	682.917	2.917	3,434	10.0
12:49:00	9.0	683.292	3.292	3,445	11.0
12:50:00	10.0	683.542	3.542	3,454	9.0
12:52:00	12.0	684.208	4.208	3,476	11.0
12:54:00	14.0	684.542	4.542	3,496	10.0
12:56:00	16.0	685.083	5.083	3,517	10.5
12:58:00	18.0	685.496	5.496	3,537	10.0
13:00:00	20.0	685.83	5.83	3,557	10.0
13:05:00	25.0	686.771	6.771	-	-
13:10:00	30.0	687.542	7.542	3,661	10.4
13:15:00	35.0	688.354	8.354	-	-
13:20:00	40.0	689.188	9.188	3,760	9.9
13:25:00	45.0	689.979	9.979	-	-
13:30:00	50.0	690.500	10.500	3,862	10.2
13:35:00	55.0	691.229	11.229	-	-
13:40:00	60.0	692.250	12.250	3,964	10.2
13:50:30	70.5	696.854	16.854	4,067	10.3
13:55:00	75.0	698.646	18.646	-	-
14:00:00	80.0	701.166	21.166	4,166	9.9
14:05:00	85.0	702.729	22.729	-	-
14:10:00	90.0	703.896	23.896	4,268	10.2
14:15:00	95.0	704.960	24.960	-	-
14:20:00	100.0	705.750	25.750	4,368	10.0
14:30:00	110	707.000	27.000	4,469	10.1
14:40:00	120	708.166	28.166	4,569	10.0
15:10:00	150	710.760	30.760	4,873	10.1
15:40:00	180	713.33	33.33	5,174	10.03
16:10:00	210	715.65	35.65	5,476.5	10.08
16:40:00	240	717.63	37.63	5,778	10.05
17:10:00	270	719.50	39.50	6,080	10.07
17:54:00	314	721.44	41.44	-	-
18:10:30	330.5	722.15	42.15	-	-
18:13:00	333			6,710	10.0
18:41:00	361	723.25	43.25	6,992	10.07
19:10:00	390	724.29	44.29	7,280.5	9.95
19:40:00	420	724.96	44.96	7,573	9.75
20:17:00	457	725.94	45.94	7,945	10.05
20:40:00	480	726.65	46.65	8,170.5	9.80

Table A3-1. (cont.)

Time (hr)	Time from beginning of pumpage (min)	Depth to water level (ft)	Water level drawdown (ft)	Flow meter reading (gal)	Well Discharge (gpm)
21:40:00	540	728.00	48.00	8,761	9.84
22:10:00	570			9,045	9.80
22:40:00	600	729.33	49.33		
23:37:00	657			9,999	10.97
23:40:00	660	730.88	50.88	-	-
01:11:00	751	732.17	52.17	-	-
01:40:00	780	732.71	52.71	-	-
02:40:00	840	733.50	53.50		
02:42:00	842			11,710	9.25
03:40:00	900	734.08	54.08		
03:42:00	902			12,290	9.67
04:45:00	965	734.71	54.71	12,921.5	10.02
05:30:00	1,010			13,365.0	9.86
05:40:00	1,020	735.16	55.16		
06:47:00	1,087	735.58	55.58	14,112	9.70
07:40:00	1,140	736.0	56.00	14,637	9.91
08:40:00	1,200	736.44	56.44	15,223.5	9.78
09:40:00	1,260	736.63	56.63	15,820.0	9.78
13:23:00	1,483			18,000	9.82
13:25:00	1,485	738.17	58.17		
14:38:00	1,558			18,732	9.76
14:46:00	1,566	738.50	58.50		
16:54:00	1,694			20,065	9.80
16:56:00	1,696	739.00	59.00		
18:34:00	1,794			21,040	9.75
18:40:00	1,800	739.87	59.87		
21:08:00	1,948			22,570	9.94
21:10:00	1,950	740.35	60.35		
21:31:00	1,971	740.50	60.50	22,784.5	9.75

that time 58.4 ft (17.8 m) of the 60.5 ft (18.4 m) of drawdown had recovered (table A3-2, fig. A3-3).

Two distinct segments appear on both figures A3-2 and A3-3. The change in slope of drawdown curve with time could be the result of several possible scenarios that may affect interpretation of the data.

A. The tested deep aquifer is semiconfined, and the shallow aquifer may leak into it. Considering this interpretation, the early part of the test represents nonsteady flow and nonleaky conditions. Leakage from the shallow aquifer starts at early drawdown when water level approaches 10 to 20 ft (3.0 to 6.1 m). A similar effect can be seen on the recovery curve. When water level recovers to 10 to 20 ft (3.0 to 6.1 m) below its initial stage, a change in slope can be observed. The presence of a shallow aquifer at the adjacent observation well (LL219) may support this explanation. Interpretation of the test data based on these conditions can be done by matching Walton's (1970) set of type curves for unsteady flow in semiconfined leaky aquifers to the time-drawdown and time-recovery plots (figs. A3-2 and A3-3). Walton developed a method of solution that followed the Theis method (Kruseman and De Ridder, 1976), but, instead of one type curve, he used a family of type curves for several values of r/B (a ratio that includes the coefficient of transmissivity, permeability, and the saturated thickness of the leaking aquitard). Transmissivity is calculated as follows:

$$T = \frac{114.6\ Q\ W(u,\ r/B)}{s}$$

Where

T = transmissivity (gpd/ft)

Q = discharge rate (gpm)

s = drawdown or the residual recovery (ft)

Table A3-2. Recovery test data from pumping test on Williams' Ranch.

Time (hr)	Time from beginning of recovery (min)	Time since pump started / Time since pump stopped (tp + Δt) / Δt	Depth to water level (ft)	Residual drawdown (s') (ft)	Water level recovery (ft)
21:31:00	0	∞	740.50	60.5	0
21:31:30	0.5	3,943	738.69	58.69	1.81
21:32:00	1.0	1,972	736.92	56.92	3.58
21:32:30	1.5	1,315	735.63	55.63	4.87
21:33:00	2.0	986.5	734.58	54.58	5.92
21:33:30	2.5	789.4	733.37	53.37	7.13
21:34:00	3.0	658.0	732.46	52.46	8.04
21:34:30	3.5	564.14	731.42	51.42	9.08
21:35:00	4.0	493.75	730.65	50.65	9.85
21:35:30	4.5	439.0	729.73	49.73	10.77
21:36:00	5.0	395.20	729.17	49.17	11.33
21:37:00	6.0	329.50	727.79	47.79	12.71
21:38:00	7.0	282.57	726.60	46.60	13.90
21:39:00	8.0	247.38	725.59	45.59	14.91
21:40:00	9.0	220.0	724.67	44.67	15.83
21:41:00	10.0	198.1	723.73	43.73	16.77
21:43:00	12.0	165.25	722.19	42.19	18.31
21:45:00	14.0	141.79	720.82	40.82	19.68
21:47:00	16.0	124.19	719.75	39.75	20.75
21:49:00	18.0	110.5	718.78	38.78	21.72
21:51:00	20.0	99.55	717.85	37.85	22.65
21:56:00	25.0	79.84	716.05	36.05	24.45
22:01:00	30.0	66.70	714.7	34.69	25.81
22:06:00	35.0	57.31	713.41	33.41	27.09
22:11:00	40.0	50.28	712.31	32.31	28.19
22:16:00	45.0	44.80	711.41	31.41	29.09
22:21:00	50.0	40.42	710.74	30.74	29.76
22:26:00	55.0	36.84	710.12	30.12	30.38
22:31:00	60.0	33.85	709.60	29.60	30.90
22:36:00	65.0	31.32	709.13	29.13	31.37
22:41:00	70.0	29.16	708.71	28.71	31.79
22:46:00	75.0	27.28	708.35	28.35	32.10
22:51:00	80.0	25.64	708.04	28.04	32.46
22:56:00	85.0	24.19	707.71	27.71	32.79

Table A3-2. (cont.)

Time (hr)	Time from beginning of recovery (min)	Time since pump started / Time since pump stopped (tp + Δt) / Δt	Depth to water level (ft)	Residual drawdown (s') (ft)	Water level recovery (ft)
23:01:00	90.0	22.90	707.40	27.40	33.10
23:06:00	95.0	21.75	707.11	27.11	33.39
23:11:00	100.0	20.71	706.83	26.83	33.67
23:21:00	110	18.92	706.35	26.35	34.15
23:31:00	120	17.43	705.89	25.89	34.61
24:01:00	150	14.14	704.23	24.23	36.27
24:31:00	180	11.95	701.28	21.28	39.22
01:01:00	210	10.39	698.17	18.17	42.33
01:31:00	240	9.21	695.85	15.85	44.65
02:01:00	270	8.30	694.34	14.34	46.16
02:31:00	300	7.57	693.10	13.10	47.40
03:01:00	330	6.97	692.25	12.25	48.25
03:31:00	360	6.48	691.46	11.46	49.04
04:01:00	390	6.05	690.98	10.98	49.52
04:34:00	423	5.66	690.35	10.35	50.15
05:01:00	450	5.38	689.90	9.90	50.60
05:31:00	480	5.11	689.37	9.37	51.13
06:31:00	540	4.65	688.59	8.59	51.91
07:01:00	570	4.46	688.20	8.20	52.30
07:34:00	603	4.27	687.83	7.83	52.67
08:10:00	639	4.08	687.42	7.42	53.08
08:31:30	660.5	3.98	687.13	7.13	53.37
09:01:00	690	3.86	686.88	6.88	53.62
10:00:00	749	3.63	686.30	6.30	54.20
11:00:00	809	3.44	685.72	5.72	54.78
12:00:00	869	3.27	685.31	5.31	55.19
13:38:00	967	3.04	684.63	4.63	55.88
15:19:00	1,068	2.85	684.03	4.03	56.47
19:00:00	1,290	2.53	683.29	3.29	57.21
05:00:00	1,890	2.04	682.08	2.08	58.42

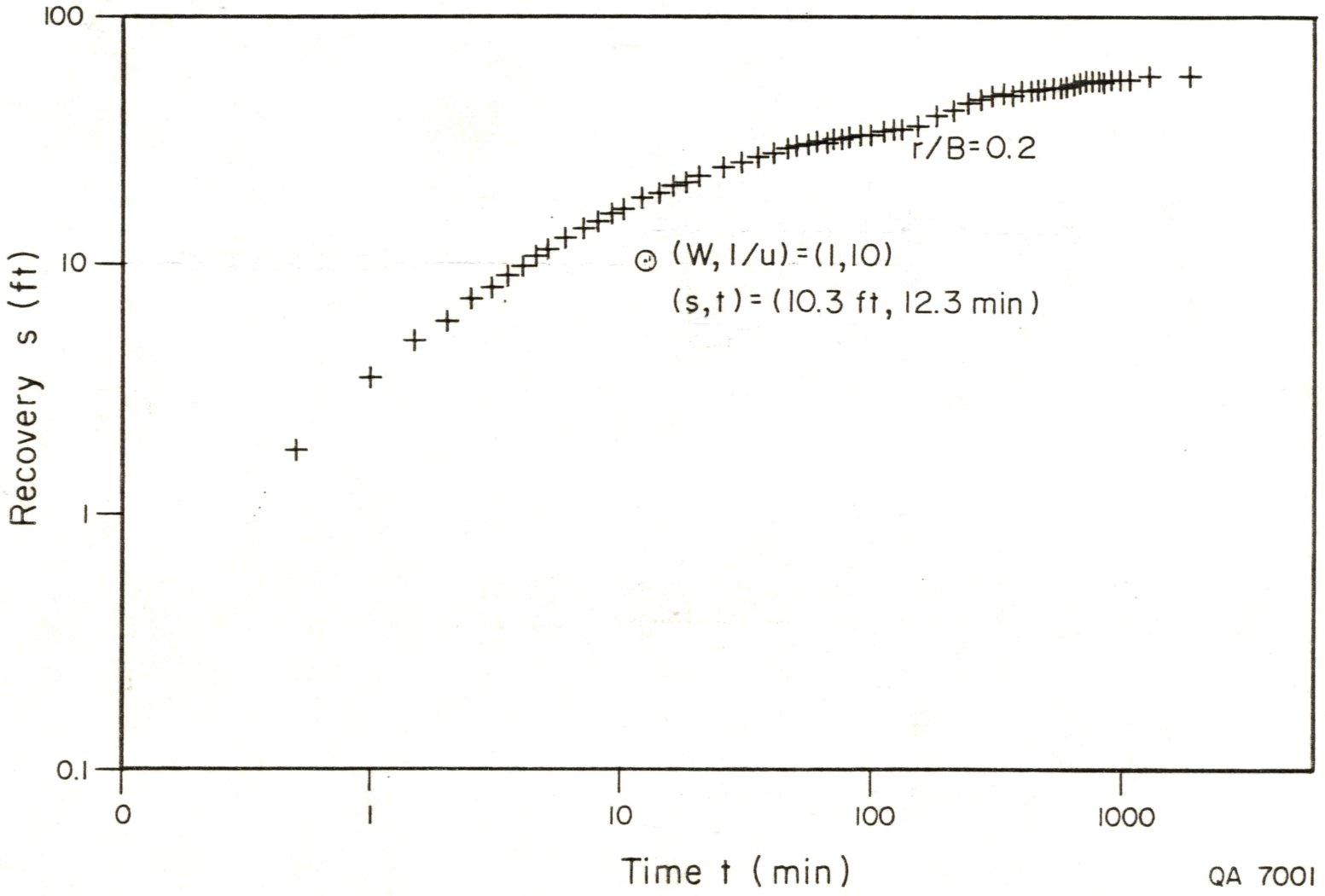

Figure A3-3. Time-recovery curve that was matched to Walton type curves. Two distinct segments appear on the curve, similarly to the time-drawdown curve.

W(u, r/B) = the well function (Kruseman and De Ridder, 1976) and the Y coordinate of the match point from the type curve.

The early part of the drawdown (30 min) may represent the flow in the pumped aquifer when no leakage from the upper aquifer was involved. The late part of the test may also include water contributed from the upper aquifer, as a result of the change in head in the deeper aquifer. Two transmissivity values were calculated for both parts of the drawdown. The early data set was matched to the nonleaky artesian type curve, and the match point had the coordinates (W, 1/u)=(1,100) and (s,t)=(4.55 ft, 380 min). The late part of the data curve was matched with the curve r/B=0.2, and the match point had the coordinates (W,1/u)=(1,100) and (s,t)=(18 ft, 1500 min) (fig. A3-2). Pumpage rate used for the calculation was the mean value of 10.01 gpm. Transmissivity values calculated from both parts of the test were 252.1 gpd/ft for the early part, and 63.7 gpd/ft for the late part (33.7 ft^2/d or 3.1 m^2/d and 8.5 ft^2/d or 0.8 m^2/d), respectively.

The early recovery part of the test (120 min) was used to check on the values calculated for the pumping period that were significantly different. By matching the data to the curve r/B=0.2, we found that the match point had the coordinates (W, 1/u)=(1,100) and (s,t)=(10.3 ft and 12.3 min) (fig. A3-3), and the calculated transmissivity was 111 gpd/ft (14.9 ft^2/d or 1.4 m^2/d). This value is higher than the value estimated for the symmetric late-pumping period during the drawdown part of the test.

B. Nonsteady flow, the aquifer is confined, and the two segments on both curves represent the permeability of the area around the borehole at the early time and the more regional pattern of permeability at a later stage. In this case, Jacob's method (Kruseman and De Ridder, 1976) can be used for interpretation of the late

part of the drawdown, and the Theis recovery method (Kruseman and De Ridder, 1976) can be used for evaluation of both stages of recovery.

Jacob developed a method to calculate the transmissivity based on the Theis formula for cases in which the value of u is small ($u = r^2S/4Tt$; r is the well diameter, S is the storativity, T is the transmissivity, and t is the test duration). U is small as t (test duration) increases, and therefore the later part of the drawdown is suitable for the analysis. Transmissivity is calculated as follows:

$$T = \frac{2.3\ Q}{4\pi\Delta s}$$

where

T = transmissivity (m^2/d)

Q = discharge rate (m^3/d)

s = drawdown (m).

Three segments were found on the drawdown curve and may represent the dewatering of three separated fracture systems, as the cone of depression extended to greater distance from the pumping well. Δs considered for the calculation were 7.5 ft/log cycle for the early phase, 31 ft/log cycle for the intermediate time, and 16 ft for the late part of the test (fig. A3-4). Calculated transmissivity values were 111, 84, and 158.6 gpd/ft (14.9 ft^2/d or 1.44 m^2/d, 11.3 ft^2/d or 1.05 m^2/d, and 21.5 ft^2/d or 1.97 m^2/d), respectively.

The Theis method was used to calculate transmissivity from the time-recovery curve following the formula:

$$T = \frac{2.3\ Q}{4\pi\Delta s'}$$

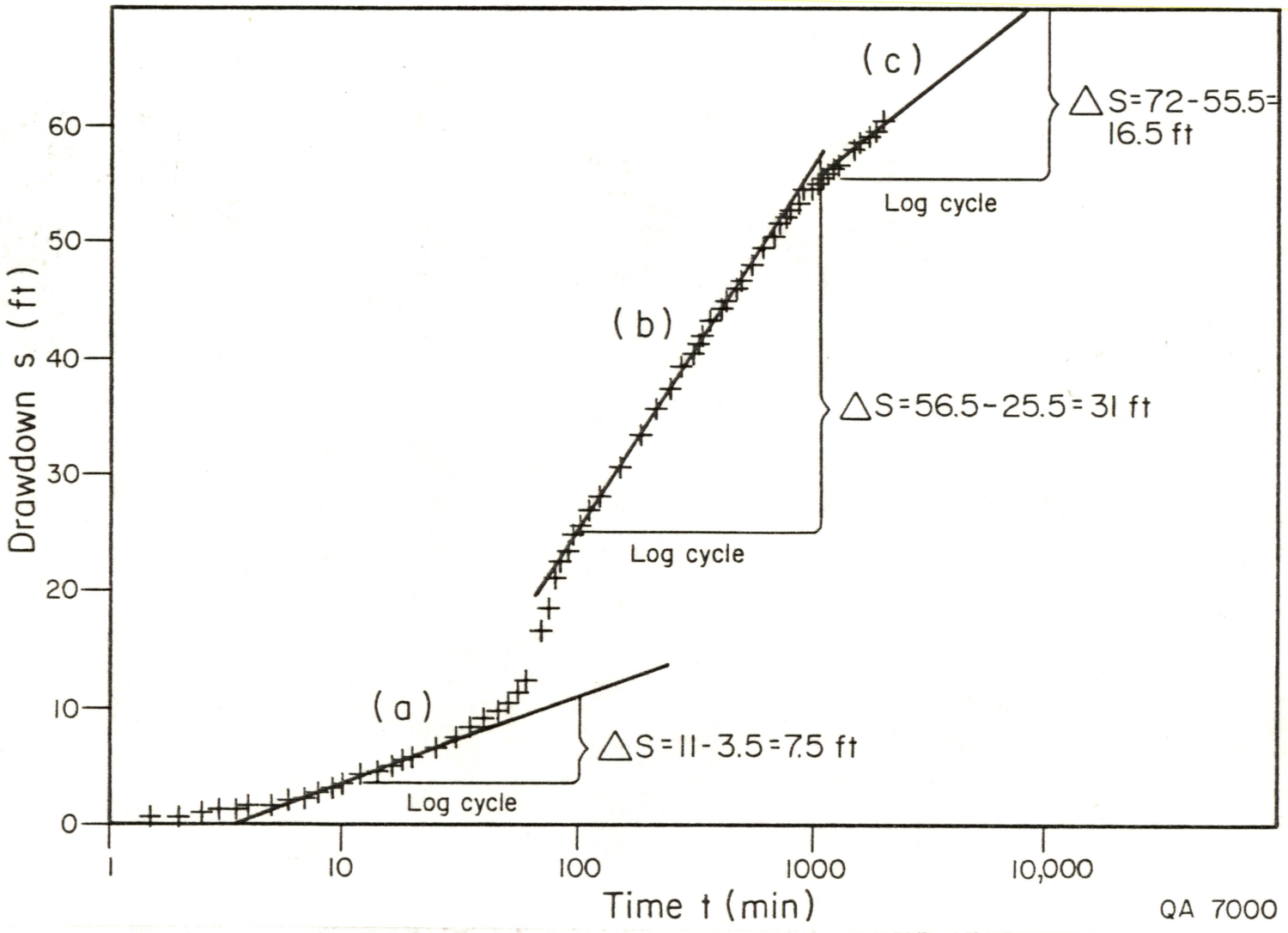

Figure A3-4. Time-drawdown plot that was interpreted by using Jacob's method. Three segments were found on the curve and may represent the dewatering of three separated fracture systems, as the cone of depression extended to greater distance from the pumping well.

where

T = transmissivity (m^2/d)

Q = discharge rate (m^3/d)

s'= residual drawdown (m)

$\Delta s'$ values considered for the calculations were 20 and 21.5 ft/log cycle for the early and late periods of recovery, respectively. Calculated transmissivity values for the early and late part of the recovery curve (fig. A3-5) were 130.6 gpd/ft and 121.5 gpd/ft (17.4 ft^2/d or 1.6 m^2/d and 16.2 ft^2/d or 1.5 m^2/d), respectively.

Transmissivity values calculated by the methods of Walton, Jacob, and Theis for both a semiconfined leaky aquifer and a confined nonleaky aquifer range from 63.7 gpd/ft to 252.1 gpd/ft, and the mean transmissivity calculated from all methods is 129.1 gpd/ft (17.3 ft^2/d or 1.6 m^2/d).

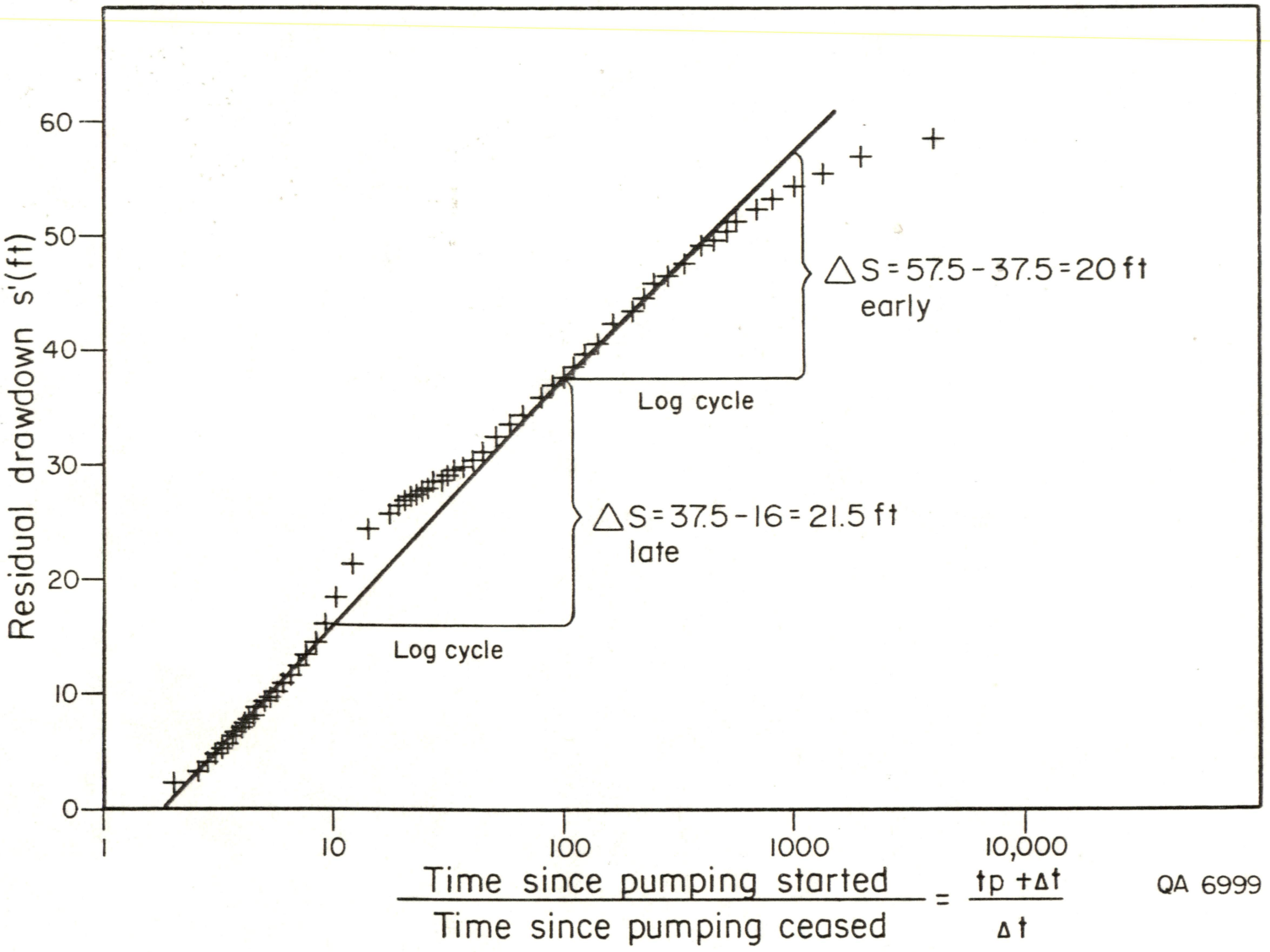

Figure A3-5. Time-recovery plot that was interpreted by using Theis' method.

Appendix 4. Geologic and hydrologic data from El Paso Natural Gas Company Pump Station #2 water wells, Hudspeth County, Texas.

The following is a synthesis of operational and maintenance records for eight wells drilled by El Paso Natural Gas Company (EPNG) to supply water to Pump Station #2. This pump station, now abandoned, is located 5.8 mi (9.4 km) south of Cornudas, Texas, and 7.5 mi (12.2 km) southwest of site HU1A. Number (#) at the beginning of each section denotes the BEG ID number for EPNG documents.

Well #1

(1) History of drilling - On November 18, 1954, it was reported that well was drilled in approximately 1929. Location is NE 1/4, NE 1/4, Sec. 24, Blk. 123 PSL.

(2) Operational data - On November 29, 1954, depth of well at 1,125 ft with a static water level of 950 ft. Capacity of well reported as 7 gpm from June 1950 to present. Water level will decrease below the pump at a higher rate and also at 7 gpm if kept at that rate longer than 30 days. Pump is a rod type cylinder pump.

(3) Well water chemical analysis - On November 29, 1954, two chemical analyses were reported (mg/l).

	5/2/50	6/2/50
pH	7.3	7.6
Total hardness as $CaCO_3$	376	428
Calcium as $CaCO_3$	190	223
Magnesium as $CaCO_3$	186	205
P alkalinity as $CaCO_3$	0	0
Total alkalinity as $CaCO_3$	230	235
Chloride as Cl	188	200
Sulfate as SO_4	295	293
Silica as SiO_2	15	14
Iron as Fe	trace	0.1

(4) Water well data. Based on the November 15, 1954 report, the following well data were summarized:

Drilling completion date	1929
Total depth (TD) of well	1,200 ft
Static water level	950 ft
Pumping capacity	7 gpm
Make of pump	Jenson Brothers
Rod size	3/4 inches
Column size	2 1/4 inches
Rated HP of pump	5
Pumping column	44 rods-25 ft @ 1,100 ft with 7-ft barrel and 8-ft perforated anchor.

This well is described as having an optimum capacity of 7 gpm and that water level will decrease below the pump at a higher pumping rate. It is also noted that water level will decrease below the pump when used at 7 gpm for more than 30 days. A production screen of unknown length was installed at 791 ft, 8 inches. This well was later plugged back to 1,125 ft.

(5) This driller's log describing the encountered section of water well #1 was prepared by M. E. Hawkins on June 20, 1950. Closing statement of the document is that well was plugged back to 1,100 ft.

Interval (ft)

From	To	Lithology and comments
110	132	Tan cream and pink dense limestone
132	140	Dense cream limestone
140	160	Cream yellow-tan and deep pink limestone, partly dolomitic
160	170	Tan and cream dense limestone (partly dolomitic) partly silty, trace chert
170	180	Yellow-tan, some cream and pink partly earthy dense dolomitic limestone
180	185	Light and limestone pebbles, some fragments of reddish-brown breccia, 20% fine to coarse clear worn sand, 20% gray clay, 80% chert
185	195	Sand and limestone conglomerate including siliceous pebbles
195	200	Light tan limestone, some quartzite pebbles
200	220	Cream partly dolomitic limestone, 30% pale gray chert

220	260	Cream limestone and pale gray chert
260	290	Cream limestone, gray and trace green tuff, 20% pyrite
290	310	Dark yellow-tan, some reddish slightly granular dolomite, 20% light chert
310	320	Dark tan granular dolomite, trace red stain and chert
320	330	Dark tan granular dolomite, 20% pink chert
330	340	Dark tan and pink dolomite, 25% gray-white and pink chert
340	360	Dark tan dolomite, trace light chert
360	370	Dark tan granular dolomite, 20% dense white chert
370	390	Dark tan dolomite
390	400	Light and dark tan and dark gray dolomitic limestone
400	410	Tan brown, some gray-black limestone
410	415	Brown and brownish gray limestone, trace dark chert
415	425	Dull tan to gray-brown limestone, trace chert and black shale
425	435	Tan and light brown limestone
435	455	Tan limestone, 10% white chert
455	475	Tan limestone, 20% cream chert
475	500	Tan limestone, 10% chert
500	520	Light and dark tan limestone, trace chert
520	530	Dark gray-brown limestone, 20% black limey shale, trace dark chert
530	545	Dark brown-gray limestone, trace chert and shale
545	560	Dark brown-gray and light tan limestone, trace black shale and chert
560	575	Tan fine crystalline limestone, 20% white chert
575	625	Brown irregular textured limestone, partly mixed with some lighter limestone
625	650	Tan and light brown limestone, 20% dark chert, trace black shale
650	660	Light tan with some gray limestone, trace black shale
660	680	Tan limestone, trace light fine-grained chert
680	690	Gray-tan partly dolomitic irregular textured limestone
690	705	Irregular textured gray-tan, some cream limestone
705	715	Brown-tan mixed with some cream limestone, 20% finer, granular dull tan chert
715	720	Limestone as above

720	730	Dark tan, some brown-black shaly granular limestone
730	745	Brown, irregular textured limestone, 20% black shale
745	760	Gray-brown irregular textured limestone
760	780	Limestone similar to above
780	800	Gray-brown, some tan limestone, 10% light chert, trace black shale
800	830	Tan limestone, Show Water
830	845	Gray-brown limestone, 25% calcite
845	875	Gray-tan limestone, trace calcite, black shale and white chert
875	900	Tan, some dark gray irregular textured limestone
900	930	Gray-tan irregular textured limestone, trace black chert
930	950	Gray-tan limestone, trace black shale
950	990	Brown limestone, some darker and shaly
990	1000	Tan to brown limestone
1000	1040	Irregular textured brown-gray limestone
1040	1060	Light and gray-tan limestone, trace black shale
1060	1070	Gray-tan rather dense limestone
1070	1090	Irregular textured light and gray-tan limestone
1090	1110	Irregular textured gray-tan limestone, 25% dark gray chert
1110	1120	Gray-tan partly shaly limestone
1120	1130	Gray-tan slightly granular dolomitic limestone
1130	1150	Tan limestone, 30% dark gray shale
1150	1170	Slightly granular and dolomitic limestone, 20% dark gray shale
1170	1190	Very coarse partly worn clear sand, 20% dark gray shale, 25% gray and tan limestone, trace glauconite Water 1190
1190	1235	Slightly dolomitic gray-tan limestone, trace black shale

Wells 2, 3, 4, and 7

(6) Memorandum dated November 24, 1954, reports the following status of water wells 2, 3, 4, and 7. Wells 2 and 3 were drilled in approximately 1929 and were abandoned in approximately 1938. The casing was pulled from both wells, and remaining boreholes were then filled with dirt. Well #4 location is listed as NE 1/4, NE 1/4, Sec. 24, PSL Blk. 123, Hudspeth County, Texas. This is 1/4 mi south of the pump station. Well #4 was also abandoned, but the dates for drilling or abandonment are not given. A plate was attached to a surface nipple on top of the

casing at time of abandonment. This well was 700 ft deep. Well #7 was drilled in 1947 and was never completed. A plate was secured to the surface casing when this well was abandoned.

Well #5

(7) Location reported as NE 1/4, NE 1/4, Sec. 24, PSL Blk. 123, 900 ft south of the pump station. Well was drilled on August 18, 1936, to a total depth of 713 ft. Casing string is given as 60 ft of 10-inch pipe and 703 ft of 4-inch pipe. Pumping equipment at this time consisted of an Allis Chalmers electric motor pump jack. This borehole is reported to be crooked at 400 ft.

(8) Driller's log (source of driller's log listed as Compressor Department, El Paso Natural Gas Company):

Interval (ft)

From	To	Lithology and comments
0	4 ft	Surface
4	21	Caliche-hard
21	45	White lime
45	80	Sandy blue limestone
80	110	White lime
110	125	Sandy blue limestone
125	185	White limestone
185	198	Black limestone
198	250	Red rock-hard
250	270	White limestone
270	295	Yellow sandy limestone
295	389	Hard gray limestone
389	400	White limestone
400	402	Gray limestone
402	452	Yellow sandstone, some limestone
452	515	Yellow limestone crevis, 479-485
515	530	White limestone
530	550	Gray limestone
550	624	White limestone
624	647	Gray limestone, crevis at 637, lost drilling water
647	700	Yellow limestone, crevis 647-653, no lost returns
700	713	Corrected to 703 water sand

(9) The chemical analysis of ground-water in well #5 given below was dated November 18, 1954:

	3/49	No date
pH	8.2	7.8
Total hardness as $CaCO_3$	376	300
Calcite as $CaCO_3$	240	223
Magnesium as $CaCO_3$	136	77
P alkalinity as $CaCO_3$	0	0
Total alkalinity as $CaCO_3$	230	260
Chloride as Cl	136	170
Sulfate as SO_4	165	---
Silica as SiO_2	36	17
Iron as Fe	0.1	0
Total solids	1092	958

(10) Appropriate portions of the maintenance record for Well #5 are listed below. Drilling operations for Well #5 began July 7, 1936, and were completed on August 18, 1936. September 18, 1957 entry includes (1) total depth of hole is 697.5 ft (212.6 m); (2) static water level is at 675 ft (205.7 m); (3) initial capacity after service of well was 8.5 gpm on 13 cycles per minute of pump jack; (4) On January 21, 1958, production rate was measured at 10.0 gpm after replacing pump parts and rods; (5) On February 17, 1958, production rate still recorded at 10 gpm.

(11) Water well maintenance report dated August 12, 1965. Reports that static water level rose from 693 ft (211 m) to 684 ft (208 m) after replacing a portion of pipe string and pump. Before servicing, the production capacity fell from 11 gpm to 5 gpm, and production barrel was faulty and sanded up.

(12) Undated operational memorandum repeats that this hole is crooked at 400 ft (121.9 m) and recommends that in the future a cable tool rig be used to reclaim all of hole (from caving). This memo also reports the static water level at well #5 for August 1965 to be ranging from 693 to 684 ft (211.2 to 208.4 m) and in October 1965 to be static at 690 ft (210.3 m). Original total depth of borehole (TD) reported to be 713 ft (217.3 m).

Well #6

(13) Location of well is NE 1/4, NE 1/4, Sec. 24, PSL Blk. 123. This is located 1/4 mile south of pump station. This well was completed at a total depth of 1,209 ft (368.5 m) in 1938. Production was reported as 12 gpm through 8-inch casing.

(14) Operational record dated November 29, 1954, states that well has a total depth of 1,214 ft (370 m) and a static water level of 1,044 ft (318.2 m). Production capacity for this well is given as 20 to 30 gpm, and it is reported that water level will decrease below the pump if rates are greater.

(15) Chemical analyses reported for two consecutive days for well #6 on November 18, 1954.

	7/24/52	7/25/52
pH	7.5	7.6
Total hardness as $CaCO_3$	430	450
Calcium as $CaCO_3$	250	250
Magnesium as $CaCO_3$	180	200
P alkalinity as $CaCO_3$	0	0
Total alkalinity as $CaCO_3$	290	270
Chloride as Cl	72	64
Sulfate as SO_4	288	310
Silica as SiO_2	9	12
Iron as Fe	trace	---
Total solids	980	1000

(16) Driller's log for Well #6.

Interval (ft)		Lithology and comments
From	To	
25	35	Buff and gray lime
35	45	Buff and gray lime, scattered sand grains
45	55	Buff and gray lime, scattered sand grains
55	65	Buff gray lime, fewer sand grains
65	80	Buff gray lime, few quartz grains
80	95	Gray buff lime, rust-colored limey shale
95	105	Gray lime, few quartz grains
105	115	40% gray buff lime, 60% calcite crystals, and few pyrite inclusions
115	127	Gray and buff lime

127	136	Brown dolomite and calcitic lime, crystalline
136	140	90% gray lime, 5% black lime, 5% black limey shale
140	150	Blue lime
150	160	Blue and gray lime
160	196	Blue and gray lime
196	208	Blue and gray lime, scattered sand grains
208	218	80% blue and gray lime, 20% sand with some pyrite
218	229	Blue and gray lime, scattered sand grains
229	233	Blue and gray lime
233	237	70% buff and blue lime, 30% partly rounded quartz grains
237	240	80% buff lime, 20% sand
240	249	90% buff lime, 10% calcitic sand
249	259	Buff lime some calcitic and quartz sand
259	269	Gray buff lime
269	271	Gray buff lime
271	295	Brown dolomitic lime, few calcitic and quartz grains
295	305	Gray buff lime, few calcite grains
305	315	Light brown lime
315	320	Dark brown lime, few calcite grains, some pyrite
320	330	Blue gray lime
330	340	Dark brown lime, few calcite grains
340	360	Dark brown and gray lime
360	370	Dark brown and gray lime, few calcite grains
370	380	Dark gray and light gray lime
380	400	Dark gray and some light brown lime
400	424	Very dark gray lime
424	430	Dark brown lime, few calcite grains
430	440	Brown lime, few calcite grains
440	450	Brown and lighter brown lime
450	490	Dark brown and gray lime
490	500	Light brown and brown lime
500	530	Brown lime
530	540	Dark brown lime
540	550	Dark brown and light lime
550	560	Light brown lime and few calcite grains
560	570	Light brown and little white lime, few calcite grains
570	580	Light and dark brown lime

580	590	Brown lime, 5%-10% calcite grains
590	600	-skipped interval on log-
600	610	Light gray lime, few calcite grains
610	620	Light brown lime
620	640	Dark brown lime
640	650	Dark brown and light brown lime
650	670	Dark gray lime, few calcite grains
670	680	Dark gray and brown lime
680	690	Light brown lime
690	715	Dark brown and brown lime
715	729	Dark brown lime
729	750	Dark gray lime, few calcite grains
750	770	Brown lime, few calcite grains
770	800	Dark brown lime, few calcite grains
800	830	Dark brown lime and brown lime
830	840	Brown lime
840	850	Brown and light brown lime
850	870	Brown lime
870	900	Dark brown lime
900	930	Brown lime
930	940	Dark brown lime
940	950	Brown lime
950	960	Dark brown and brown lime
960	980	Brown lime
980	1000	Brown and light brown lime
1000	1010	Light brown lime
1010	1018	Dark brown lime
1018	1030	Brown lime
1030	1038	Dark brown lime
1038	1062	Brown lime
1062	1068	Brown and light brown lime
1068	1086	Brown lime, semi-frosted quartz grains
1086	1087	Dark brown lime
1087	1094	Light brown lime, few green limey shale flakes, few quartz grains, light brown lime contains fossil remnants
1094	1099	Dark brown lime, numerous frosted quartz grains
1099	1104	Brown lime, numerous frosted quartz grains

1104	1115	Light brown lime, few frosted quartz grains
1115	1120	Light brown lime, some pyrite inclusions
1120	1128	Dark brown lime
1128	1150	Brown lime
1150	1160	Brown lime, few frosted quartz grains
1160	1170	Brown lime, few calcite grains
1170	1175	Dark brown fossiliferous grains
1175	1180	Dark brown lime
1180	1189	Brown lime
1189	1204	Dark brown lime
1204	1209	Dark brown lime and gray lime--TD

Well #8

(17) Well data sheet gives location for this well as NE 1/4, NE 1/4, Sec. 24, PSL Blk. 123 (outside southwest corner of plant location). This well, completed on June 26, 1951, was drilled by Holland Page, Jr., to a TD of 1,288 ft (392.5 m). Well was temporarily plugged and abandoned March 28, 1956, and restored to production on January 20, 1958.

(18) This document is a memorandum to W. H. Miller from M. E. Hawkins reporting the results of pump tests on well #8.

Date	Time	Gallons per minute (gpm)
11/26/51	12:30 p.m.	start test
11/26/51	12:30-4:30 p.m.	45
11/26/51	4:30-11:30 p.m.	30
11/26-27/51	11:30 p.m.-8:30 a.m.	25
11/27/51	8:30 a.m.-10:00 p.m.	20
11/27-28/51	10:00 p.m.-6:30 a.m.	15
11/28-12/5/51	6:30 a.m. to present	12

(19) The following is a synthesis of a combined driller's log and operational report for water well #8.

Date	Interval (ft)	Lithology and comments
6/2/51	0-43	Caliche
6/3/51	43-45	Lime
	45-65	Yellow lime
	65-75	Brown lime
	75-80	Yellow lime
	80-86	Yellow lime
	86-94	Gray lime
6/4/51	94-95	Light brown hard lime
	95-100	Light brown hard lime
	100-106	Lime ballard gray lime
6/5/51	106-114	Lime gray
	114-120	Lime brown hard
	120-124	Lime brown hard
	124-134	Gray lime
	134-140	Gray lime
	140-143	Gray shale
	143-155	Gray lime shells
6/6/51	155-165	Lime, broken medium, little water at 158-160
	165-171	Lime gray hard
	171-175	Lime, broken, little more water at 171-175
	175-190	Broken lime
	190-195	Gray shale
	195-205	Gray lime
6/7/51	205-225	Lime hard sharp
	225-233	Lime hard sharp
	233-239	Sand, report increase in water
	239-240	Hard gray lime
6/8/51	240-245	Lime gray hard
	245-253	Lime broken
	253-270	Lime-sand medium
	270-276	Lime-sand
	276-295	Yellow lime hard

6/9/51	295-310	Lime gray brown hard
	310-325	Brown lime hard
6/10/51	325-340	Lime brown hard
	340-348	Lime
6/17/51	348-355	Lime hard
	355-358	Lime hard
6/18/51	358-360	Lime hard
	360-370	Lime hard
	370-377	Black lime
6/19/51	377-383	Hard lime
	383-397	Hard lime, testing water, 1.5 bailers per hour
6/20/51	397-401	Hard lime
	401-410	Brown lime
	410-421	Brown lime
6/21/51	421-443	Brown lime
	443-450	Brown lime
6/24/51	450-455	Brown lime hard
	455-464	Brown lime hard
	464-480	Brown lime
6/25/51	480-493	Brown lime
	493-513	Brown lime
6/26/51	513-525	Brown lime hard
	525-557	Brown lime
6/27/51	557-571	Lime shells
	571-607	Brown lime
6/28/51	607-618	Broken lime hard
	618-649	Black lime, tested production at 0.5 bailer per hour
6/29/51	649-685	Lime
6/30/51	685-698	Lime
7/1/51	698-710	Lime hard
	710-743	Black lime
7/3/51	743-760	Black lime

7/4/51	760-771	Lime black
	771-777	Gray lime
	777-790	Brown lime
	790-804	Black lime
7/5/51	804-825	Gray lime
	825-843	Blue lime
7/6/51	843-875	Gray lime
7/7/51	875-885	Gray lime hard
	885-908	Gray lime
7/8/51	908-920	Gray lime
	920-933	Gray lime hard
	933-940	Gray lime, tested water production, rate at 1.5 bailers per hour
7/9/51	940-952	Gray lime
	952-963	Hard gray lime
	963-973	Hard gray lime
7/10/51	973-983	Gray lime
7/13/51	983-985	Black lime
7/14/51	985-997	Black lime
	997-1021	Blue gray lime
7/15/51	1021-1051	Blue gray lime hard
7/16/51	1051-1070	Black lime
	1070-1093	Blue gray lime
7/17/51	1093-1131	Blue gray lime
7/18/51	1131-1150	Shale-gray lime
7/19/51	1150-1180	Blue gray lime, possible water from 1170 to 1180, begin testing water-no results
	1180-1200	Black lime
7/20/51	1200-1217	Blue gray lime, testing production-initial rate of 2.5 bailers per hour, increased to 10 bailers per hour
7/21/51	1217-1235	Blue gray lime, tested 5 bailers per hour, hit small crevice at 1225
7/22/51	1235-1266	Shale and lime

7/23/51	1266-1288	Shale and lime, recorded 400 ft (121.9 m) of fluid in the hole, bailed from 11:30 a.m. to 5:30 p.m. (75 bailers full), during one hour delay for equipment repair-water level rose 100 ft, at 530 ft, 65 bailers water 500 ft
7/24/51	1288	Continued bailing, water rose approximately 25 ft (7.6 m) averaged bailing 15 bailers per hour-lowered the water level 40 ft (12.2 m) -shut down 45 minutes and water level rebounded to original level of 250 ft (76.2 m) (Note-the water level of 250 ft mentioned in this entry is unclear because the last entry noted water level of approximately 530 ft (161.5 m)
7/25/51	1288	Started production test. Before starting-water level measured at 590 ft (179.8 m), recovered 23 bailers in 1 hour, water level at 948 ft (288.9 m), after bailing 1,640 gallons bailed (6207.4 L)-bailed 23 to 24 gallons per hour-maximum drawdown measured was 200 ft (60.9 m)
7/26/51	1288	420 ft (128.0 m) of fluid in the hole at beginning of production test-recovered 21 bailers containing 1,425 gal (5393.6 L) lowering water table 100 ft (30.4 m) unable to lower water table below 200 ft (60.8 m)-end of test.

(20) The following chemical analysis as prepared for water well #8 by D. C. Kelly is dated November 18, 1954.

	7/24/51	12/--/51
pH	7.6	7.4
Total hardness as $CaCO_3$	400	405
Calcium as $CaCO_3$	230	240
Magnesium as CaCO3	170	265
P alkalinity as $CaCO_3$	0	0
Total alkalinity as $CaCO_3$	215	230
Chloride as Cl	80	104
Sulfate as SO_4	108	336
Silica as SiO_2	18	17
Iron as Fe	trace	---
Total solids	---	1578

(21) An operational report dated March 1952 provides information about water found in the following intervals in water well #8:

158 ft- 165 ft
171 ft- 175 ft
1170 ft-1190 ft

Static water level is recorded at 626.5 ft (190.9 m). Other remarks in this memo include (1) well does not have a sand trap, (2) is not gravel packed, (3) does have a foot valve, and 4) well does not pump sand.

Appendix 5. Chemical and isotopic composition of ground-water samples, HU1A and HU1B sites, Hudspeth County.

Major ions (mg/L) and temperatures (°C).

Aquifer A+

BEG ID	Well Name	Coordinates		Ca^{2+}	Mg^{2+}	Na^{+}	K^{+}	HCO_3^{-}	SO_4^{2-}	Cl^{-}	NO_3^{-}	TDS	Temp.
LL128	Temple Well	31°44'40"	105°05'25"	320	116	278	11.3	236	820	530	40	2363.07	22
LL129	Guillen Exxon Well	31°44'48"	105°12'06"	193	79.7	113	5.2	178	680	117	24	1404.12	25
LL130	Desert Inn Well	31°45'56"	105°21'22"	178	73.5	269	7.0	345	553	305	2.7	1745.37	24
LL131	Cornudas Cafe Well	31°46'45"	105°28'09"	146	63.7	325	10.0	293	580	312	3.8	1743.9	24
LL132	Williams Ranch House Well	31°41'31"	105°30'09"	95.1	37.1	100	2.7	299	170	78	92	884.03	25
LL133	Puett Well	31°46'38"	105°26'53"	199	86.6	462	12.7	332	950	405	<1.0	2461.77	23
LL134	Hobo Well-Deep	31°41'44"	105°33'07"	157	73.2	308	5.8	352	710	202	<1.0	1826.76	22
LL135	Jardin Well	31°33'27"	105°21'25"	169	60.9	964	40.5	412	580	1300	<1.0	3551.72	23
LL136	Sparks Windmill	31°46'18"	105°16'45"	605	193	259	11.7	243	2210	245	<1.0	3802.95	22
LL137	Sparks House Pump Well	31°45'39"	105°18'04"	497	121	310	9.2	263	1470	401	<1.0	3094.9	20
LL138	Williams #4 Well	31°46'21"	105°33'09"	176	80.5	238	5.9	283	740	172	<1.0	1722.28	22
LL139	Stewart #2 Well	31°48'30"	105°32'52"	358	133	303	5.8	430	1490	122	2.4	2858.58	21
LL140	Adobe House Tank Well	31°41'10"	105°25'18"	111	48.6	249	7.9	328	510	147	26	1445.18	22
LL141	Bravo Well	31°36'14"	105°24'27"	95.2	69.8	381	5.9	177	690	275	76	1786.92	25
LL142	Three Sisters Well	31°36'10"	105°28'18"	118	60.1	290	3.7	251	570	209	99	1616.51	22
LL143	Sumrall Well	31°45'57"	105°05'20"	252	95.2	303	9.1	290	660	500	10	2126.47	23
LL144	Foster House Well	31°51'44"	105°21'44"	213	86.8	340	8.4	300	730	410	1.3	2103.23	26
LL145	Foster South Well	31°47'15"	105°22'47"	141	59.4	182	4.3	340	530	110	7.0	1384.09	21
LL146	Stewart #1 Well	31°48'29"	105°32'56"	258	102	225	4.9	400	1040	91	<1.0	2145.50	19
LL147	Beard #1 Well	31°46'07"	105°37'02"	166	87.6	408	7.1	400	840	340	6.0	2267.56	22
LL148	Red Well	31°37'47"	105°14'20"	153	60.4	416	18.3	320	540	490	10	2020.67	20
LL149	Sampson Well	31°42'04"	105°12'45"	216	86.2	267	9.0	280	590	410	30	1898.45	22
LL152	Gibbs Well	31°49'17"	105°20'17"	203	82.9	328	10.3	310	700	380	1.0	2027.10	21
LL153	Dyer #2 Black Mountain South Well	31°31'20"	105°09'33"	113	52.8	324	14.6	370	290	400	9	1581.12	22
LL154	Flattop Well-Figure 2 Ranch	31°37'49"	105°02'10"	218	80.4	265	9.7	290	550	420	16	1856.72	24
LL155	Dyer #3 Well	31°28'16"	105°13'16"	150	77	400	14.5	370	700	340	13	2077.08	19

Appendix 5. (cont.)

Trace ions (mg/L) and isotopic composition.

Aquifer A+

BEG ID	Well name	TWC ID	As^{3+}	Cd^{2+}	Li^{+}	Fe^{2+}	Sr^{2+}	Ba^{2+}	Br^{-}	F^{-}	$\delta^{18}O$**	δD**	Tritium	$\delta^{34}S$**	$\delta^{13}C$**	PMC†	^{14}C Age††
LL128	Temple Well	48-24-1	<0.05	<0.03	0.07	*0.02	8.04	0.06	0.5	3.0	-9.18	-68.8	4.1	16.11	-5.77	13.47	7,639
LL129	Guillen Exxon Well	48-23-201	<0.05	<0.03	*0.05	0.08	8.25	0.06	0.5	5.2	-9.19	-72.7	2.7	12.11	-5.78	9.56	10,488
LL130	Desert Inn Well	48-14-7	<0.05	<0.03	0.08	0.04	6.14	0.03	0.7	5.1	-9.17	-70.3	3.8	5.56	-8.49	6.74	16,556
LL131	Cornudas Cafe Well	48-13-7	<0.05	<0.03	0.10	<0.02	4.49	0.05	0.7	5.0	-9.18	-69.8	3.5	4.53	-6.07	10.54	10,084
LL132	Williams Ranch House Well	48-20-6	<0.05	<0.03	*0.04	0.03	3.77	0.61	0.6	5.0	-6.90	-50.9	13.7	8.61	-8.00	21.02	6,660
LL133	Puett Well	48-13-8	<0.05	<0.03	0.16	1.62	5.58	0.03	1.0	5.0	-10.21	-81.1	2.3	5.71	-6.36	5.36	16,061
LL134	Hobo Well-Deep	48-20-5	<0.05	<0.03	0.09	1.42	0.09	0.02	0.8	7.2	-8.01	-64.2	2.3	7.70	-8.92	18.46	8,635
LL135	Jardin Well	48-30-4	<0.05	<0.03	0.45	6.97	0.45	0.08	1.4	9.0	-9.15	-67.4	2.8	15.72	-6.79	5.08	17,046
LL136	Sparks Windmill	48-14-9	<0.05	<0.03	0.14	16.3	0.14	0.03	0.7	6.6	-10.53	-81.5	3.3	11.29	-3.64	5.99	10,529
LL137	Sparks House Pump Well	48-14-8	<0.05	<0.03	0.14	2.24	0.14	*0.01	0.7	6.2	-9.53	-71.3	3.2	10.37	-4.67	11.32	7,328
LL138	Williams #4 Well	48-12-8	<0.05	<0.03	0.09	11.8	0.09	0.08	0.8	6.3	-7.91	-65.1	6.8	10.12	-9.65	13.98	11,583
LL139	Stewart #2 Well	48-12-5	<0.05	<0.03	0.10	0.25	0.10	0.03	0.8	5.7	-10.44	-79.6	<0.8	-1.24	-10.35	4.34	21,832
LL140	Adobe House Tank Well	48-21-5	<0.05	<0.03	0.11	5.24	0.11	0.04	0.9	8.5	-9.73	-76.0	8.2	7.05	-5.67	13.02	7,775
LL141	Bravo Well	48-29-3	<0.05	<0.03	0.15	<0.02	0.15	0.02	1.9	9.0	-2.72	-35.3	3.4	5.84	-7.99	46.52	84
LL142	Three Sisters Well	48-29-1	<0.05	<0.03	0.11	0.17	0.11	0.12	1.9	7.7	-8.16	-66.5	<0.8	7.23	-6.27	23.50	3,725
LL143	Sumrall Well	48-16-7	<0.050	<0.03	0.09	<0.02	0.09	0.04	0.39	1.3	-9.26	-64.8	<0.8	11.13	-6.80	19.64	5,880
LL144	Foster House Well	48-14-1	<0.050	<0.03	0.12	0.10	0.12	0.10	0.75	2.7	-9.47	-69.1	2.2	7.81	-7.54	49.5	modern
LL145	Foster South Well	48-13-9	<0.050	<0.03	0.08	0.07	0.08	0.02	0.81	3.0	-9.82	-75.4	4.5	4.26	-7.59	9.71	12,610
LL146	Stewart #1 Well	48-12-5	<0.050	<0.03	0.08	13.0	0.08	0.04	0.93	3.0	-9.79	-73.2	1.9	-0.72	-10.04	4.84	20,678
LL147	Beard #1 Well	48-12-7	<0.050	<0.03	0.13	0.11	0.13	0.09	0.92	3.0	-8.36	-63.8	3.0	6.58	-8.01	6.31	16,618
LL148	Red Well	48-23-7	<0.050	<0.03	0.22	3.10	0.22	0.06	0.96	3.3	-9.71	-75.0	4.5	5.91	-7.46	13.13	9,974
LL149	Sampson Well	48-23-1	<0.050	<0.03	0.11	0.05	0.11	0.03	0.63	2.3	-8.99	-68.6	1.4	9.28	-6.38	16.70	6,691
LL152	Gibbs Well	48-14-4	<0.050	<0.03	0.13	0.03	0.13	0.11	0.69	2.7	-9.69	-72.9	1.2	6.74	-7.58	7.60	14,628
LL153	Dyer #2 Black Mountain South Well	48-31-9	<0.050	*0.03	0.16	0.07	0.16	0.04	0.82	2.7	-8.42	-61.8	<0.8	5.58	-7.09	10.96	11,047
LL154	Flattop Well - Figure 2 Ranch	48-24-9	<0.050	<0.03	0.09	0.35	0.09	0.12	0.50	1.5	-8.90	-61.8	8.1	11.04	-7.40	25.54	4,406
LL155	Dyer #3 Well	48-39-1	<0.050	<0.03	0.19	0.65	0.19	0.07	1.46	3.0	-7.31	-54.8	21.4	2.91	-6.76	9.08	12,210

Appendix 5. 'cont.)

Major ions (mg/L) and temperatures (°C).

Aquifer B+

BEG ID	Well Name	Coordinates		Ca^{2+}	Mg^{2+}	Na^{+}	K^{+}	HCO_3^{-}	SO_4^{2-}	Cl^{-}	NO_3^{-}	TDS	Temp
LL150	South Well	31°35'29"	105°30'08"	97	50.7	247	4.3	240	470	140	63	1321.86	20
LL151	Dyer #1 Ranch House	31°29'45"	105°21'59"	89.3	58	519	6.7	400	830	230	105	2246.66	21
LL156	Baylor - New Well	31°28'05"	105°22'59"	66.3	36.6	164	3.3	200	230	130	99	936.36	22
LL157	Baylor - Old Well	31°27'38"	105°24'51"	85.2	22.4	87.3	3.3	240	110	61	100	715.38	20

Aquifer B+

BEG ID	Well name	TWC ID	As^{3+}	Cd^{2+}	Li^{+}	Fe^{2+}	Sr^{2+}	Ba^{2+}	Br^{-}	F^{-}	$\delta^{18}O$**	δD**	Tritium	$\delta^{34}S$**	^{13}C**	PMC†	^{14}C Age††
LL150	South Well	48-28-3	<0.050	<0.03	0.10	0.06	0.10	0.16	1.74	3.7	-8.27	-63.0	0.9	6.87	-5.40	35.77	modern
LL151	Dyer #1 Ranch House	48-38-1	<0.050	<0.03	0.14	0.03	0.14	0.02	2.06	3.7	-8.19	-64.7	<0.8	6.34	-5.65	11.82	8,544
LL156	Baylor-New Well	48-37-3	<0.050	<0.03	0.07	<0.02	0.07	0.04	1.31	3.0	-7.38	-57.4	9.5	6.65	-4.73	39.43	modern
LL157	Baylor-Old Well	48-37-3	<0.050	<0.03	0.06	0.19	0.06	0.14	0.60	3.0	-7.04	-46.4	32.0	9.00	-4.75	90.77	modern

\+ see fig. 7 for distribution
< less than indicated value
* reported value near detection limit
** $\delta^{18}O$ and $\delta^{2}H$ defined relative to SMOW. $\delta^{34}S$ is given as deviation from the Canyon Diablo Meteorite standard. $\delta^{13}C$ defined relative to Pee Dee Belemnite carbonate.
† PMC is percent of modern carbon
†† ^{14}C age was corrected by using $\delta^{13}C$ values

Appendix 6.

A. Chemical and isotopic composition of ground-water samples, Fort Hancock site (Kreitler and others, 1986).

Major ions (mg/L) and temperatures (°C).

BEG ID	Well name	Coordinates		Ca^{2+}	Mg^{2+}	Na^{+}	K^{+}	HCO_3^{-}	SO_4^{2-}	Cl^{-}	NO_3^{-}	TDS	Temp.
LL107	48-42-1 Windmill	31°22'12"	105°50'52"	169.0	35.3	1250	7.7	161	2270	520	1.3	4421.6	24.5
LL108	48-42-404 Well	31°18'56"	105°51'27"	34.7	11.9	410	4.5	263	395	259	5.1	1388.1	22.5
LL109	48-41-618 Well	31°17'31"	105°52'45"	23.8	23.9	486	14.6	96	315	555	<0.5	1517.5	
LL110	48-41-2 Well	31°19'37"	105°54'55"	387.0	91.7	881	12.8	495	770	1450	<0.5	3604.1	19.0
LL111	48-33-9 Windmill	31°23'18"	105°53'18"	26.8	10.5	327	4.2	242	360	168	11.4	1154.4	21.0
LL112	Head of Canyon WM	31°31'42"	105°42'05"	61.6	19.3	177	5.4	282	168	116	26.5	861.7	14.0
LL113	Wilkey Well no. 1	31°23'23"	105°40'48"	77.1	43.1	237	3.4	336	438	88	11.8	1241.5	20.0
LL114	Wilkey Well no. 2	31°22'48"	105°39'07"	131.0	24.6	55	1.5	284	275	10	11.3	801.4	11.0
LL115	Gunsight Windmill no. 1	31°25'03"	105°30'20"	37.3	22.1	454	7.4	411	570	137	<0.5	1649.2	19.0
LL116	Owens Well	31°22'31"	105°45'50"	48.4	15.3	362	3.5	278	525	128	<0.5	1369.4	14.0
LL126	Low Level Well	31°24'14"	105°43'32"	70.7	6.9	549	4.4	60	710	416	18.3	1850.	17.0
Springs:													
LL106	Thaxton Sp	31°28'11"	105°42'57"	26.8	22.9	475	4.6	501	520	148	11.3	1718.3	9.0

Trace ions (mg/L) and isotope composition[1] in ground-water samples.

BEG ID	Well name	Coordinates		As^{3+}	Cd^{2+}	Li^{+}	Fe^{2+}	Sr^{2+}	Ba^{2+}	Br^{-}	F^{-}	$\delta^{18}O$	$\delta^{2}H$	Tritium	$\delta^{34}S$	$\delta^{13}C$	PMC[2]	^{14}C Age[3]
LL107	48-42-1 Windmill	31°22'12"	105°50'52"	0.012	<0.03	0.26	0.04	3.20	0.02	2.66	1.05	-8.0	-59	<0.8	+1.0	-16.8	16.6	14,748
LL108	48-42-404 Well	31°18'56"	105°51'27"	0.017	<0.03	0.10	0.05	1.01	0.04	1.25	2.37	-6.9	-48	<0.8	+3.8	-9.6	61	Modern
LL109	48-41-618 Well	31°17'31"	105°52'45"	<0.010	<0.03	0.21	0.02	1.43	0.01	0.59	0.39	-7.4	-71	27.2	+16.9			
LL110	48-41-2 Well	31°19'37"	105°54'55"	<0.010	<0.03	0.26	1.35	6.69	0.06	2.27	0.61	-8.8	-74	21.8	+4.7	-12.0	116	Modern
LL111	48-33-9 Windmill	31°23'18"	105°53'18"	<0.010	<0.03	0.10	0.49	0.81	0.02	1.01	2.03	-7.3	-51	<0.8	+7.2	-10.1	21.8	8,288
LL112	Head of Canyon Windmill	31°31'42"	105°42'05"	<0.010	<0.03	0.06	0.10	1.72	0.02	1.14	2.79	-7.1	-50	11.8	+5.8	-8.0	43	833
LL113	Wilkey Well no. 1	31°23'23"	105°40'48"	<0.010	<0.03	0.05	0.71	3.90	0.03	0.77	1.60	-7.7	-58	3.74	+5.2	-9.4	36	3,529
LL114	Wilkey Well no. 2	31°22'48"	105°39'07"	<0.010	<0.03	0.03	<0.02	7.50	0.03	0.44	0.90	-7.5	-54	20.67	+10.9	-11.3	60	868
LL115	Gunsight Windmill no. 1	31°25'03"	105°30'20"	<0.010	<0.03	0.12	2.15	3.32	0.03	1.15	3.10	-10.7	-83	0.5	-0.5	-7.9	9.6	13,071
LL116	Owens Well	31°22'31"	105°45'50"	<0.010	<0.03	0.07	0.20	2.87	0.12	1.10	4.30	-8.0	-62	1.52	+7.0	-7.8	8.9	13,520
LL126	Low Level well	31°24'14"	105°43'32"	<0.050	<0.03	0.10	0.13	8.30	0.19	2.10	4.30	-8.3	-61		+4.1	-18.1	3.3	27,400
Springs:																		
LL106	Thaxton Sp	31°28'11"	105°42'57"	<0.010	<0.03	0.13	0.02	1.63	0.02	1.34	5.57	-7.5	-58	<0.8	-1.8			

Appendix 6. (cont.)

B. Chemical composition of ground water from selected wells (Texas Water Development Board [TWDB] 1985).

BEG ID	TWDB ID	Ca^{2+}	Mg^{2+}	Na^{+}	K^{+}	HCO_3^-	SO_4^{2-}	Cl^-	F^-	NO_3^-	TDS
LL170	48-07-101	324	139	168	-	193	1,300	145	-	31.0	2,220
LL171	48-07-102	598	164	250	-	214	2,142	267	2.0	8.7	3,555
LL172	48-07-206	459	225	640	-	172	2,230	594	3.1	286.0	4,563
LL173	48-07-207	364	136	119	-	227	1,220	156	1.8	14.1	2,140
LL174	48-07-210	326	158	267	-	240	1,180	405	1.8	51.0	2,520
LL176	48-07-304	332	124	175	-	248	860	408	1.8	7.0	2,045
LL177	48-07-405	435	219	471	-	195	1,630	800	2.4	110.0	3,779
LL178	48-07-414	324	134	481	-	260	1,120	750	1.9	29.5	2,983
LL180	48-07-501	358	264	510	-	138	1,670	890	2.1	39.0	3,817
LL183	48-07-606	368	220	338	-	259	1,230	670	2.1	42.0	3,011
LL184	48-07-607	350	137	121	-	238	910	415	1.5	3.5	2,070
LL185	48-07-706	264	82	392	1.2	294	703	667	1.1	4.87	2,276
LL187	48-07-801	538	306	952	-	231	2,117	1,512	1.8	44.20	5,603
LL188	48-07-803	500	199	820	-	123	2,110	1,120	2.6	42.0	4,869
LL189	48-07-901	215	87	160	-	95	700	320	1.4	3.50	1,548
LL190	48-07-904	522	248	773	-	255	1,646	1,400	1.6	22.60	4,757
LL192	48-06-201	560	166	40	-	229	1,910	20	2.7	0.40	2,831
LL193	48-06-601	520	178	58	-	201	1,900	27	2.7	0.40	2,804
LL194	48-15-203	266	77	378	1.1	293	681	615	1.1	5.01	2,184
LL195	48-15-301	280	81	326	-	293	720	550	1.6	7.00	2,125
LL202	47-09-803	222	99	156	-	279	660	256	-	3.50	1,549
LL203	47-09-805	171	70	82	-	283	439	126	1.0	0.10	1,044

1) $\delta^{18}O$ and $\delta^{2}H$ defined relative to SMOW. $\delta^{34}S$ is given as deviation from the Canyon Diablo Meteorite standard. $\delta^{13}C$ defined relative to Pee Dee Belemnite carbonate.
2) PMC is percent of modern carbon.
3) ^{14}C age was corrected by using $\delta^{13}C$ values except for sample LL126.

Appendix 7. Lithologic and structural descriptions of test holes.

Two boreholes drilled as part of this study were continuously cored from the top of bedrock to a total depth of 150 ft (46 m). Lithologic logs for both boreholes are presented below.

HU1A (fig. A7-1)

Bedrock was encountered in HU1A-BEG #1 at a depth of 8 ft (2.4 m). Alluvial cover from 0 to 5 ft (0-1.5 m) consisted of tan to brown, sand to silty sand, with minor occurrences of caliche. From 5 ft (1.5 m) to 8 ft (2.4 m) the alluvium became increasingly coarser with gravels of predominantly rhyolite composition. The dark-red rhyolite porphyry has pink feldspar and clear glassy quartz phenocrysts that range in size from 0.1 to 0.4 inches (0.2 to 1.0 cm). Chlorite is a common alteration product. Limonite and hematite stains also occur on fracture surfaces in the core. Fifty percent of the rhyolite porphyry core from site HU1A is fractured. Lithologic descriptions, fractured intervals, and fracture orientations are presented below.

HU1B (fig. A7-2)

Bedrock was encountered in HU1B-BEG#1 at a depth of 18 ft (5.4 m). Alluvial cover at this site consisted of tan to brown sand with abundant caliche nodules from 0 to 8 ft (0 to 2.4 m); tan to yellow clay with variable amounts of brown sandstone gravels and minor inclusions of interbedded silts and sands from 8 to 18 ft (2.4 to 5.4 m). Cretaceous bedrock encountered at 18 ft (5.4 m) consisted of a limestone breccia to 20.3 ft (6.2 m). Cretaceous Cox sandstone consists at

this location of a predominantly gray cross-bedded sandstone interbedded with thin purple layers of quartz grains, and was recorded from 20.3 ft (6.2 m) to 30.8 ft (9.3 m). This interval recorded variable amounts of fracturing. Oxidation of iron minerals in this interval was prevalent.

From 30.8 ft (9.2 m) to total depth at 150 ft (45.7 m) the stratigraphic interval was Cretaceous Campagrande limestones. This interval is dominated by nodular limestones in the upper section, becoming more conglomeratic in the lower section. Lithologic descriptions, fracture, and solution occurrence are presented below. Logging descriptions used are based on the system of Bebout and Loucks (1984).

Appendix 8. Climate and vegetation controls on surface recharge.

Differences in annual rates of precipitation, evaporation, temperature, and dominant plant ecosystems between sites HU1A and HU1B on the Diablo Plateau and the Fort Hancock site in the Hueco Bolson may influence the potential for surface recharge. Distinct differences between the two areas in climate, surface and near-surface lithologies, and vegetation have been reviewed to determine how they may affect surface recharge. Further study is required to quantify actual levels of evapotranspiration at both areas before final conclusions are drawn.

Trans-Pecos Climate

Regional climatic data for Hudspeth and El Paso Counties have been previously discussed (Kreitler and others, 1986). The region has a subtropical arid climate (Larkin and Bomar, 1983) characterized by (1) high mean temperatures and marked fluctuations over broad diurnal and annual ranges and (2) low mean precipitation with widely separated annual extremes (Orton, 1964). Rainfall in this climate is inadequate to support vegetation other than desert and semi-desert types.

Precipitation and temperature (minimum and maximum) data were selected for five monitoring stations in the area (fig. A8-1; table A8-1) (National Weather Service, 1986a, b, c). Three of these are located within the Hueco Bolson at the El Paso Airport, in Fabens, and in Fort Hancock. Two stations on the Diablo Plateau were also monitored. They are at Sierra Blanca, south of the study area, and at Cornudas, northwest of the study area. Only the El Paso Airport station had complete records for extended lengths of time. Data from the other four stations are incomplete.

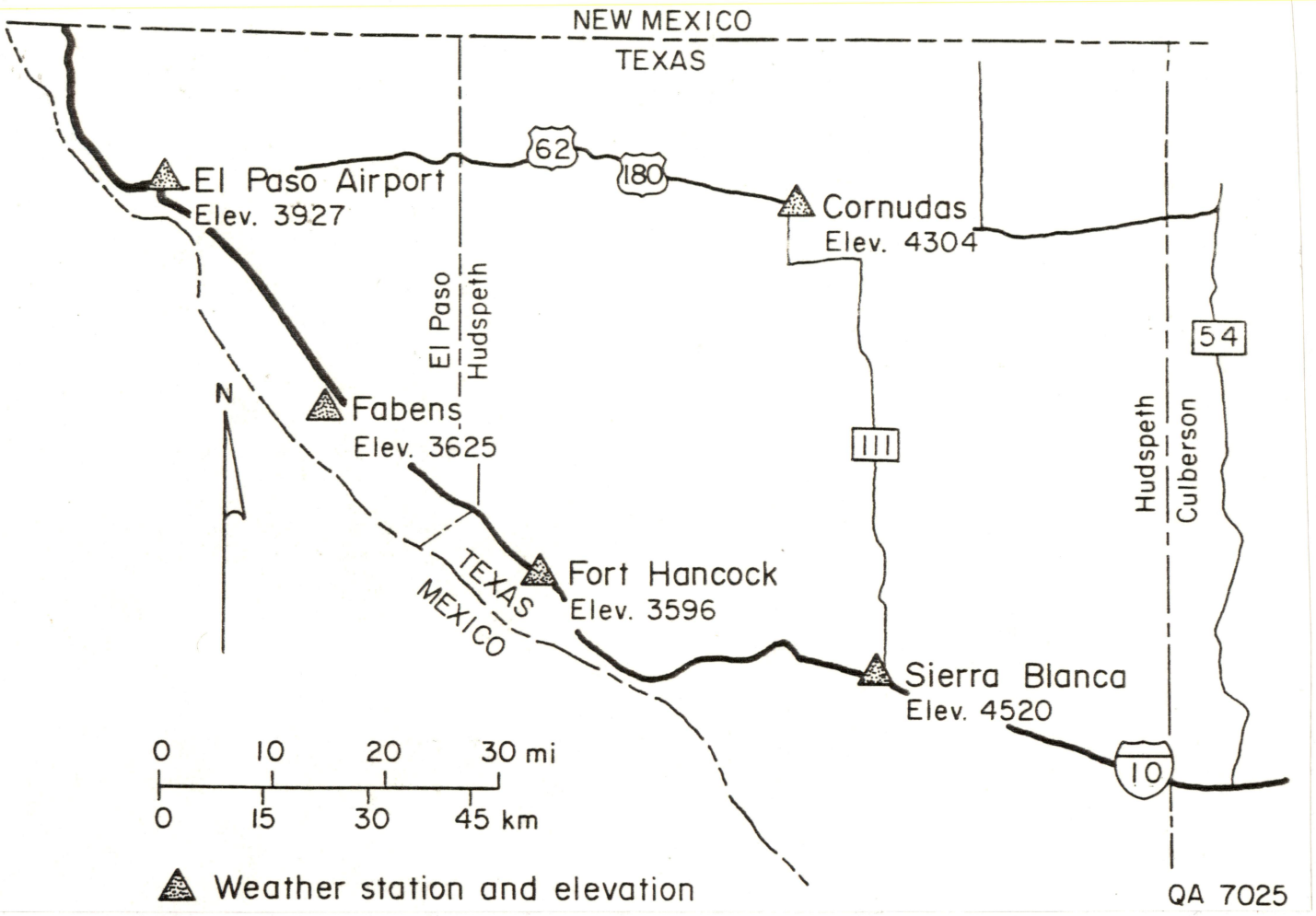

Figure A8-1. Weather stations location map. Three stations (El Paso, Fabens, and Fort Hancock) are in the Hueco Bolson area, whereas two stations (Sierra Blanca and Cornudas) are in the Diablo Plateau.

Table A8-1. Climatic data for Hueco Bolson and Diablo Plateau in the study area.

Monitor Station (Elevation in ft)	Latitude/ Longitude	Annual Average			Summer Average (June - Sept.)		
		Rainfall inches`	Minimum Temperature °F	Maximum Temperature °F	Rainfall 'inches`	Minimum Temperature °F)	Maximum Temperature (°F)
Cornudas Service Station (4304)	31°47'00" 105°28'00"	10.2	42.5	77.7	6.24	59.1	91.9
El Paso WSO AP (3927)	31°48'00" 106°24'00"	9.53	49.0	77.9	5.56	65.5	94.0
Fabens (3625)	31°30'00" 106°09'00"	9.65	45.2	77.8	6.96	62.5	91.6
Fort Hancock (3596)	31°17'00" 105°51'00"	10.27	44.1	79.8	6.48	61.9	95.0
Sierra Blanca (4520)	31°11'00" 105°21'00"	13.45	43.9	77.3	9.28	59.7	90.2

National Weather Service (NWS) records were used to describe the climate of the study area. Monthly totals for precipitation and monthly averages for minimum and maximum temperatures were recorded at the above-mentioned five stations. No year with incomplete data was used; data from some stations represent different years. Ten complete years of data were assembled for each station except Fort Hancock, which had only 7 years of precipitation data. Mean annual, monthly, and summer (June to September) values for precipitation and temperatures were calculated along with their standard deviation. The results are presented in table A8-1.

Most annual precipitation occurs as afternoon thundershowers from June to September. These thundershowers are the result of moist air from the Gulf of Mexico moving northwest into the Trans-Pecos area during the hurricane season. At the Cornudas service station, annual precipitation has averaged 10.2 inches (25.9 cm) and average summer precipitation is 6.24 inches (15.8 cm) or 61% of the annual total over 33% of the time. Similar values were observed at the other stations.

Changes in elevation have a direct effect on both temperature and precipitation patterns. The difference in elevation between Cornudas and Fort Hancock is approximately 708 ft (215 m), and the difference in average temperatures is 2.1°F for maxima and 1.6°F for minima. Average precipitation totals for both Cornudas and Fort Hancock are 10.2 inches (25.9 cm) and do not reflect the difference in elevations. Sierra Blanca, however, records a greater average annual precipitation of 13.45 inches (34.1 cm).

The degree to which an increase in temperature within the Hueco Bolson affects potential evaporation, and thus evapotranspiration changes between the bolson and plateau is unknown. Quantitative data on potential evaporation in the area are from two stations in Ysleta, both of which are in the bolson east of El Paso. The adjusted annual mean evaporation for these stations ranges from 93.1 inches (2.4 m)

in 1944 to 116.4 inches (3 m) in 1956 (Dougherty, 1975). Scalapino (1950) reported that the annual potential evaporation in the Dell City area is nine times greater than the annual precipitation. If the only variables in the two systems were precipitation and temperature, the potential for evapotranspiration in the bolson would be greater, and, thus, the potential for surface recharge to the water table would be more probable on the Diablo Plateau.

Fort Hancock Area - Hueco Bolson Plant Ecosystems

Common plant ecosystems in the Hueco Bolson north of Fort Hancock are representative of desert shrublands (taxonomic identification assisted by Kenneth Moore, personal communication, 1986; Correll and Johnston, 1970). Most of the annual vegetative production is from woody plants with running mesquite (*Prosopis sp.*) dominant in areas of rolling sandy loams and the creosote bush (*Larrea tridentata*) more dominant in gravelly areas. Annual plant production from herbaceous plants is low, averaging 500 pounds per acre (ppa). Commonly, bare land surface exists between woody plants, a controlling factor in the low plant production. Annual grasses may also constitute a large part of the plant production.

Other woody plants common in the area are javelina bush (*Condalia ericoides*), yucca (*Yucca sp.*), and cactus (Cactaceae family). Minor populations of four-wing salt bush (*Atriplex canescens*) and broomweed or snakeweed (*Xanthocephalum sp.*) are also present. Perennial grasses in the area include bush muhly (*Muhlenbergia porteri*), dropseed (*Sporobolus sp.*), fluffgrass (*Erioneuron pulchellum*), and burro grass (*Scleropogon brevifolius*).

HU1A - HU1B Diablo Plateau-Plant Ecosystems

The area on the Diablo Plateau in the vicinity of HU1A and HU1B is a desert grassland. Numerous annual and perennial grasses may be found in the area but only sparse occurrences of woody vegetation. Annual plant production from desert grasslands may be considerably higher than has been reported for desert shrublands, ranging from 1,000 to 5,000 ppa. Dominant annual grasses of the area include blue grama (*Bouteloua gracilis*), black grama (*Bouteloua eriopoda*), tobosa grass (*Hilaria mutica*), plains bristlegrass (*Setaria macrostachya, S. texana,* and *S. leucopila* collectively), and side-oats grama (*Bouteloua curtipendula*).

Perennial grasses may also represent a large segment of the desert grassland ecosystem. Several of these species are *Muhlenbergia, Sporobolus*, along with vine-mesquite (*Panicum obtusum*), burro grass (*Scleropogon brevifolius*), and fluffgrass *(Erioneuron pulchellum*). In local areas that receive additional water from runoff, such as in draws, Cane bluestem (*Andropogon sp.*) and Sacaton grass (*Sporobolus sp.*) may also be dominant part of the ecosystem.

Woody vegetation is rare in the desert grassland, except where the soil is sandy or gravelly. Woody vegetation that occasionally dominates the draws includes vine ephedra (*Ephedra pedunculata*), several species of the cactus family, the creosote bush (*Larrea tridentata*), desert sumac (*Rhus microphylla*), yucca (*Yucca sp.*), and the javelina bush (*Condalia cricoides*).

Discussion

The correlation between temperature, precipitation, and dominant plant ecosystem discussed above influences evapotranspiration rates and potential for surface recharge. High tritium levels in several sampled wells on the Diablo Plateau indicate surface

recharge activity significantly higher than that measured in the Hueco Bolson, north of Fort Hancock (fig. 14, this report; Kreitler and others, 1986). Greater rainfall and lower temperatures may be directly related to active surface recharge on the Diablo Plateau. However, increases in precipitation may not affect surface recharge in the Diablo Plateau because the denser plant populations may absorb more water, whereas shrublands lose water during runoff infiltration due to less extensive or less efficient root systems. There is a large difference between plant production in the bolson (500 ppa) and on the plateau (up to 5,000 ppa). Quantification of evapotranspiration rates in both areas would facilitate a better understanding of recharge mechanism and recharge potential in the bolson and on the plateau.